RUPTURE STATUS PREDICTION, BASED ON THE MORPHOLOGY AND HEMODYNAMIC PARAMETERS OF CEREBRAL ANEURYSMS: A MACHINE LEARNING BASED STUDY

Dr. BHUSHAN SADASHIV AKHADE

MCh NEUROSURGERY THESIS

2023

SREE CHITRA TIRUNAL INSTITUTE FOR MEDICAL SCIENCES AND TECHNOLOGY, TRIVANDRUM

An Institution of National Importance established by an Act of the Indian Parliament (Act No.52 of 1980)

Dept. of Science and Technology, Govt. of India

www.sctimst.ac.in

RUPTURE STATUS PREDICTION BASED ON THE MORPHOLOGY AND HEMODYNAMIC PARAMETERS OF CEREBRAL ANEURYSMS: A MACHINE LEARNING BASED STUDY

A THESIS SUBMITTED BY

Dr BHUSHAN SADASHIV AKHADE

TO

SREE CHITRA TIRUNAL INSTITUTE FOR MEDICAL SCIENCES AND TECHNOLOGY, TRIVANDRUM.

IN PARTIAL FULFILMENT OF THE REQUIREMENTS

FOR THE AWARD OF

MCh NEUROSURGERY

2023

DECLARATION BY THE STUDENT

CERTIFICATE

I Dr Bhushan Sadashiv Akhade hereby certify that I had personally carried out the work depicted in the thesis titled, "**RUPTURE STATUS PREDICTION, BASED ON THE MORPHOLOGY AND HEMODYNAMIC PARAMETERS OF CEREBRAL ANEURYSMS: A MACHINE LEARNING BASED STUDY.**

No part of this thesis has been submitted for the award of any other degree or diploma prior to this date.

Signature

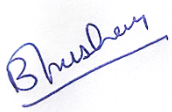

Name of the Candidate

Date-30/08/2023 Dr Bhushan Sadashiv Akhade

SREE CHITRA TIRUNAL INSTITUTE FOR MEDICAL SCIENCES AND TECHNOLOGY,TRIVANDRUM

Thiruvananthapuram– 695 011, Kerala, India

(An Institute of National Importance under Govt. of India)

Phone: 91-471-2443152 Fax: 91-471-2446433, Email: sct@sctimst.ac.in

Web site: www.sctimst.ac.in

CERTIFICATE BY THE RESEARCH GUIDE

Name of the Guide: Prof. B Jayanand Sudhir

Department: Neurosurgery

This is to certify that Dr Bhushan Sadashiv Akhade department of Neurosurgery of this institute has fulfilled the requirements prescribed for the MCh degree of the Sree Chitra Tirunal Institute for Medical Sciences and Technology, Trivandrum.

The thesis entitled, **"RUPTURE STATUS PREDICTION, BASED ON THE MORPHOLOGY AND HEMODYNAMIC PARAMETERS OF CEREBRAL ANEURYSMS: A MACHINE LEARNING BASED STUDY"** was carried out under my direct supervision. No part of the thesis was submitted for the award of any degree or diploma prior to this date.

Clearance was obtained from the Institutional Ethics Committee for carrying out the study.(IEC/841/MARCH-2023)

Signature

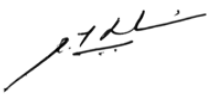

Name of the Guide
Prof. B Jayanand Sudhir

Date 30/08/2023

SREE CHITRA TIRUNAL INSTITUTE FOR MEDICAL SCIENCES AND TECHNOLOGY,TRIVANDRUM

Thiruvananthapuram– 695 011, Kerala, India

(An Institute of National Importance under Govt. of India)

Phone: 91-471-2443152 Fax: 91-471-2446433, Email: sct@sctimst.ac.in

Web site: www.sctimst.ac.in

APPROVAL OF THESIS

The thesis entitled

"RUPTURE STATUS PREDICTION, BASED ON THE MORPHOLOGY AND HEMODYNAMIC PARAMETERS OF CEREBRAL ANEURYSMS: A MACHINE LEARNING BASED STUDY"

Submitted by

Dr Bhushan Sadashiv Akhade

for the degree of

MCh Neurosurgery

Of

SREE CHITRA TIRUNAL INSTITUTE FOR MEDICAL SCIENCES AND TECHNOLOGY, TRIVANDRUM

is evaluated and approved by

Prof. B Jayanand Sudhir

(Guide) (External Examiner)

ACKNOWLEDGEMENTS

First and foremost, I bow my head to the Almighty for giving me strength, endurance and perseverance which made me capable of carrying out the present work successfully. Words are insufficient to express the love, labour and selflessness that everyone has given and expressed during the last 3 years of tenure in this department.

I owe a deep sense of gratitude to Prof. B Jayanand Sudhir , Addtional Professor, Department of Neurosurgery for his invaluable advice, encouragement, and guidance, without which this work would not have been possible. His critical remarks, suggestions, helped me in achieving a high standard of work.

The guidance of Prof Krishnakumar K and Prof Easwer H V , has been invaluable and I am extremely grateful and indebted for his contributions and suggestions, which were of invaluable help during the entire work. They will always be a constant source of inspiration to me.

I am deeply indebted to Prof. George C Vilanilam, Dr. Prakash Nair, Dr. Ganesh Divakar, Dr. Mathew Abraham, Dr. Gowtham for their constant encouragement and support.

I thank Prof. Prasad Patnaik B.S.V, Professor, Department of Applied Mechanics,Indian Institute of Technology Madras for his valuable guidance and constant encouragement.

I thank my seniors Dr. Darshan Ravi, Dr. Sreenath Nair for their constant support.

I thank my colleagues Dr. Sam Scaria, Dr. Suraj Gopal, Dr. Lokesh, Dr.Akhilesh, Dr. Ram kishan, Dr. Vamshi , Dr. Ashutosh, Dr. Pooja, Dr. Niroop, Dr. Arvin, Dr. Sagar, Dr. Ankush, Mr Harikrishnan P, Ms Larib Hassan (IIT Madras) and my wife, parents for their help and guidance in this study.

I owe a deep sense of gratitude to my institute and all my patients without whom this work would not have been possible.

I am extremely grateful to Department of Science and Technology, Government of India. The study was supported by a grant (SUPRA: Scientific and Useful Profound Research Advancement SPR/2020/000298 Computational Fluid Dynamics based tools to the aid of clinical decision making in the management of intracranial aneurysms) from Science Engineering Research Board (SERB), Department of Science and Technology, Government of India.

Dr. BHUSHAN SADASHIV AKHADE

TABLE OF CONTENTS

LIST OF FIGURES

LIST OF TABLES

LIST OF ABBREVIATIONS

Abbreviation	Full Form
1. IA	Intracranial Aneurysms
2. HPC	High Performance Computing
3. CFD	Computational Fluid Dynamics
4. ML	Machine Learning
5. ANOVA	Analysis of variance
6. VIF	Variance inflation factor
7. PCA	Principal component analysis
8. ANN	Artificial neural network
9. DBSCAN	Density-based spatial clustering of applications with noise
10. SVM	Support vector machine

SYNOPSIS

RUPTURE STATUS PREDICTION, BASED ON THE MORPHOLOGY AND HEMODYNAMIC PARAMETERS OF CEREBRAL ANEURYSMS: A MACHINE LEARNING BASED STUDY

Background and Aim: Intracranial aneurysms are common condition in neurosurgical practice. A key factor governing clinical management of cerebral aneurysms is the rupture status. Crucial clinical situations arise when it is difficult to identify the ruptured aneurysm in case of multiple aneurysms. In this realm, morphological and hemodynamic features of aneurysms often provide valuable and reliable clues. This work aims to assess the significance of the morphological and hemodynamic factors in predicting the rupture status of intracranial aneurysms using statistical and machine learning tools.

Methods: Hundred consecutive cerebral aneurysms (64 ruptured, 36 unruptured) were studied. Geometric models were derived from using computational modelling computed tomographic angiography (CTA) or digital subtraction angiography (DSA). These models were created by performing image segmentation of angiographic images. The geometrical models were processed using software to extract key morphological and hemodynamic indices and ratios. The morphological and hemodynamic factors were tabulated, and statistically analysed. Further, machine

learning algorithms were used to obtain the best prediction of aneurysm rupture status. This was performed by supervised and unsupervised learning and testing the dataset.

Results: The aforementioned workflow was used to gather morphological and hemodynamic parameters for further statistical and machine learning-based inferences. Aspect ratio, bottle neck ratio, Dome height, parent vessel diameter, aneurysm surface area, surface area/volume ratio and RRT, mean WSS and p Mean were identified as the best parameters based on the hypothesis test. With the supervised learning methods our results shows that ANN model followed by Logistic regression algorithm proved to be effective in predicting the rupture status with accuracy of around 80 %.

The unsupervised machine learning algorithms shows that a higher inflow angle, abnormally large aneurysms and low wall shear stress can be related to higher rupture status which were consistent with other studies. And spectral algorithm grouped anuerysms with a silhouette score of 0.76 and 0.68 for both types of data.

Conclusion: Supervised learning algorithms shows ANN model followed by Logistic regression proved to be effective in predicting the rupture status.And unsupervised algorithms were used, out of which spectral algorithm grouped anuerysms with a silhouette score of 0.76 and 0.68 for both types of data.

KEYWORDS: Cerebral Aneurysm, Intracranial Aneurysm, Morphology, Risk Assessment; Machine Learning Classification Models.

INTRODUCTION

1. INTRODUCTION

Intracranial aneurysms are relatively common. The true risk arises when an aneurysm ruptures, resulting in a subarachnoid haemorrhage. However, symptoms from unruptured aneurysms may be primarily due to a mass effect or thrombosis. Spontaneous subarachnoid haemorrhage (SAH), a serious condition that can be fatal and result in permanent impairment, is primarily caused by the rupture of aneurysms. Therefore, it is highly desirable to assess the aneurysm rupture risk.

The overall 28-day case mortality rate following aneurysm rupture is 42.7 %, and survivors-dependency rates are about 50 % (Timothy Ingall et al., 2000).About 3.2 percent of adults (mean age, 50 years) globally have cerebral aneurysms, yet only 0.25 percent rupture.(Thompson, Brown, Amin-Hanjani, Broderick, Cockroft, Connolly, Duckwiler, Harris, Howard, SCC lay Johnston, et al., 2015) Treatment recommendations for unruptured aneurysms requires knowledge about the stability of the aneurysm. According to several investigators, size is the most crucial factor in determining aneurysm stability. (kassell1983.pdf, n.d.)

Due to the widespread use of computed tomography angiogram (CTA) and magnetic resonance angiogram (MRA) during the past few decades, an increase in the number of unruptured aneurysms has been discovered. Notably, a significant portion of accidentally discovered aneurysms (<87.6%) have small diameters (<3–4 mm) and are generally asymptomatic.(Murayama et al., 2016) It is still debatable how to handle patients with small aneurysms that have not ruptured. Based on the data of the low annual growth and rupture rates of small aneurysms, some researchers advise patients with aneurysms of 3 mm to not undertake preventative treatment or imaging follow-up.(Malhotra et al., 2017) However, in reality, acute catastrophic aneurysmal subarachnoid haemorrhage being the chief concern, small unruptured

aneurysms are frequently treated. Discriminating aneurysm stability is important, especially in tiny ones, because expanding aneurysms have a higher risk of rupture than those with a constant size.

Multiple cerebral aneurysms are present in up to 20% of those who have aneurysmal subarachnoid haemorrhage (SAH).(Hadjiathanasiou et al., 2020) In situations where a patient has multiple intracranial aneurysms, it is sometimes difficult to identify the aneurysm that has ruptured. Clinicians rely on results of cranial imaging, such as the pattern of the haemorrhage in computed tomography (CT) to pinpoint the aneurysm that has ruptured. Based on the CT findings, including the haemorrhage pattern on side of aneurysm, large irregular shaped (multilobulated or aneurysm with bleb), the neurovascular team determines which aneurysm had the highest likelihood of having ruptured.(Hadjiathanasiou et al., 2020)However, in other instances, when two or more aneurysms are in immediate proximity of cisternal blood and the bleeding pattern lacks lateralization, it might be difficult to identify the ruptured aneurysm.

We used an advanced statistical/ machine-learning model for the prediction of an aneurysm rupture, which could help neurovascular teams in such situations. Numerous morphological factors have been linked to the identification of a ruptured aneurysm, including size ratio, flow angle, height/width ratio, aspect ratio, and deviated angle(Kashiwazaki and Kuroda, 2013) Aspect ratio, ellipticity index, non-sphericity index, and undulation index were shown to be statistically significant between the ruptured and unruptured cases than pure size-based morphological indices. (Xiang et al., 2011a)

There have also been reports of early uses of artificial intelligence in aneurysm detection, risk classification, and prediction. To forecast the rupture risks of anterior communicating artery aneurysms, Liu et colleagues built a 2-layer feed-forward neural network and achieved an overall prediction accuracy of 94.8 percent. (Liu et al., 2018a)

The purpose of this study was to create a machine-learning model utilising clinical, hemodynamic and morphological parameters, in order to identify the rupture status of an intracranial aneurysm. These models might develop to serve as a foundation for clinical judgement while treating brain aneurysms.

AIMS & OBJECTIVES

AIMS AND OBJECTIVES

1)To assess the significance of the morphological and hemodynamic factors in predicting the rupture status of intracranial aneurysms using statistical and machine learning tools.

2)To apply supervised learning and clustering methods to analyze the data and identify subgroups with distinct characteristics

3) To apply unsupervised learning and clustering methods to analyze the data and identify subgroups with distinct characteristics

REVIEW OF LITERATURE

REVIEW OF LITERATURE

Multiple well known risk factors are contributing to the formation, growth, and rupture of IAs such as genetics, age, hypertension, smoking, size, and site of the aneurysms (UCAS Japan Investigators et al., 2012). However, the actual mechanisms that lead to an aneurysm rupture are not well understood yet.

Predicting the future behaviour of cerebral aneurysms was the target of several studies in recent years. When an unruptured cerebral aneurysm is diagnosed, the physician has to decide about the treatment method. Often more giant aneurysms are diagnosed at higher risk of rupture and are candidates for intervention. However, several clinical and morphological parameters are introduced as risk factors. Therefore, some small size aneurysms with a higher growth rate and rupture risk may be missed.

Treatment method of unruptured aneurysm depends on the aneurysm size. The ISUIA study and the UCAS study both concluded that size is a significant risk factor for rupture.(UCAS Japan Investigators et al., 2012; Wiebers et al., 2003)

In both ISUIA and UCAS studies, aneurysms smaller than 7 mm have been associated with very low risk profiles for rupture(Wiebers et al., 2003)

Aneurysms below the threshold size of 7 mm still account for a noticeable number of ruptures(Robertson et al., 2015)

Therefore, it is necessary to be aware of the future behavior of the aneurysm. Estimating the 3D flow pattern and stress distribution and predicting the disease's progression trend may be possible by computational studies.

CFD can help surgeons decide about the best treatment method and prevent unnecessary interventions.

It is not possible to study the true natural history of UIAs in future prospective follow-up cohorts.

Risk factors for aneurysmal rupture include aneurysm size and aneurysm site, with higher risks for larger aneurysms and aneurysms in the posterior circulation (Juvela et al., 2000; UCAS Japan Investigators et al., 2012; Wiebers et al., 2003).Various other factors like multiple aneurysms,(UCAS Japan Investigators et al., 2012) female sex,(Wermer et al., 2007) young age, (UCAS Japan Investigators et al., 2012) and cigarette smoking(Juvela et al., 2000) have been suggested as risk factors.

The treatment decisions of unruptured IAs may improve to a large extent with an accurate prediction model based on the different types of risk factors aiming to identify patients with a high risk of aneurysmal rupture.(Detmer et al., 2018) Treatment of unruptured IAs would be indicated when the risk of rupture from natural history is higher than the risk of treatment and follow-up.

Despite great progress in methodological developments and many studies using patient specific data, there are still significant controversies about the precise governing processes and divergent conclusions from apparently contradictory results.

Dr Jacoba et al undertook a pooled analysis of individual patient data to establish predictors of aneurysm rupture in patients with unruptured intracranial aneurysms and to provide a risk prediction chart that allows physicians to easily determine the 5-year risk of aneurysm rupture on the basis of a set of routinely assessed patient and aneurysm characteristics(Greving et al., 2014) and proposed PHASES score,(population, hyperten sion, age, size of aneurysm, earlier

aneurysm rupture, site of aneurysm)which is an easily applicable aid for prediction of the risk of rupture of incidental intracranial aneurysms(Greving et al., 2014)

PHASES aneurysm risk score	Points
(P) Population	
North American, European (other than Finnish)	0
Japanese	3
Finnish	5
(H) Hypertension	
No	0
Yes	1
(A) Age	
<70 years	0
≥70 years	1
(S) Size of aneurysm	
<7·0 mm	0
7·0–9·9 mm	3
10·0–19·9 mm	6
≥20 mm	10
(E) Earlier SAH from another aneurysm	
No	0
Yes	1
(S) Site of aneurysm	
ICA	0
MCA	2
ACA/Pcom/posterior	4

To calculate the PHASES risk score for an individual, the number of points associated with each indicator can be added up to obtain the total risk score. For example, a 55-year-old North American man with no hypertension, no previous SAH, and a medium-sized (8 mm) posterior circulation aneurysm will have a risk score of 0+0+0+3+0+4=7 points. According to figure 3, this score corresponds to a 5-year risk of rupture of 2·4%. SAH=subarachnoid haemorrhage. ICA=internal carotid artery. MCA=middle cerebral artery. ACA=anterior cerebral arteries (including the anterior cerebral artery, anterior communicating artery, and pericallosal artery). Pcom=posterior communicating artery. posterior=posterior circulation (including the vertebral artery, basilar artery, cerebellar arteries, and posterior cerebral artery).

Table 4: **Predictors composing the PHASES aneurysm rupture risk score**

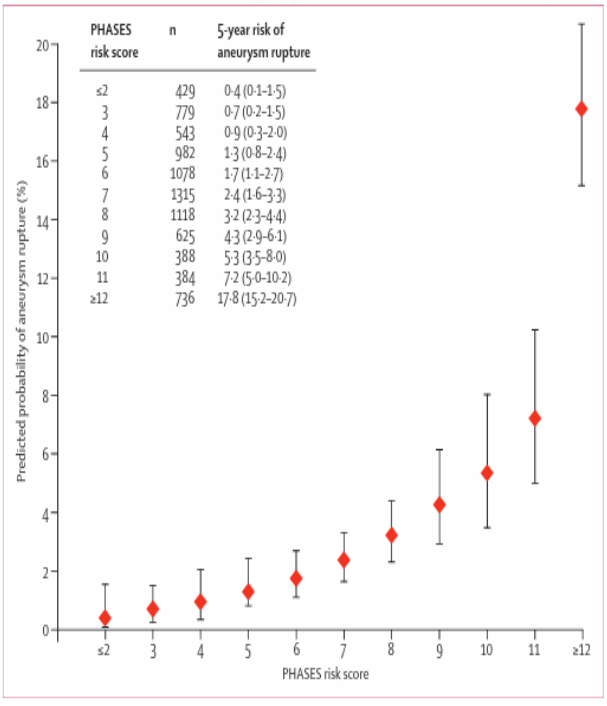

Figure 3: Predicted 5-year risk of aneurysm rupture according to PHASES score

The overall accuracy of the PHASES risk calculation is 54%, precision 51%, and recall of 54%.(Malik et al., 2023).

Unruptured intracranial aneurysm treatment score(UIATS) by Etminan et al (Etminan et al., 2015) for management of unruptured intracranial aneyrysm(UIA) given. The scores assigned to each patient aneurysm or treatment related feature on both management columns of the scoring form "in favour of UIA repair" and "in favour of UIA conservative management" are totaled up to determine a management recommendation for a UIA. This will result in two numerical values, one promoting surgical or endovascular aneurysm repair and the other recommending conservative care.

When there is a 3 point or more score difference, the direction, i.e the difference between the estimated numerical values on either side of the recommendation columns, will offer a specific management proposal (i.e., aneurysm repair or conservative management). The recommendation is "not decisive" in instances with identical aneurysm treatment and conservative management scores (2 point difference or less), and any management strategy may be justified. Each aneurysm must be assessed separately in cases involving multiple aneurysms, which will lead to individual recommendations for each aneurysm.

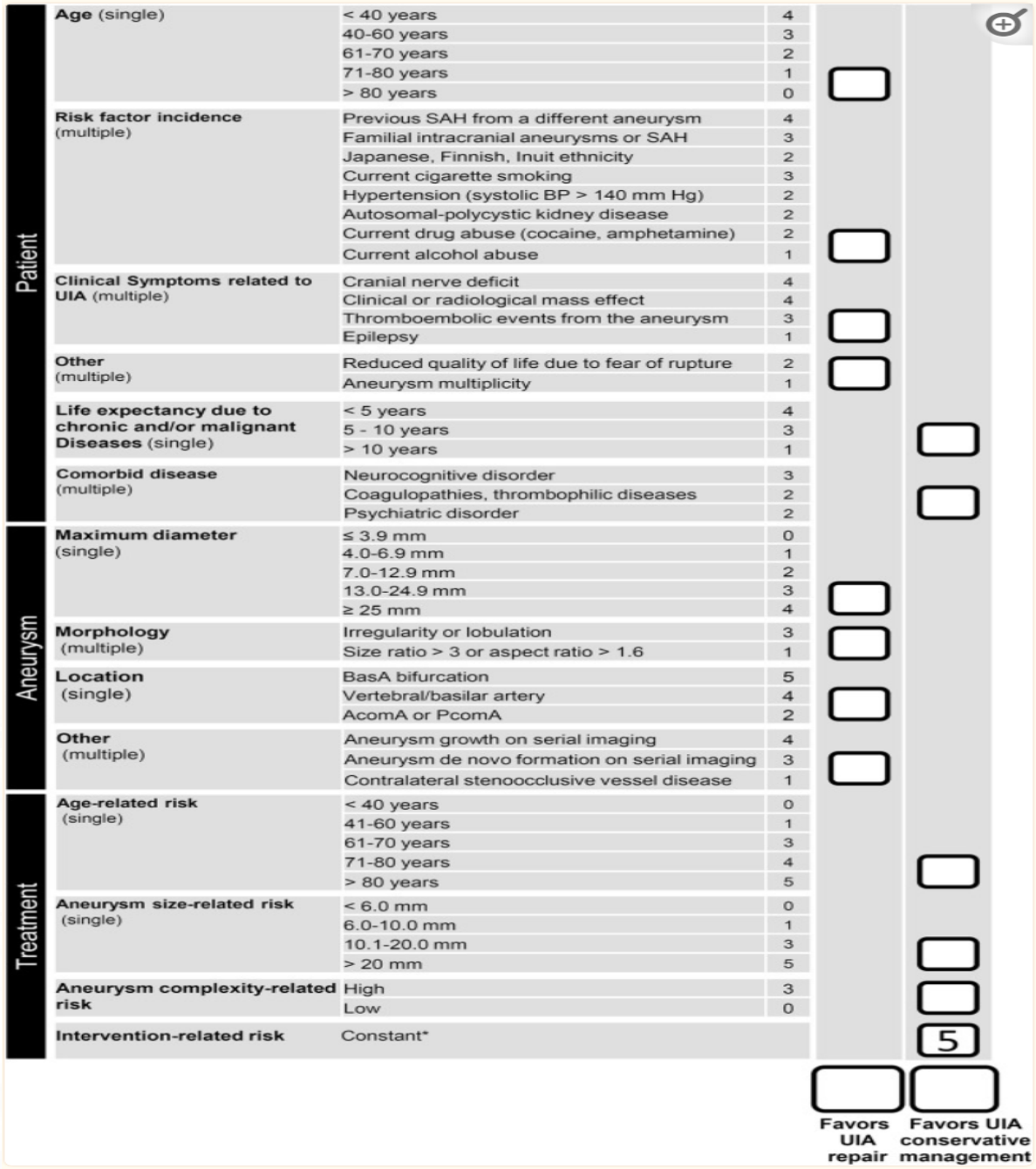

Patient	**Age** (single)	< 40 years	4		
		40-60 years	3		
		61-70 years	2		
		71-80 years	1	☐	
		> 80 years	0		
	Risk factor incidence (multiple)	Previous SAH from a different aneurysm	4		
		Familial intracranial aneurysms or SAH	3		
		Japanese, Finnish, Inuit ethnicity	2		
		Current cigarette smoking	3		
		Hypertension (systolic BP > 140 mm Hg)	2		
		Autosomal-polycystic kidney disease	2		
		Current drug abuse (cocaine, amphetamine)	2	☐	
		Current alcohol abuse	1		
	Clinical Symptoms related to UIA (multiple)	Cranial nerve deficit	4		
		Clinical or radiological mass effect	4		
		Thromboembolic events from the aneurysm	3	☐	
		Epilepsy	1		
	Other (multiple)	Reduced quality of life due to fear of rupture	2	☐	
		Aneurysm multiplicity	1		
	Life expectancy due to chronic and/or malignant Diseases (single)	< 5 years	4		
		5 - 10 years	3		☐
		> 10 years	1		
	Comorbid disease (multiple)	Neurocognitive disorder	3		
		Coagulopathies, thrombophilic diseases	2		☐
		Psychiatric disorder	2		
Aneurysm	**Maximum diameter** (single)	≤ 3.9 mm	0		
		4.0-6.9 mm	1		
		7.0-12.9 mm	2		
		13.0-24.9 mm	3	☐	
		≥ 25 mm	4		
	Morphology (multiple)	Irregularity or lobulation	3	☐	
		Size ratio > 3 or aspect ratio > 1.6	1		
	Location (single)	BasA bifurcation	5		
		Vertebral/basilar artery	4	☐	
		AcomA or PcomA	2		
	Other (multiple)	Aneurysm growth on serial imaging	4		
		Aneurysm de novo formation on serial imaging	3	☐	
		Contralateral stenoocclusive vessel disease	1		
Treatment	**Age-related risk** (single)	< 40 years	0		
		41-60 years	1		
		61-70 years	3		
		71-80 years	4		☐
		> 80 years	5		
	Aneurysm size-related risk (single)	< 6.0 mm	0		
		6.0-10.0 mm	1		
		10.1-20.0 mm	3		☐
		> 20 mm	5		
	Aneurysm complexity-related risk	High	3		☐
		Low	0		
	Intervention-related risk	Constant*			5

Favors UIA repair

Favors UIA conservative management

(Etminan et al., 2015)

Unruptured intracranial aneurysm treatment score(UIATS) overestimates the treatment indications of patients of working age and that its specificity for the lifelong occurrence of UIA rupture is low, and its predictive value in terms of receiver operating curves was modest. The UIATS recommended UIA treatment for 99% of the patients, but 24% had an aneurysm rupture(Juvela, 2019).

The overall accuracy of UIATS risk calculation was 59%, precision 59%, and recall was 59%(Malik et al., 2023).

All the UIATS factors with additional UIA locations and sex were tested with Cox regression analysis by Seppo Juvela to identify the variables which best predicted a future aneurysm rupture.(Juvela, 2019).

The best new treatment score consisted of 4 variables: age <40 years (2 points), current smoking (2 points), UIA size ≥7 mm (3 points), and location (anterior communicating artery, 5 points; internal carotid bifurcation, 4 points; and posterior communicating artery, 2 points). Scores of 5 to 12 points were associated with high cumulative UIA rupture rates (16%–60% at 10 years and 49%–80% at 30 years), favoring UIA treatment. Scores of 1 to 4 points (3% at 10 years and 18% at 30 years) favored conservative treatment and needed additional indications for treatment. Patients with a score of 0 points should not be treated(Juvela, 2019).

The PHASES and UIATS scores may only provide weak assistance in the clinical decision-making process of aneurysm treatment, particularly when it comes to the prediction of tiny aneurysms (those less than 5 mm).(Malik et al., 2023).

Because of its ability to deal with any geometry, image based computational fluid dynamics (CFD) has been progressively used to investigate the role of hemodynamics in the underlying mechanisms governing the natural history of cerebral aneurysms. It is known that the hemodynamics of the aneurysm plays a significant role in the pathophysiology of IAs (Cebral and Raschi, 2013).

Recently, computational fluid dynamics has become a popular tool in studying the hemodynamics of the IAs and predicting their rupture risk (Valen-Sendstad and Steinman, 2014). It has also been noticed that several morphological parameters may contribute to the IA rupture.(Kleinloog et al., 2018; Ujiie et al., 2001).

The morphology and growth of intracranial aneurysm are very complex due to the diverse nature of fluid mechanics. Because of the living nature of blood vessels, mechanical stimuli are transduced into biological signals, triggering inflammatory cascades leading to blood vessel wall remodeling. For this reason, cerebral aneurysmal hemodynamics has a significant role in the aneurysmal biophysical pathogenesis, evolution, and risk of rupture .(Soldozy et al., 2019)

In the current study, machine learning models performed better than conventional statistical model such as LR. Although machine learning models are powerful, they are often more complex, which makes them difficult to understand like a “black box.” This is a significant drawback if machine learning models were to be used in clinical setting. Clear reasoning is very important in medical decision making, especially for deadly disease such as cerebral aneurysms. They demonstrated that by using the SHAP method, machine learning models can be made more interpretable, and the underneath reasoning behind each prediction can be revealed, which can facilitate its use in clinical setting.(Ou et al., 2020)

Malik et al (Malik et al., 2023) introduce the concept of aneurysmal rupture criticality prediction(ARCP) and compare how risk factors and risk factor combinations are associated with aneurysmal rupture. This novel approach to aneurysmal rupture identifies new, high-risk patterns of rupture and can be used to guide clinical decision making for patients with nontraditional risks.

Their findings suggest that the ML techniques described here are reliable and the fine-grained location-specific models are more accurate than the global model. Additionally, weighted ensemble models can improve the accuracy of the global model.

The natural history of intracranial aneurysms consists of three stages: genesis, enlargement, and rupture. Each phase of the natural history of intracranial aneurysms depends on cell matrix processes and material properties of the wall.

There is significant controversy regarding the mechanisms responsible for growth and ultimate rupture of cerebral aneurysms. The controversy can be divided into two main schools of thought: high flow effects and low flow effects.(Sforza et al., 2009) In each theory, the hemodynamic environment within the aneurysm interacts with the cellular elements of the wall to result in a weakening of the wall.

The high flow theory focuses on the effects of elevation of wall shear stress (WSS), which can cause endothelial injury and thus initiate wall remodeling and potential degeneration. On the other hand, the low flow theory points to low flows within aneurysms as causing localized stagnation of blood flow against the wall in the dome, which causes a dysfunction of flow induced nitric oxide and triggers inflammation processes that lead to wall degradation.

However, because of the practical difficulties associated with measuring hemodynamic quantities in vivo, it has been difficult to exploit this potentially important information for basic biologic or clinical studies.

CFD for a cerebral aneurysm using the patient specific geometry model was first reported by DA Steinman et al. in 2003 (Steinman et al., 2003). Their results illustrate the importance of anatomic realism in determining the resulting flow dynamics, and their techniques serve as the first key step toward incorporating patient specific fluid dynamic information into a clinical setting.

Steinman et al(Steinman et al., 2003) observed high speed flow entering the aneurysm at the proximal and distal ends of the neck, promoting the formation of both persistent and transient vortices within the aneurysm sac. This produced dynamic patterns of elevated and oscillatory wall shear stresses distal to the neck and along the sidewalls of the aneurysm. A more practical limitation of this modeling approach was time required for stimulational, approximately 1 week was required to run this simulation on an economic, single processor desktop workstation.

Then Shojima et al were able to demonstrate that the average WSS of the aneurysm was significantly lower than that of the parent vessel.(Shojima et al., 2004). Their results suggest that in contrast to the pathogenic effect of a high WSS in the initiating phase, a low WSS may facilitate the growing phase and may trigger the rupture of a cerebral aneurysm by causing degenerative changes in the aneurysm wall.(Shojima et al., 2004)

Then Tateshima et al studied the flow pattern of a wide necked internal carotid artery-ophthalmic artery aneurysm by using Doppler velocimetry and particle imaging velocimetry. They found maximal flow velocities at the inflow and outflow zone at peak systole measuring 46.8% and 24.9% of that in the parent vessel and found that their side-wall aneurysm did not show a simple flow pattern as previously assumed.(Tateshima et al., 2003)

The flow patterns of inflow and outflow zones were very difficult to predict based on the limited flow information provided on standard digital subtraction angiography, even in an aneurysm with a relatively simple dome shape.(Tateshima et al., 2003).

They emphasize the need for 3D flow studies based on 3D imaging of aneurysm geometry for better understanding of aneurysmal behaviour after endovascular coil packing.

Hoi et al observed elevated aneurysm WSS and enlargement of impingement zones in sidewall aneurysms, located at curved arterial segments, when the arterial curvature increased.(Hoi et al., 2004).

authour postulate that lateral saccular aneurysms located on more curved arteries are subjected to higher hemodynamic stresses. Saccular aneurysms with wider necks have larger impact zones. The large impact zone at the distal side of the aneurysm neck correlates well with other findings, implicating this zone as the most likely site of aneurysm growth or regrowth of treated lesions.(Hoi et al., 2004)

Meng et al. found that a combination of high WSS and high positive WSS gradient were associated with vascular and molecular changes that predispose the arterial wall for aneurysm development(Meng et al., 2007)

They surgically created new branch points in the carotid vasculature of 6 female adult dogs,in vivo angiographic imaging and computational fluid dynamics simulations revealed in addition to hemodynamic parameters, many morphological parameters also helpful in predicting risk of rupture in aneurysm.

As rupture status predictors, selective morphological quantities such as the aspect ratio, the aneurysm neck, and the non sphericity index have been proposed.(Raghavan et al., 2005; Weir, 2003).Quantified shape is more effective than size in discriminating between ruptured and unruptured aneurysms. (Raghavan et al., 2005).

Some studies suggested that morphology variables and hemodynamic parameters are mutually causal: geometry dictates flow conditions, and flow affects pathobiology, eventually promoting aneurysm formation, and ultimately affecting the vessel shape (Meng et al., 2014).

Moreover, the authors hypothesized that high magnitudes of WSS drive mural cell-mediated destructive remodelling, producing small, thin wall translucent aneurysms, whereas low WSS drives inflammatory cell mediated destructive remodelling, giving rise to giant, thick walled aneurysms.(Meng et al., 2014).

Hemodynamics is as important as morphology in discriminating aneurysm rupture status.(Xiang et al., 2011b)

All 3 models morphological (based on size ratio), hemodynamic (based on WSS and oscillatory shear index), and combined-discriminate intracranial aneurysm rupture status with high AUC values.(Xiang et al., 2011b).

Few studies employed the logistic regression (ML) model to assess the risk of rupture using the oscillatory shear index (OSI), the time averaged wall shear stress (TAWSS), and the size ratio (SR) of the aneurysm(Meng et al., 2014; Xiang et al., 2016)

Review of literature in last decade

The Morphology of Aneurysm

It is believed that morphological factors of IAs have an essential role in the prediction of aneurysm rupture.

When Detmer et al. studied 1931 aneurysms, they discovered that the ruptured aneurysms' aspect ratio (AR), which is the ratio of the maximum perpendicular height to the average neck diameter (calculated as twice the average distance from the neck centroid to the edge of the neck), was higher than that of the unruptured aneurysms.(Detmer et al., 2018)

Liu et al. studied the morphological difference in 96 ruptured and 96 unruptured IAs. They noted that AR in ruptured IAs was (1.8±0.7), whereas it was (1.2±0.5) in unruptured IAs ($p < 0.001$) (Liu et al., 2019).

In their analysis of 79 aneurysms, Huang et al. found that 57 of the ruptured aneurysms showed substantially high AR (p 0.05) in half of them.(Huang et al., 2018)

However, a different case-control study conducted by Mocco et al. on 57 ruptured aneurysms (case) and 197 unruptured aneurysms (control) revealed that AR is not a statistically significant predictor of aneurysm rupture.(Mocco et al., 2018).

Skodvin et al. found that in a case series of 29 ICAs, the median AR before rupture was 1.5 (range, 0.8-4.0), as opposed to 1.9 (range, 0.8-6.7) after rupture ($p = 0.008$).(Skodvin et al., 2017).

Lastly, Zhang et al. discovered that AR is considerably higher in ruptured ICAs ($p = 0.004$) after comparing 20 ruptured and 20 unruptured IAs in a cross-sectional investigation.(A. Can and Du, 2016).

The size ratio (SR) of an aneurysm which is the ratio between maximum aneurysm height and parent artery diameter is another morphological factor that can be a risk factor of aneurysm rupture. This association was clearly demonstrated by Detmer et al. in their study, however Liu et al study .'s indicated that SR had insignificant effect on ruptured IAs.(Liu et al., 2019).

Huang et al. discovered that ruptured aneurysms had significantly high SR (Huang et al., 2018). Mocco et al. also showed that SR has a significant risk of IA rupture (Mocco et al., 2018). Therefore, the majority of earlier studies demonstrated that largerer SR, which equals larger aneurysms, has a higher risk rate of rupture.

Height, which is defined as the maximum perpendicular distance of the dome from the neck plane, showed no statistical significance in the study conducted by Liu et al. (Liu et al., 2019). Huang et al study, however revealed a substantial relationship between height and aneurysm rupture.(Huang et al., 2018).Mocco et al. and Skodvin et al. noted that perpendicular height is an important predictor for the rupture of IAs (Mocco et al., 2018; Skodvin et al., 2017). Zhang et al. also noticed a significant difference in the maximum height of ruptured aneurysms in comparison with unruptured ones (Zhang et al., 2014). As a result, the majority of these studies found a correlation between aneurysm height and the probability of rupture, which might be utilised as a predictor when evaluating specific individuals.

The bottle-neck factor is defined as the ratio between width, which is the largest diameter that is orthogonal to the greatest distance between the neck plane center and any point on the aneurysm dome, and neck diameter. It is another morphological factor that was studied as a risk for IA rupture. Detmer et al. noticed a significant relationship between the bottle-neck factor and the risk of IA rupture(Detmer, Hadad, et al., 2019). Huang et al. also found a statistically significant link between the bottle-neck factor and ruptured aneurysms in another study.(Huang et al., 2018). However, this significant relationship could not be seen in the study by Skodvin et al. (Skodvin et al., 2017).

According to a review article by Ambekar et al., aneurysms containing daughter sacs are more likely to rupture, with a 1.63 hazard ratio.(Ambekar et al., 2016). Concurrent to these results, Skodvin et al. noticed in their case series that aneurysms with one or more than one daughter cyst are more liable for rupture (Skodvin et al., 2017). However, there was no statistically significant difference in the presence of daughter cysts between ruptured and unruptured aneurysms.(Liu et al., 2019).

The presence of the daughter sac was not found to be a statistically significant predictor of aneurysm rupture by Mocco et al.(Mocco et al., 2018).

Other more complicated parameters such as undulation index, aneurysm (inclination) angle, ellipticity index, non-sphericity index, vessel angle, the relationship among aneurysm neck, parent artery and daughter branches, daughter artery ratio and lateral angle ratio, height-to width ratio, bulge location, volume-to-ostium ratio, convexity ratio, isoperimetric ratio have been studied too as the risk of rupture in unruptured aneurysms but are still not well established.

Ellipticity index, non-sphericity index and undulation index are a few parameters used to quantify an aneurysm's irregular shape. In an attempt to identify the morphologic determinants of aneurysm rupture status, Xiang et al, found that non-sphericity index, undulation index, and ellipticity index heavily influenced the discrimination between ruptured and unruptured aneurysms(Xiang et al., 2011b)

Hemodynamic Factors

Computational fluid dynamics: It is a computational technique that makes streamlines (virtual vectors) inside a blood vessel and IA by data analysis from CT or MR angiography or rotational digital subtraction angiography. It is useful for studying fluid dynamics like WSS inside a blood vessel or ICA (Cebral et al., 2015; Sun et al., 2012).

WSS is the tangential and frictional force exerted by blood flow on the blood vessel wall (Longo et al., 2017). It is one of the most studied hemodynamic factors as a risk in the formation, growth, and rupture of IA. Detmer et al. noticed in their study that ruptured IAs have larger maximum wall shear stress (WSSmax), mean WSS (WSSmean), WSS in the aneurysm parent vessel (WSSves), and maximum normalized WSS (MWSSnorm). Interestingly, when normalizing the WSSmean concerning the WSS in the parent artery, it was significantly lower in ruptured aneurysms (Detmer, Chung, et al., 2019).

In another study, Liu et al. found statistically significant differences between ruptured and unruptured aneurysms regarding the ratio between WSS maximum (WSSm) of aneurysm and WSS maximum (WSSm) of parent vessel (pWSSm). However, there was no significant difference regarding the ratio between WSS average (WSSa) of aneurysm and parent vessel WSS average (pWSSa) .

Huang et al. discovered that ruptured aneurysms have larger SAR-TAWSS which is extracted by an equation from the relationship between time-averaged wall shear stress (TAWSS), which is defined as the standard time average of each nodal WSS vector magnitude at the wall across a cardiac cycle (Longo et al., 2017), and aneurysmal surface area (Huang et al., 2018).

Doddasomayajula et al. noted that ruptured aneurysms had more concentrated WSS distributions and lower minimum WSS ($p = 0.003$) than unruptured aneurysms (Doddasomayajula et al., 2017). Kaneko et al. found that the average WSS of the aneurysm was 1.2 Pa, which was lower than that of the parent artery 4.2 Pa (Kaneko et al., 2018). The results of the study conducted by Qiu et al. strongly suggest that both high and low WSS were able to cause a rupture in wide-necked aneurysms (Qiu et al., 2017).

In a meta analysis conducted by Can and Du, there was a positive relationship between high WSS and aneurysm formation and low WSS and aneurysm rupture of bifurcation aneurysms. However, this relationship was negative in side wall aneurysms (Anil Can and Du, 2016). Ruptured aneurysms have a lower minimum WSS than unruptured ones, according to Zhang et al. (Zhang et al., 2014). Accordingly, there is a big controversy whether high or low WSS will influence the formation, growth, and rupture of IAs and more sophisticated studies are needed to analyze this issue. WSS gradient (WSSG) reflects the change in the magnitude of the WSS vector in the flow direction, concerning the streamwise distance (Longo et al., 2017). It is used in unruptured IAs with complex geometries and/or with arising vessels (Longo et al., 2017). It can be thought of as the change in WSS along the length of the blood vessel (Dolan et al., 2013).

Liu et al. didn't find a statistically significant difference in WSSG between ruptured and unruptured aneurysms(Liu et al., 2019). Concomitantly Can and Du in their metaanalysis did not see a significant difference in WSSG between these two groups (Anil Can and Du, 2016).

Oscillatory shear index (OSI) indicates WSS fluctuations magnitude and describes the tangential force oscillation as a function of the cardiac cycle (Longo et al., 2017). OSI measures temporal, rather than spatial variation in the flow direction. According to Detmer et al., ruptured aneurysms had a considerably higher mean OSI and maximum OSI (OSI max) than unruptured aneurysms (OSI mean) (Detmer, Chung, et al., 2019). WSSG between ruptured and unruptured aneurysms was statistically significant, according to Liu et al.(Liu et al., 2019).

Using an equation derived from the link between OSI and aneurysmal surface area, Huang et al. found that ruptured aneurysms have greater SAR-OSI. (Huang et al., 2018). Aneurysms that have ruptured, however, do not exhibit significantly different pooled OSI when compared to aneurysms that have not ruptured, according to Can and Du's meta-analysis of the distribution of OSI. (Anil Can and Du, 2016). The OSI between ruptured and unruptured aneurysms did not significantly differ, in study by Zhang et al.(Zhang et al., 2014).

Low wall shear stress area (LSA) indicates the areas of the aneurysm wall exposed to a WSS value <10% of the mean parent vessel WSS. Liu et al. did not find a statistically significant difference in low wall shear stress area ratio (LSAR normalized by the dome area) between ruptured and unruptured aneurysms (Liu et al., 2019). LSA did not reach a statistically significant difference between ruptured and unruptured aneurysms in the observation of Doddasomayajula et al. (Doddasomayajula et al., 2017).

On the contrary, Qiu et al. found that LSAR was one of the hemodynamic factors predictive of rupture(Qiu et al., 2017) . The meta-analyses conducted by Can and Du showed significantly higher LSA in the ruptured IAs (Anil Can and Du, 2016). Similar to this, Zhang et al. also observed that the ruptured aneurysms had much higher LSA than the unruptured aneurysms.(Zhang et al., 2014).

There are many other hemodynamic factors under study like relative residence time, gradient oscillatory number, aneurysm formation indicator, and shear concentration index.

Hemodynamic stressors may trigger an inflammatory cascade in the wall of the blood vessels, which may influence the thickness of the blood vessel wall and the morphology and thickness of the wall of IA. Besides, these stressors may induce atherosclerotic changes in the wall of the blood vessel and IA.

Most of the studies were done on ruptured aneurysms and further studies are needed on hemodynamics in unruptured aneurysms to assess the risk of rupture.

At clinical practice we routinely encountered a case of subarachnoid hemorrhage with multiple intracranial aneurysms. Predominance of cisternal bleed was noted on the side of a smaller, smooth-walled aneurysm, while the aneurysm on the side opposite to the bleed was larger and irregular in shape. In such situations, there is a felt need for advanced techniques, which can predict the rupture status of aneurysm

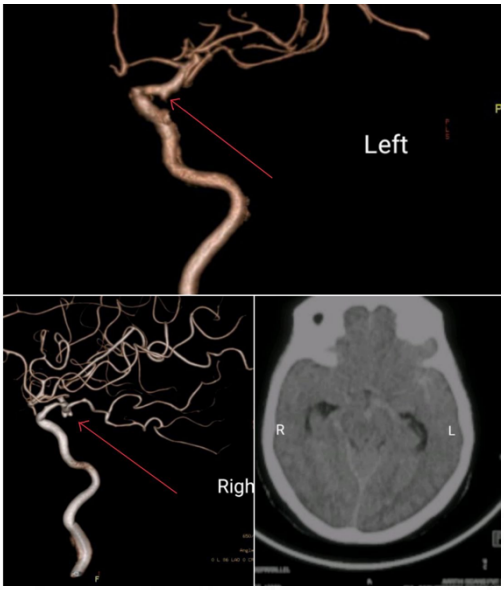

Figure 2.1- SAH in multiple intracranial aneurysms.

Clinical judgement of the rupture status of an aneurysm relies on multiple factors including a proper clinical history and review of the angiographic images. Larger and irregular aneurysms are deemed to have ruptured; but the situation is complicated if there is a mismatch with the amount of cisternal blood(Björkman et al., 2017)

According to a retrospective study, irregular shape was the most important predictor of aneurysm rupture regardless of size, accounting for 18% of ruptured aneurysms that were under 4 mm and 38% that were over 7 mm.(Lindgren et al., 2016)

The aim of current radiological methods is to diagnosis of cerebral aneurysm and no current imaging study helps to predict of aneurysm rupture. So there is always need for some models,which can predict cerebral aneurysm rupture.

As once the aneurysm ruptures, the overall 28-day case fatality rate is 42%(T. Ingall et al., 2000) , and the dependency rate in survivors is ≈50% (Alleyne, 2010).

Despite the minimal risk of rupture, these small aneurysms are being treated because of the concern of catastrophic aneurysmal subarachnoid hemorrhage. However, no treatment comes without risks; the overall mortality rate and morbidity 30 days after treatment in patients without previous hemorrhage are 9.7% and 13.7% in open surgical and endovascular groups, respectively (DO, 2003). As growing aneurysms are at a high rupture risk compared with those with stable size (Malhotra, 2017), estimating the aneurysm rupture potential is worthwhile, especially in small ones.

Possible cause of cerebral aneurysm formation and the role of CFD

The process of aneurysm formation is not fully elucidated, Tanaka et al. proposed that chronic inflammation of the cerebral arteries is due to genetics and molecular biology which is closely associated with the pathogenesis of cerebral aneurysm initiation. Blood flow characteristics were found to affect chronic inflammation of the cerebral arteries, besides smoking, ingesting alcohol, and decreased estrogen levels (Tanaka, 2018)

W. Kaspera et al. found that degenerative lesions caused by hemodynamic stress play an important role in cerebral aneurysms initiation. Animal studies showed that exposure to hemodynamic stress associated with an increased blood flow leads to degenerative changes of the internal elastic lamina and muscularis media of the arterial wall immediately adjacent to the apex of bifurcation and aneurysm formation (Kaspera, 2014)

According to Murayama et al., Image-aided computational fluid dynamics provide a better understanding to identify the mechanism responsible for the formation, growth, and rupture of aneurysms. These techniques facilitate the possible ways to improve the diagnosis and evaluation of patients by including morphological information with already available anatomical data. Also, CFD techniques play a significant role in endovascular treatment planning and endovascular device designing (Murayama et al., 2019)

Importance of good quality mesh generation in Imaging Aided CFD:

Marchandise et al. proposed that to imply CFD simulation techniques in patient-specific geometries robust mesh generation is necessary. The accuracy and efficiency of numerical methods depend upon the quality of mesh created. Researchers have studied the impact of mesh quality in patient-specific geometries. Mesh quality parameters such as aspect ratio, orthogonality, skewness, smoothness, etc indicate whether the mesh is suitable for computation or not. The presence of badly shaped cells makes an unsuitable mesh and increases the local effective spatial discretization error (Marchandise et al., 2012).

Study on the implementation of Image Aided Computation Fluid Dynamics (CFD):

High-resolution image is acquired from imaging techniques such as digital subtraction angiography (DSA) or CT angiography are used to conduct CFD analysis. In CFD analysis of cerebral aneurysms, Murayama et al. considered blood as a Newtonian fluid with specific values of density and viscosity. In flow analysis, the flow field was mostly assumed to be incompressible laminar flow because the Reynolds number (based on vessel diameter and flow speed) was in the range of several hundred. After applying computational preconditions, including assumed blood material properties and boundary conditions, the blood flow was simulated, solving the 'Navier–Stokes' equations(Murayama et al., 2019)

Nanduri, Pino-Romainville, and Celik et al., followed the procedure for patient-specific modelling and characterization of cerebral aneurysms from angiogram images and concluded that flow patterns are independent of the mean flow velocity and viscosity but are highly dependent on the geometry. This finding makes the accurate reconstruction of the geometry more critical (Nanduri et al., 2009)

MATERIALS AND METHODS

CHAPTER 3

MATERIALS AND METHODS

Study group:

100 patient-specific cerebral aneurysms (unruptured, ruptured) were distinguished using computational modelling and computational fluid dynamics (CFD) simulations. Sixteen morphological and nine hemodynamic parameters with Three clinical parameters like Age, Sex and Type of the aneurysm were computed, and their discrete prediction capability was evaluated using traditional statistical techniques, such as hypothesis testing, confusion matrix, and accuracy, among others. After evaluating the most significant parameters from the dataset, selected for predicting rupture status on the machine learning model.

CT angiography images were collected for patients with intracranial Aneurysms treated at SCTIMST (Sree Chitra Tirunal Institute for Medical Sciences & Technology, Trivandrum) Hospital. All images collected were examined for suitability to be included in the study. Hundred consecutive patients with unruptured and ruptured aneurysms datasets with the aneurysm location, age and gender were collected.

Inclusion criteria :

- All patients with Aneurysm, both bled and unbled will be participants of this study.
- Both sexes.

Exclusion criteria :

- patients with SAH secondary to AVM/ trauma
- Patients who underwent coiling of the aneurysm.

FUNDING: THE CURRENT STUDY REPRESENTS THE INTERIM RESULTS OF AN ONGOING PROSPECTIVE STUDY FUNDED BY SCIENCE AND ENGINEERING RESEARCH BOARD, GOVERNMENT OF INDIA, UNDER THE SCIENTIFIC AND USEFUL PROFOUND RESEARCH ADVANCEMENT (SUPRA) SCHEME (GRANT NO. SPR/2020/000298). THE AUTHOR CONFIRMS THAT THE RESEARCH IS AN ORIGINAL WORK UNDERTAKEN BY HIM AT THE SAID INSTITUTE. THE AUTHOR ALSO CONFIRMS THAT THERE ARE NO CONFLICTS OF INTEREST OR DISCLOSURES TO MAKE

Workup plan:

GEOMETRY EXTRACTION

The patient-specific geometry can be extracted with Clinical imaging techniques (CT or MRI) and Computational resources. All collected images were examined for suitability to be included in the study. Only cases whose 3D images were of sufficient quality after accurate segmentation and reconstruction were included as CFD analysis critically depends on accurate 3D geometry. All 100 aneurysms (36 Unruptured and 64 Ruptured)were reconstructed from CTA or DSA using the open-source software called a slicer.

It is extremely important to accurately and effectively analyze the morphological characteristics for modelling patient-specific geometry. Figure 3.1 describes the steps involved in converting medical imaging raw data to geometry extraction.

Medical image segmentation refers to extracting the desired object (organ) from a medical image (2D or 3D), which can be done manually, semi-automatically or fully automatically.

Angiograms are extracted from different imaging techniques like Computerized Tomography (CT), DSA. This medical image data is in the form of 2D planes. Depending on the imaging technique used,enhancements are carried out before segmentation. The segmentation output is in the form of (.STL) file, which can be directly imported into mesh creation software like ICEM CFD and mesh is generated. The patient-specific realistic geometry obtained is used further for CFD studies.

3D reconstruction in surface-triangulation format and isolation of the region of interest (Aneurysm+ adjacent vessels) were performed using open-source software 3D Slicer (SLICER, Harvard University, NIH) and MeshLab (MESHLAB, ISTI - CNR). To allow accurate geometric measurements of both the aneurysm and parent vessel, they were computationally separated at the Aneurysm neck using cutting tools in ANSYS ICEM CFD software (ANSYS, Inc., Canonsburg, PA) and ParaView.

The Aneurysm neck plane was defined as the plane intersecting the location from where the aneurysmal sac pouched outward from the parent vessel. The 3D geometries and simulations were then analyzed to provide various morphologic and hemodynamic parameters using ICEM CFD, ParaView (Sandia National Laboratories, Kitware Inc.) and Pyradiomics (Open-Source Python Package).

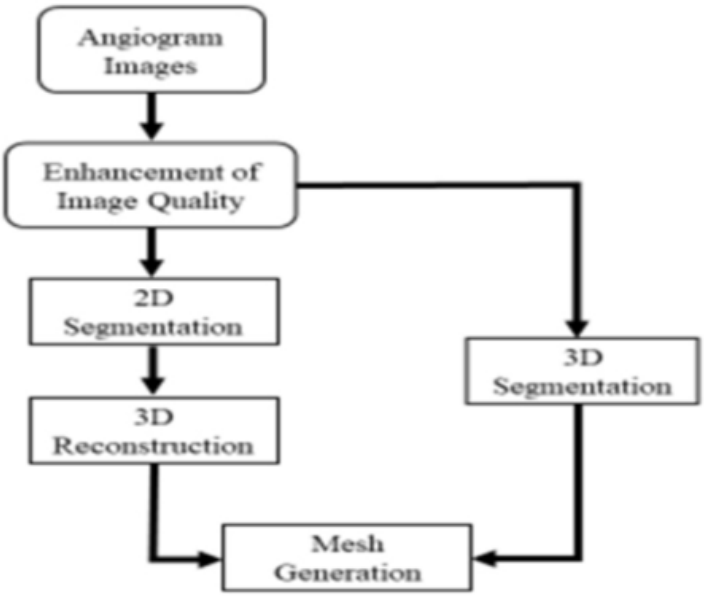

Fig 3.1 - Flow Chart conversion of medical imaging raw data to realistic geometry model.

Morphological Parameters

The aneurysm dome region symbolises the weaker portion of the wall (and a probable site for rupture), and hence is our major region of interest from the medical images. Thirteen morphological parameters were extracted. The illutstration shown below 3.1 is taken from the work done in lab. at IIT Chennai.

Parameter	**Method of Extraction (Tools)**
Dome Height (mm)	Paraview + ICEM CFD
Dome Perpendicular Height (mm)	Paraview + ICEM CFD
Dome Width (mm)	Paraview + ICEM CFD
Neck Diameter (mm)	Paraview + ICEM CFD
Parent Vessel Diameter (mm)	Paraview + ICEM CFD
Inflow Angle (degrees)	ICEM CFD
Surface Area (mm^2)	ICEM CFD
Volume (mm^3)	ICEM CFD
Aspect Ratio	Derived Parameter
Size Ratio	Derived Parameter
BottleNeck Ratio	Derived Parameter
Neck to Parent Vessel Ratio	Derived Parameter
Area to Volume Ratio	Derived Parameter

Table 3.1: Morphological parameters

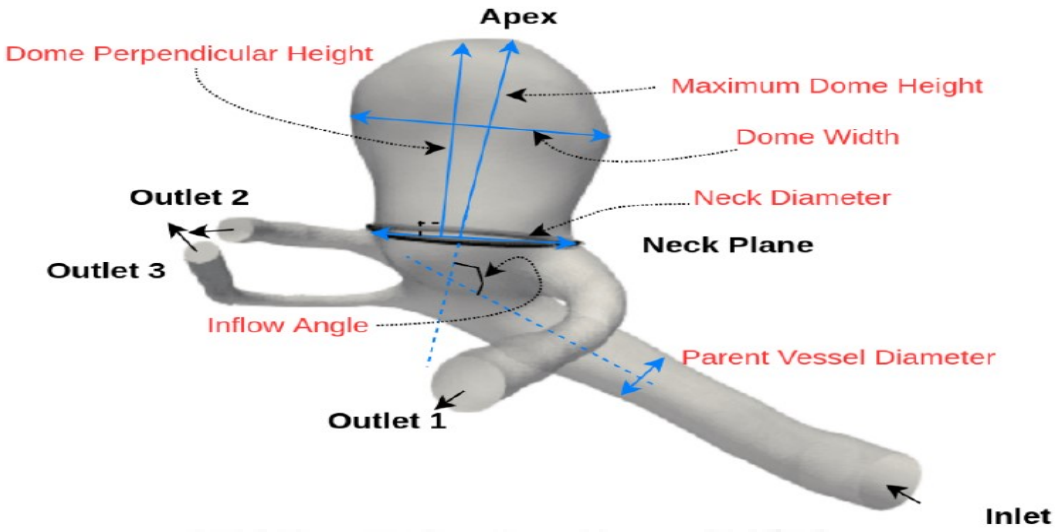

Figure 3.2: Illustration of morphology parameter's definition

The following definitions for the morphological parameters were adapted from the works by Dhar *et al.*(S et al., 2008) and Raghavan *et al.* (Raghavan et al., 2005)

Maximum Dome Height: The Maximum Dome Height refers to the greatest distance between the centroid of the aneurysm neck plane and any point located on the dome of the aneurysm.

Dome Perpendicular Height: The Aneurysm Size, also known as the Maximum Dome Height, is defined as the maximum perpendicular distance between the aneurysm dome and the neck plane. It represents the largest distance from the centroid of the neck plane to any point on the aneurysm dome, indicating the overall size of the aneurysm.

Neck Diameter: Aneurysm Neck Diameter is defined as the average diameter of the neck plane of the aneurysm. In cases where the neck plane has an irregular shape, this parameter is computed by averaging multiple measurements taken at different points along the neck plane.

Dome Width: The Dome Width is defined as the maximum diameter of the aneurysm dome when measured in a plane that is perpendicular to the neck plane. If there is no bulge or protrusion beyond the neck plane, then the Dome Width is equal to the Neck Width.

Parent vessel diameter: Parent Vessel Diameter is defined as the average diameter of the artery comprising the parent vessel of the aneurysm. This measurement represents the average size of the artery from which the aneurysm originates. Based on the above-described parameters, the following ratio-based parameters were computed:

Aspect Ratio (AR): The Aneurysm Aspect Ratio is defined as the ratio between the perpendicular height of the aneurysm dome and the width of its neck. This parameter has been widely used in various morphological studies and serves as a measure of the elongation of the aneurysm. It provides valuable information about the shape and geometry of the aneurysm, helping to characterize its elongation or roundness.

Dome Neck Ratio: It is defined as the ratio of maximum dome height to neck width.

Bottleneck Ratio: The Bottleneck Ratio is defined as the ratio between the dome width and the neck diameter of an aneurysm. This ratio can range from 1 to infinity. In cases where the ratio is significantly greater than 1, it indicates an obstruction to the flow of blood into the aneurysmal sac. This abnormality in the bottleneck ratio suggests abnormal hemodynamics, potentially implying a higher risk of complications or rupture.

Neck Width to Parent Vessel Width Ratio: The ratio of the neck width of the aneurysm to the parent vessel diameter. A higher ratio suggests a relatively narrower neck compared to the parent vessel diameter, which can result in altered blood flow patterns and potentially affect the risk of rupture or other hemodynamic abnormalities within the aneurysm.

Further, the Aneurysm Dome Surface Area and Aneurysm Dome Volume were computed using Ansys ICEM CFD – where the dome represents the part of the aneurysm above the neck plane.

Hemodynamic Parameters

In the study, unstructured meshes consisting of tetrahedral components were generated for each 3D model of the aneurysm using ANSYS ICEM CFD software. Near-wall prism layers were included in the mesh to ensure accurate resolution of the boundary layer. The numerical solution of the unsteady, incompressible Navier-Stokes equations was performed using OpenFOAM, a software package developed by CFD Direct Ltd. The simulations were conducted under pulsatile flow conditions to mimic the pulsating nature of blood flow. The aneurysm wall was assumed to be rigid, and the following boundary conditions were applied: no-slip conditions at the wall and zero pressure at the outlet. The blood was mathematically represented as a Newtonian fluid with a density of 1060 kg/m3 and a viscosity of 0.0035 Ns/m2. To ensure numerical stability, three pulsatile cycles were simulated. The output scalar and vector fields were analyzed using the data from the last cycle for each scenario. This analysis allowed for the examination of various flow parameters and characteristics within the aneurysm.

The following definitions for the hemodynamic parameters were adapted from the work by Sheikh *et al.* (2020)

Wall Shear Stress (WSS) : The Wall Shear Stress (WSS) refers to the tangential stress exerted by the frictional force of blood flow on the inner wall of a blood vessel. In the case of pulsatile flow, the time-averaged WSS (TAWSS) was calculated by integrating the magnitude of WSS at each node over the entire cardiac cycle. The formula for TAWSS is:

$$TAWSS = \frac{1}{T}\int_0^T |wss_i|\, dt$$

Where *wssi* represents the instantaneous shear stress vector, and *T* represents the duration of one cardiac cycle. *TAWSS* provides an evaluation of the average WSS over the entire cardiac cycle and is typically measured in Pascals (Pa). Normal values for TAWSS range from 1.5 to 10 Pa.

Parameter	**Method of Extraction (Tools)**
Mean Wall Shear Stress (meanWSS)	OpenFOAM
Mean pressure (Pmean)	OpenFOAM
Wall shear stress gradient (WSSG)	OpenFOAM
Time Averaged Wall Shear Stress (TAWSS)	OpenFOAM
Gradient oscillatory number (GON)	OpenFOAM
Relative residence time (RRT)	OpenFOAM
Oscillatory Shear Index (OSI)	OpenFOAM

Table 3.2: Hemodynamic parameters

The calculation is based on the accurate time-averaged magnitude of the shear stress vector at each point on the vessel wall. The *meanWSS*, on the other hand, refers to the averaged WSS (already time-averaged) over the dome area, which is the entire luminal surface of the aneurysm sac. It provides an average measure of WSS within the dome area. *WSSG*, or Wall Shear Stress Gradient, measures the change in WSS magnitude in the direction of flow. It is calculated by taking the spatial derivative of WSS with respect to the streamwise distance. The time-averaged

WSSG is then further averaged over the dome area to provide an average measure of the WSS gradient within the aneurysm. *Pmean* is the mean pressure across the dome.

Oscillatory Shear Index (OSI): The Oscillatory Shear Index (OSI) is a nondimensional parameter that describes the extent of oscillation in the flow path during a pulse flow calculated as the directional change of Wall Shear Stress (WSS) throughout the cardiac cycle.

The formula for OSI is as follows:

$$OSI = \frac{1}{2}\left\{1 - \frac{\left|\int_0^T wss_i dt\right|}{\int_0^T |wss_i|\, dt}\right\}$$

Here, *wssi* represents the shear stress vector, and *T* represents the duration of one cardiac cycle. The numerator of the equation computes the absolute integral of the shear stress vector over the cardiac cycle, while the denominator calculates the integral of the absolute magnitude of the shear stress vector over the same duration. It ranges from 0 to 0.5, where 0 represents steady flow and 0.5 indicates intense oscillation. OSI is commonly used to assess the disturbance of the flow field in the aneurysm wall. The OSI is then averaged over the dome area, which encompasses the entire luminal surface of the aneurysm sac. This provides an average measure of the disturbance in the flow field within the aneurysm.

Relative residence time (RRT): RRT is an important hemodynamic parameter used to characterize the distribution of blood flow near the vortex within the aneurysm and quantify the residence time of blood cells circulating in proximity to the aneurysm wall. It serves as a measure of disturbed flow. RRT is calculated using the time-averaged Wall Shear Stress (WSS) vector magnitude and the Oscillatory Shear Index (OSI). The formula for RRT is as follows:

$$RRT = \frac{1}{(1 - 2 \times OSI) \times WSS} = \frac{1}{\frac{1}{T}\left|\int_0^T WSS_i dt\right|}$$

RRT has the capability to quantify and differentiate between regions of the aneurysm wall that are thin or thick. The variations in RRT values across different wall regions provide insights into the disturbed flow patterns and potentially help identify areas of higher risk within the aneurysm.

Gradient oscillatory number (GON): GON is a hemodynamic indicator used to quantify the distortion of tangential forces exerted by blood flow on the vascular wall in the context of cerebral aneurysm initiation. It operates under pulsatile flow conditions and ranges from 0 to 1. GON is a non-dimensional parameter that reflects the degree of temporal fluctuations in the spatial Wall Shear Stress Gradient (WSSG) vector within one cardiac cycle. The formula for GON is as follows:

$$GON = 1 - \frac{\left|\int_0^T G dt\right|}{\int_0^T |G| dt}$$

G is the spatial WSS gradient vector, and *T* is the duration of one cardiac cycle. GON provides a measure of the different flow pattern conditions experienced by the vascular wall over a complete cardiac cycle.

Supervised learnings

Supervised learning is the types of machine learning in which machines are trained using well "labelled" training data, and on basis of that data, machines predict the output. Supervised learning can be separated into two types of problems when data mining—classification and regression:

Classification uses an algorithm to accurately assign test data into specific categories. It recognizes specific entities within the dataset and attempts to draw some conclusions on how those entities should be labelled or defined. Common classification algorithms are linear classifiers, support vector machines (SVM), decision trees, k-nearest neighbour, and random forest, which are described in more detail below.

Regression is used to understand the relationship between dependent and independent variables. It is commonly used to make projections, such as for sales revenue for a given business. Linear regression, logistical regression, and polynomial regression are popular regression algorithms.

The machine learning classification is a two-step process: the learning and prediction steps. The model is developed based on given training data in the learning step. In the prediction step, the model predicts the response to given data.

Decision Tree Algorithm

The Decision Tree algorithm comes under the family of supervised ML algorithms. The decision tree algorithm is quite efficient in regression and classification problems. Using a Decision Tree is to create a training model that can predict the class or value of the target variable by constructing simple decision trees with the most crucial parameter at the top (training data).

In a Decision tree, there are two nodes: the Decision Node and Leaf Node. Decision nodes are used to make decisions and have multiple branches, whereas Leaf nodes are the output of those decisions and do not contain any further branches.(Decision Tree Algorithm in Machine Learning - Javatpoint, n.d.)

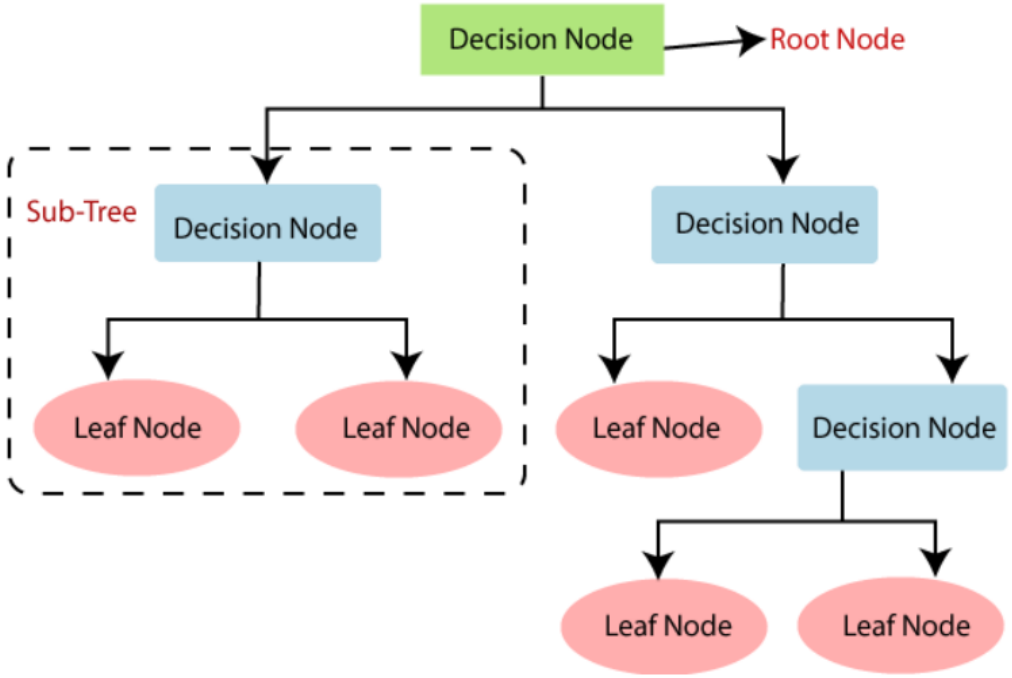

Fig 3.3- Decision Tree Algorithm

In Decision Trees, class labels are predicted by starting from the tree root. We compare the values of the root attribute with the record's attribute. We take the branch corresponding to that value and then shift it to the next node based on the comparison.

Support Vector Machine

Support Vector Machine or SVM is a very popular method in Supervised Learning algorithms, which can be used for Classification and Regression problems.

The goal of the SVM algorithm is to produce the best line or decision boundary that can be segregated in the n-dimensional space into different classes so that a new data point fits well into one of the class clusters. This best line boundary that separates out data best is called the hyperplane. SVM chooses the extreme points/vectors that help in creating the hyperplane. These severe cases are called support vectors, and so this algorithm is called the Support Vector Machine. The diagram below shows the two different categories that are classified using a decision boundary or hyperplane:(Support Vector Machine (SVM) Algorithm - Javatpoint, n.d.)

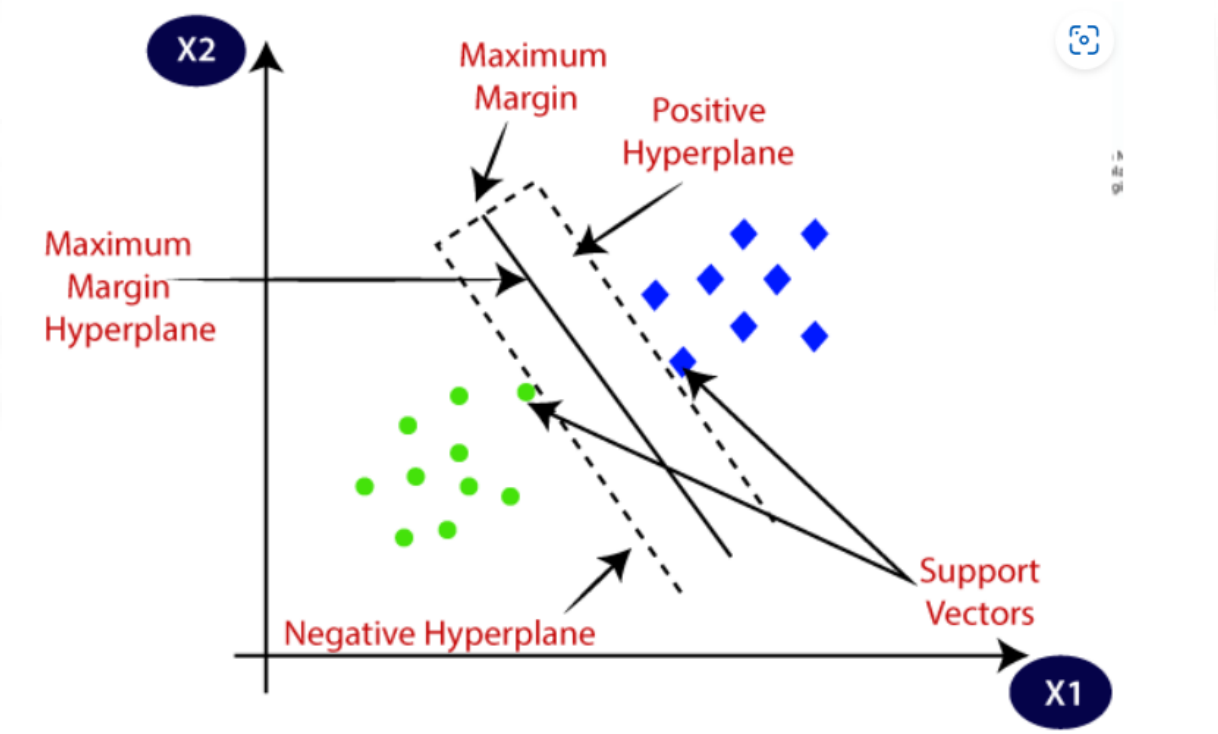

Fig 3.4- Support Vector Machine Classifier

K-Nearest Neighbours

K-Nearest Neighbour is one of the simplest Machine Learning algorithms belonging to the family of Supervised Learning techniques. The k-NN algorithm can be used for classification and regression. K-NN algorithm assumes the similarity between the new case/data and available cases and puts the new case into the most similar category to the available ones. K-NN algorithm stores all the available data and classifies a unique data point based on the similarity. When new data appears, it can be easily classified into a good suite category using the K- NN algorithm.

K-NN is a non-parametric algorithm, which means it does not make any assumptions on underlying data. It is also called a lazy learner algorithm because it does not learn from the training set immediately instead, it stores the dataset, and at the time of classification, it acts on the dataset. KNN algorithm at the training phase stores the dataset, and when it gets new data, it classifies that data into a much similar category to the latest data. (*GeeksforGeeks*, 2017)

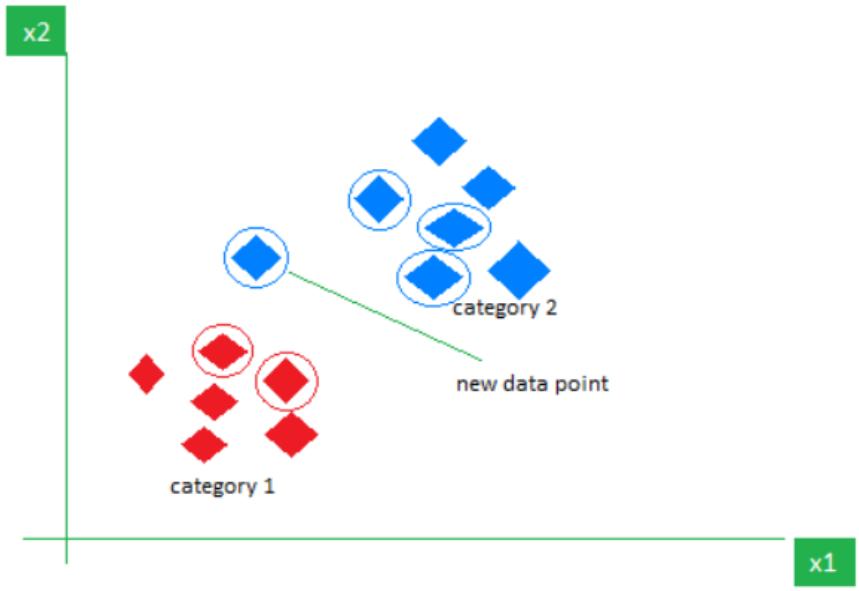

Fig 3.5- K-Nearest Neighbor

Random Forest Algorithm

Random Forest is a popular machine learning algorithm that belongs to the supervised learning technique. It can be used for both Classification and Regression problems in ML. It is based on the concept of ensemble learning, which combines multiple classifiers to solve a complex problem and improve the model's performance.

As the name suggests, "Random Forest classifier contains several decision trees on various subsets of the given dataset and takes the average to improve the predictive accuracy of that dataset." Instead of relying on one decision tree, the random forest takes the prediction from each tree and, based on the majority votes of predictions, predicts the final output.

Since the random forest combines multiple trees to predict the class of the dataset, some decision trees may predict the correct output while others may not. But together, all the trees predict the correct output. Therefore, below are two assumptions for a better Random Forest classifier:

• There should be some actual values in the feature variable of the dataset so that the classifier can predict accurate results rather than a guessed result.
• The predictions from each tree must have very low correlations.

One of the most essential features of the Random Forest Algorithm is that it can handle the data set containing continuous variables and categorical variables. The more significant number of trees in the forest leads to higher accuracy and prevents the problem of overfitting.(Machine Learning Random Forest Algorithm - Javatpoint, n.d.)

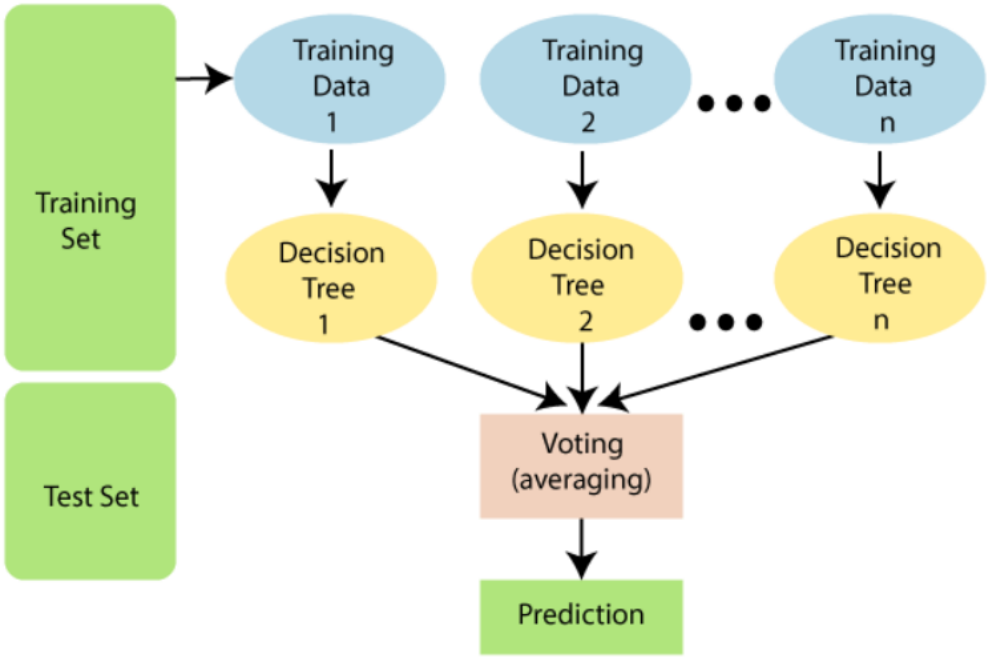

Fig 3.6- Random Forest Algorithm

XGBoost

XGBoost is a decision-tree-based ensemble Machine Learning algorithm that uses a gradient boosting framework. For small-to-medium structured/tabular data, decision tree-based algorithms are considered performant algorithms.

XGBoost is an implementation of Gradient Boosted decision trees. In this algorithm, decision trees are created in sequential form. Weights play a vital role in XGBoost. Weights are assigned to all the independent variables, which are then fed into the decision tree, which predicts results. The weight of variables predicted wrong by the tree increases, and these variables are then fed to the second decision tree. These individual classifiers/predictors then ensemble to give a strong and more precise model. It can work on regression, classification, ranking, and user-defined prediction problems.

The term "gradient boosting" comes from "boosting" or improving a single weak model by combining it with several other weak models to generate a collectively robust model. Gradient boosting is an extension of boosting where the process of additively developing weak models is formalized as a gradient descent algorithm over an objective function. Gradient boosting sets targeted outcomes for the next model to minimize errors. Targeted outcomes for each case are based on the gradient of the error (hence the name gradient boosting) for the prediction.

XGBoost is scalable and highly accurate Implementation of gradient boosting pushes the limits of computing power for boosted tree algorithms, built mainly for energizing machine learning model performance and computational speed. With XGBoost, trees are built in parallel. It follows a level-wise strategy, scanning across gradient values and using these partial sums to evaluate the quality of splits at every possible split in the training set(*NVIDIA Data Science Glossary*, n.d.)

Unsupervised Learning

Unsupervised learning is a type of machine learning in which models are trained using unlabeled dataset and are allowed to act on that data without any supervision.

k-Means Algorithm

The k-means algorithm is a widely used unsupervised learning method for clustering data. Given a dataset $\mathbf{X} = \{x_1,...,x_n\}$ in a d-dimensional Euclidean space R^d, the goal is to find c cluster centers $A = \{a_1,...,a_c\}$.

The algorithm iteratively minimizes the k-means objective function $J(z,A) = \sum_{i=1}^{n} \sum_{k=1}^{c} z_{ik} |x_i - a_k|^2$, where $z = [z_{ik}]_{n \times c}$ is a binary variable indicating whether data point x_i belongs to cluster k. The k-means algorithm updates the cluster centers and memberships based on the following equations Sinaga and Yang (2020):

Cluster center update: $$a_k = \frac{\sum_{i=1}^{n} z_{ik} x_i}{\sum_{i=1}^{n} z_{ik}}$$

Membership update: $$z_{ik} = \begin{cases} 1 & \text{if } |xi - ak|^2 = \min 1 \leq k \leq c \; |xi - ak|2 \\ 0, & \text{otherwise} \end{cases}$$

Here, $|x_i - a_k|$ represents the Euclidean distance between data point x_i and cluster center a_k. By iteratively updating the cluster centers and memberships, the k-means algorithm aims to find the optimal cluster assignments that minimize the objective function, leading to meaningful clustering of the data. The number of clusters k is decided by the elbow method which is discussed in the further sections. This algorithm works best when we have globular clusters.

The k-means technique has a number of advantages, including its ease of use, scalability, and efficacy in clustering huge datasets. It can also be used to find natural groupings or patterns in data without prior understanding of the underlying structure. However, this method has noteworthy issues, including sensitivity to initial cluster centres and a tendency to converge to a local minimum rather than the global minimum.

DBSCAN Algorithm

DBSCAN (Density-Based Spatial Clustering of Applications with Noise) is a density-based clustering algorithm that overcomes some limitations of the k-means algorithm. Unlike k-means, DBSCAN does not rely on the mean value of cluster elements, but instead identifies clusters based on the density of data points. DBSCAN operates under the assumption that clusters are dense regions in space separated by areas of lower density. It defines clusters as groups of data points that are closely packed together, while regions with lower density are considered noise or outliers.

One advantage of DBSCAN is its ability to handle clusters of arbitrary shape and size. It is not restricted to spherical clusters like k-means. Additionally, DBSCAN does not require prior knowledge of the number of clusters (k) in the data, as it automatically detects clusters based on density. DBSCAN works by defining a neighborhood around each data point and identifying core points, which have a sufficient number of neighboring points within a specified distance. It then expands clusters by connecting core points to their neighboring points, forming dense regions. Data points that do not belong to any cluster are considered outliers or noise.

By utilizing the concept of density, DBSCAN provides robust and flexible clustering, making it particularly useful for datasets with irregular or unknown cluster structures, and eliminating the need to predefine the number of clusters.

For DBSCAN algorithm, there are two parameters ϵ and *minPts* Nagesh Singh Chauhan (2022, https://www.kdnuggets.com/2020/04/dbscan-clusteringalgorithm-machine-learning.html)

1. ϵ - maximum distance between points for them to be considered neighbors
2. *minPts* - The minimum number of points (a threshold) to form a dense region (cluster)

The basic algorithmic steps are as follows:

1. Select an arbitrary point from the dataset.
2. Check if there are at least *minPts* points within a distance of ϵ from the selected point. If there are, mark all these points as part of the same cluster.
3. Expand the cluster by recursively repeating the neighborhood computation for each neighboring point, considering only points that have not been assigned to a cluster yet.
4. Continue this process until no more points can be added to the cluster.
5. Select another unvisited point from the dataset and repeat the process until all points have been visited.
6. Any points that were not assigned to a cluster are considered outliers or noise.

ϵ and *minPts* are chosen and derived from the number of dimensions (D) and the distance plot. The distance plot is a plot of distance to the k = *minPts* − 1 nearest neighbor ordered from the largest to the smallest value. Usually, we take *minPts* >= D+1 and ϵ as the value which provides the elbow in the distance plot for clustering . In our study, the parameters obtained were ϵ=0.5 and *minPts* = 8.

Spectral Clustering

Spectral clustering is a popular algorithm used for clustering data points based on the similarity of their features. It utilizes spectral graph theory to transform the data into a lower-dimensional space and perform clustering in that space. There is no assumption about the shape/form of the clusters. The purpose of spectral clustering is to group together data that is linked but not necessarily compact or clustered inside convex bounds.

The basic operations of the algorithm are as follows Ng *et al.* (Ng et al., 2001)

The given set of points S in R^l can be clustered into k subsets using the following steps:

1. Form the affinity matrix $A \in R^{n \times n}$, where $A_{ij} = \exp\left(-\frac{|s_i - s_j|^2}{2\sigma^2}\right)$ if $i \neq j$, and $A_{ii} = 0$. This matrix measures the similarity between pairs of points based on their Euclidean distance.

2. Define the diagonal matrix D such that the (i,i)-element is the sum of the i-th row of matrix A. Construct the matrix $L = D^{-1/2}AD^{-1/2}$.

3. Find the k largest eigenvectors $x_1,x_2,...,x_k$ of matrix L (chosen to be orthogonal to each other in the case of repeated eigenvalues). Stack these eigenvectors in columns to form the matrix $X = [x_1,x_2,...,x_k] \in R^{n \times k}$.

4. Create matrix Y by re-normalizing each row of matrix X to have unit length,

i.e., $Yij = Xij/\text{qP}j\ Xij2$.

5. Treat each row of matrix Y as a point in R^k and cluster them into k clusters using an algorithm such as k-means or any other distortion-minimizing algorithm.

6. Assign the original point s_i to cluster j if and only if row i of matrix Y was assigned to cluster j.

By following these steps, the spectral clustering algorithm leverages the affinity matrix, the graph Laplacian, and the spectral embedding to effectively cluster the data points into subsets based on their similarities in the lower-dimensional space.

Unlike k-means, the spectral clustering algorithm can identify clusters which are not enclosed within convex boundaries and also identifies groups among connected datapoints. All the 3 algorithms mentioned above, have been used for cluster analysis on our data making use of python libraries.

RESULTS AND ANALYSIS

CHAPTER -4

RESULTS and ANALYSIS

The number of females are slightly more in the study compared to males. Unruptured aneurysms have an equal split with respect to gender, while there are more females with ruptured aneurysms. According to the data, most of the aneurysms were found in adults between the ages of 40 to 70 and the average age was 52 years 3.3. All of the 8 patients who had smoking habits were having ruptured aneurysms. 25 out of 35 patients who were diagnosed with hypertension had ruptured aneurysms.

Rupture Status

	Ruptured	Unruptured	Total
Sex Female/Male	26/38	18/18	44/56
Total	64	36	100

Table 4.1: Demographic information based on gender

The blood flow to brain and locations of aneurysms are illustrated in fig 4.2. In our data, ACOM aneurysms were more in number (35+) followed by MCA, PCOM and other types.

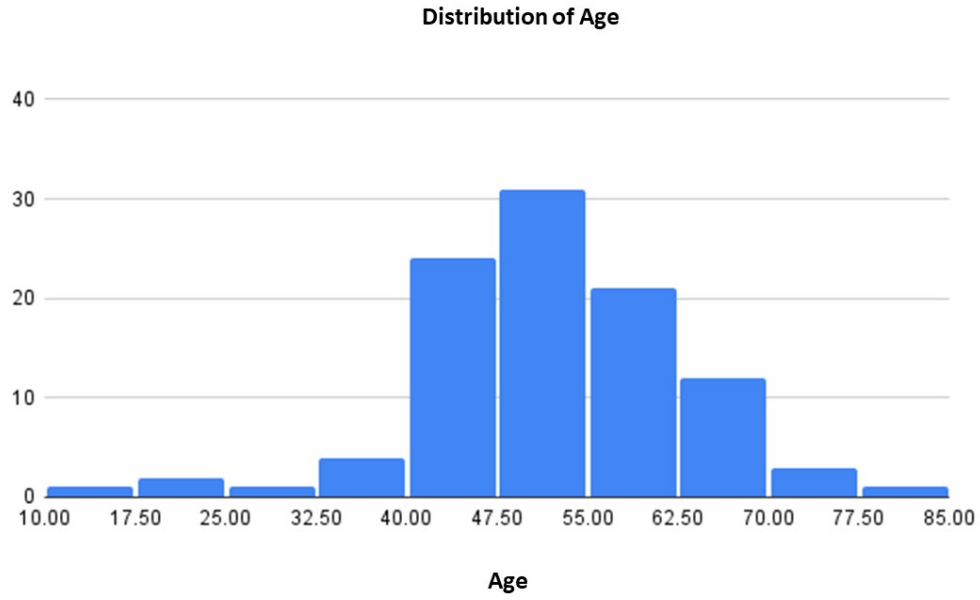

Figure 4.1: Distribution of patient age

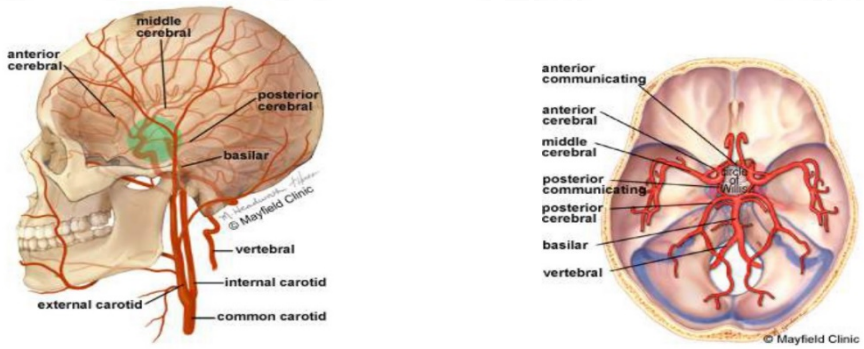

(a) Blood supply to the brain

(b) Circle of Willis

Figure 4.2: Brain blood supply schematics illustration. The frontal view provides a depiction of the arteries that supply blood to the brain, while the top view illustrates the Circle of Willis and the branching pattern of arteries. Figure taken from Jain and Siegen (Jain, 2016)

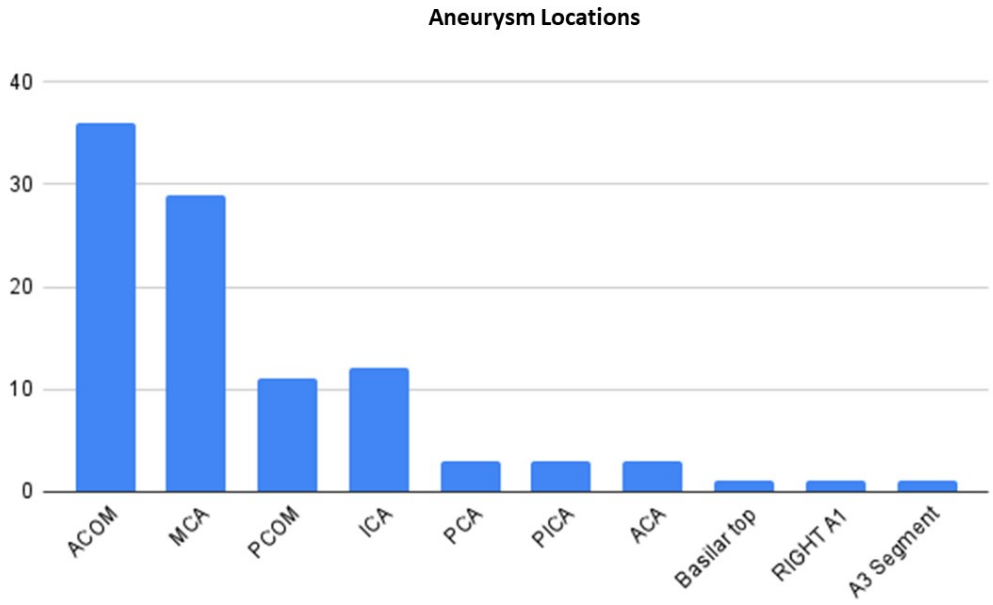

Figure 4.3: Distribution of aneurysm locations

Statistical Analysis

Descriptive Statistics

13 morphological parameters were extracted from for all the 100 cases. Aneurysm volume was the attribute with the highest range and variance, closely followed by area. A total of 87 samples were available for calculation of 7 hemodynamic parameters during the study, of which 60 were ruptured. Wall Shear Stress parameters were having the highest range and variances.

Hypothesis Testing

The Mann-Whitney U-test is used to compare the differences between two independent groups when the dependent variable is ordinal or continuous but not normally distributed. It is often viewed as the nonparametric equivalent of the Students T-test, but Mann–Whitney U-Test is used with nonparametric data (typically, ordinal data) whereas the Student's t-Test for Independent Samples is used with data that meet the assumptions associated with parametric distributions.

The Morphological Parameters

	N	Minimum	Maximum	Mean	Std. Deviation
Dome Height	100	0.86	22.33	6.3264	4.82242
Dome Perpendicular Height	100	0.75	21.13	5.5377	4.40643
Dome Width	100	1.66	28.05	7.5726	5.41668
Neck Diameter	100	1.66	21.78	6.2407	3.66305
Parent Vessel Diameter	100	0.85	10.06	3.0966	1.26282
Inflow Angle	100	79	176	138.4069	21.68978
Surface Area	100	4.03	6113.31	362.0303	768.19536
Volume	100	5.3	14875.9	677.02	1983.67151
Aspect Ratio	100	0.29	2.54	0.8398	0.33863
Size Ratio	100	0.3	2.65	0.9563	0.35612
BottleNeck Ratio	100	0.66	2.02	1.1603	0.24962
Neck/ParentVessel Ratio	100	0.57	4.55	2.0068	0.79588
Area/Volume Ratio	100	0.25	7.56	1.573	1.24008

Table 4.2: Analysis on morphological parameters

Hemodynamic Parameters

	N	Minimum	Maximum	Mean	Std. Deviation
MeanWSS	87	0.15	81.85	5.4942	11.80468
TAWSS	87	0.19	85.95	6.4025	12.68596
OSI	87	0	0.09	0.0216	0.01645
RRT	87	0.02	11.12	1.4313	2.1898
WSSG	87	0.02	26.11	1.7182	3.82386
GON	87.	0.01.	30.	1.5989.	3.92629
Pmean	87.	0.03	5.46	0.5969.	0.8434

Table 4.3: Analysis on hemodynamic parameters

Mann–Whitney U-Test is used when we have data that deviate from acceptable distribution patterns, or for when there are noticeable differences in the number of subjects in the two comparative groups MacFarland *et al.* The major assumptions for carrying out a Mann-Whitney test are that the two groups must be independent and that the dependent variable is ordinal or numerical (continuous) (Bilker and Wang, 1996)

Let $X_1,...,X_n$ be an i.i.d. sample from X, and $Y_1,...,Y_m$ an i.i.d. sample from Y , and both samples independent of each other. The corresponding MannWhitney U statistic is defined as:

$$U = \sum_{i=1}^{n} \sum_{j=1}^{m} S(X_i, Y_j),$$

with

$$S(X,Y) = \begin{cases} 1, & \text{if } X > Y \\ \frac{1}{2}, & \text{if } X = Y \\ 0, & \text{if } X < Y \end{cases}$$

This U statistic is then compared to standard tables and the significance values are found. From the histogram plots of all the variables, most of them were evidently not following a normal distribution, and there sample sizes are different ($n1 = 64, n2 = 36$). Hence we can proceed to use the Mann-Whitney U-test. In this study, our null hypothesis states that there is no correlation between rupture status and input parameters. Unequal variances were assumed. The tests were performed using the IBM SPSS Statistics software.

A p-value of less than 0.05 indicates that the difference of medians of the parameters for ruptured and unruptured aneurysms are statistically significant. Hence we can conclude that morphological parameters like Dome Height, Neck Diameter, Parent Vessel Diameter, Inflow Angle, Surface Area, Volume and Aspect Ratio are significant for the analysis. Hemodynamic parameters exhibited less significant differences in ruptured and unruptured aneurysms, with the most significant parameter being RRT followerd by GON, MeanWSS and OSI.

Mann Whitney U Test - Morphology

	Ruptured (n = 64)		Unruptured (n = 36)		
	Mean	Std.Dev	Mean	Std.Dev	Significance (pvalue)
Dome Height	6.1068	4.74226	6.7062	5.00093	0.05
Dome Perp. Height	5.1903	4.19025	6.1386	4.75631	0.133
Dome Width	7.3302	5.30284	7.9919	5.65736	0.157
Neck Diameter	6.1434	3.71534	6.4092	3.61516	0.044
Parent Vessel Dia	3.0348	1.40798	3.2034	0.9706	0.026
Inflow Angle	0.8104	0.35862	0.8905	0.29882	0.042
Surface Area	0.9455	0.37872	0.975	0.31737	0.047
Volume	1.1442	0.25072	1.1883	0.24861	0.038
Aspect Ratio	2.041	0.75348	1.9476	0.87195	0.048
Size Ratio	140.1428	23.37412	135.4512	18.39945	0.205
BottleNeck Ratio	308.5371	805.01962	454.5591	700.89092	0.126
Neck/ParentVessel	583.6314	2063.82952	838.557	1853.14971	0.219
Area Volume Ratio	1.5793	0.99354	1.5621	1.59499	0.12

Table 4.4: Significance test on morphology parameters

Mann Whitney U Test – Hemodynamics

	Ruptured (n = 64)		Unruptured (n = 36)		
	Mean	Std.Dev	Mean	Std.Dev	Significance (pvalue)
MeanWSS	4.8703	10.07377	6.5665	14.41993	0.061
TAWSS	5.8526	11.25714	7.3477	14.97525	0.103
OSI	0.0209	0.01682	0.0228	0.01599	0.059
RRT	1.5039	2.09622	1.3064	2.37132	0.048
WSSG	1.6857	3.32968	1.7742	4.60939	0.087
GON	2.4593	17.51619	0.1201	0.07489	0.053
PMean	0.5366	0.71118	0.7005	1.03674	0.098

Table 4.5: Significance test on hemodynamic parameters

Correlation of Parameters

Pearson's Linear Correlation Coefficient is defined as

$$r = \frac{\sum (x_i - \bar{x})(y_i - \bar{y})}{\sqrt{\sum (x_i - \bar{x})^2 \sum (y_i - \bar{y})^2}}$$

where $\bar{x}$ = mean of the values of the x-variable $\bar{y}$ = mean of the values of the y-variable x_i = values of the x-variable in a sample y_i = values of the y-variable in a sample r = correlation coefficient

From the correlation plots 4.4, we can clearly see that there are highly linearly correlated parameters in the dataset. Dome shape charecteristics like height, perpendicular height and width are highly correlated. Similarly, volume and area are inevitably interusable, All the derived parameters were correlating with Aspect Ratio. Among the hemodynamic parameters, all the Wall Shear Stress parameters were found to be highly linked. OSI and RRT were also correlated linearly

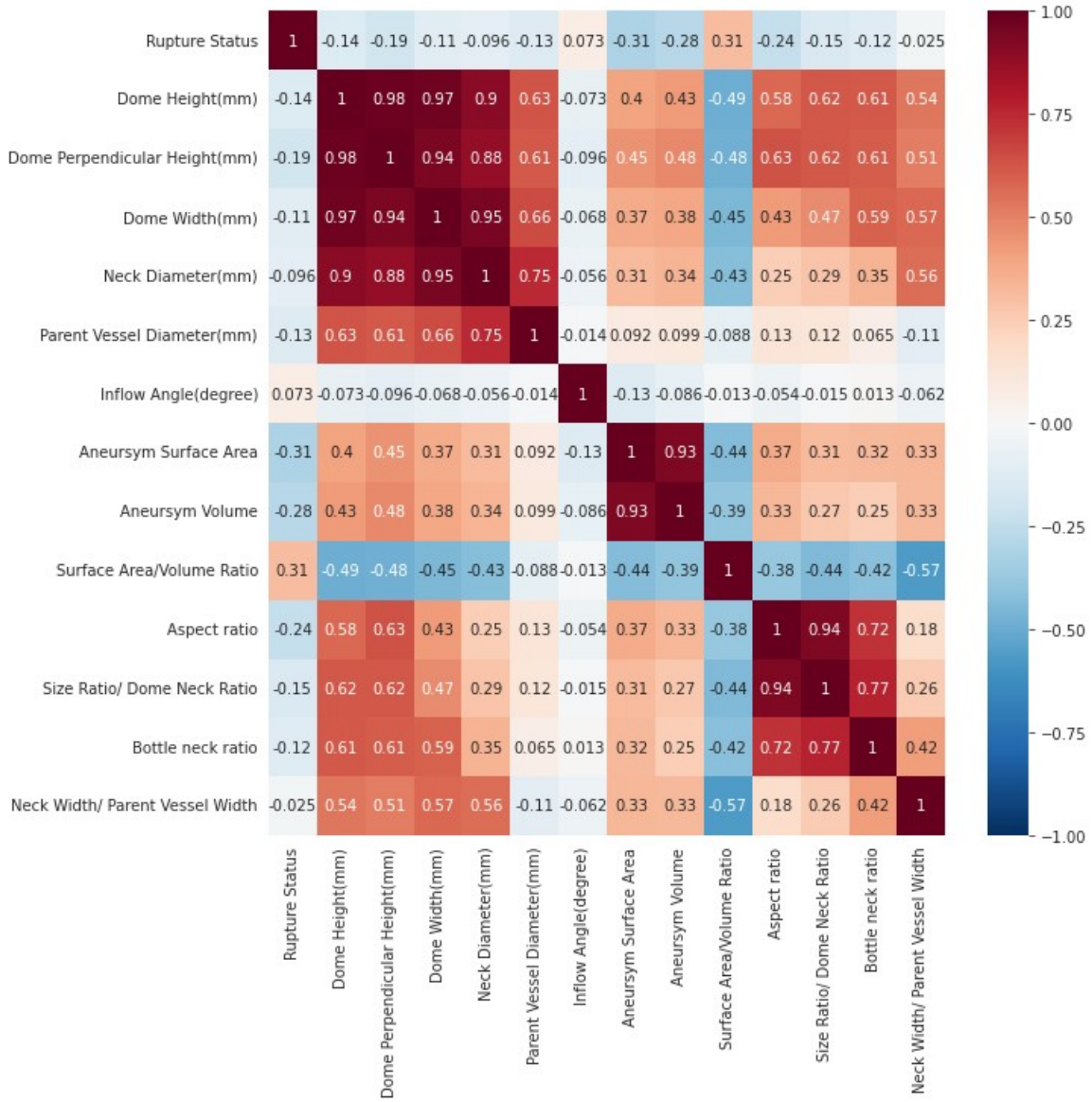

Figure 4.4: Linear Correlation of morphological parameter

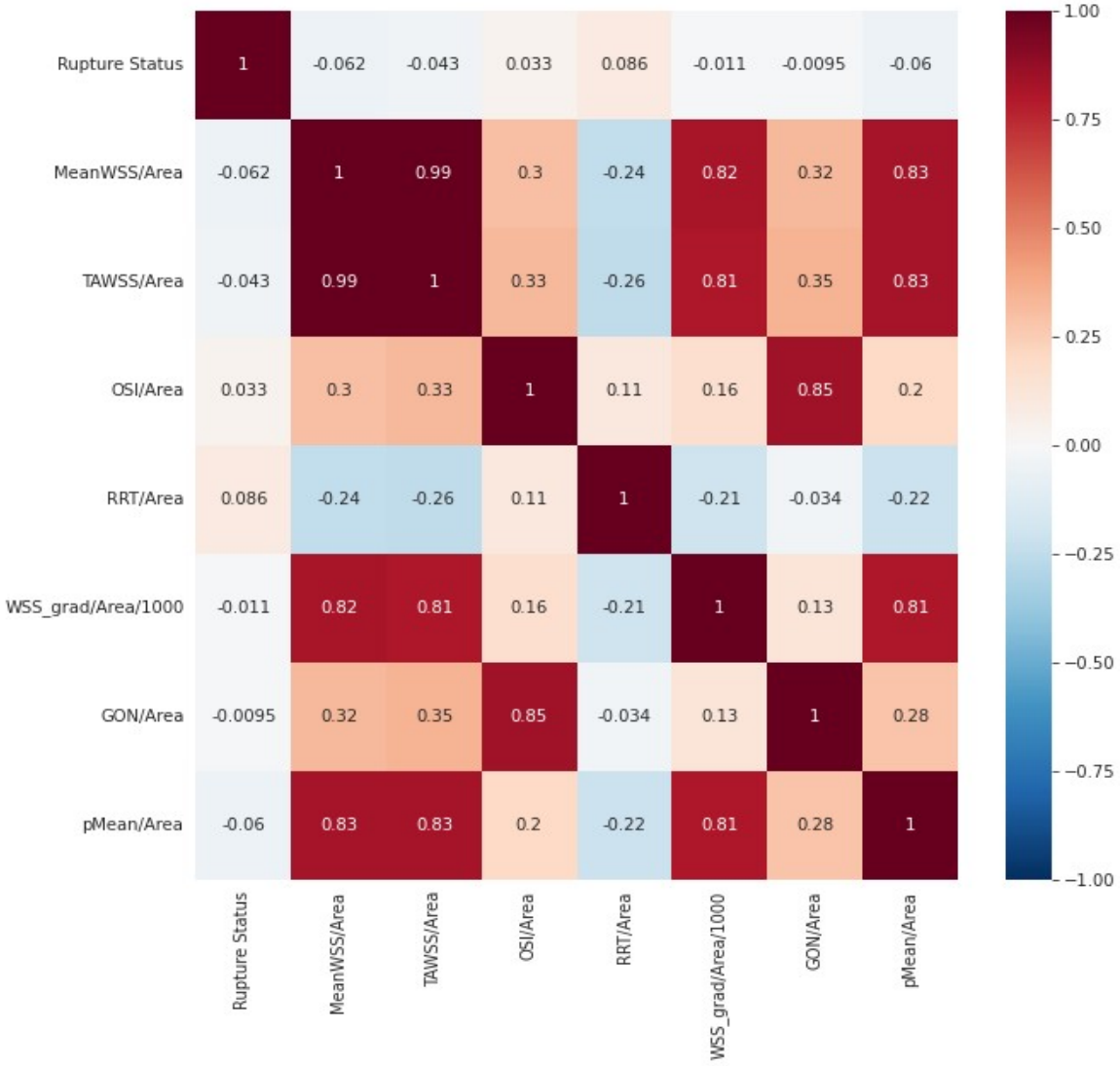

Figure 4.5: Linear Correlation of hemodynamic parameters

MACHINE LEARNING APPROACH (supervised machine learning algorithms)

The process involved conducting ANOVA f tests to identify significant features and utilizing the Variance Inflation Factor to eliminate correlated parameters among those significant features. Subsequently, machine learning models such as logistic regression, Random Forest, XG Boost, Support Vector Machine, Decision Tree, K Nearest Neighbor and artifical neural networks were trained using the selected parameters to develop the optimal model.

The Machine learning classification model is being used since our model output is in the form of ruptured or unruptured (binary).

ANOVA f tests

Analysis of variance (ANOVA) uses F-tests to statistically assess the equality of means when you have three or more groups

The F-statistic is simply a ratio of two variances. Variances are a measure of dispersion, or how far the data are scattered from the mean. Larger values represent greater dispersion.

Variance is the square of the standard deviation. For us humans, standard deviations are easier to understand than variances because they're in the same units as the data rather than squared units. However, many analyses actually use variances in the calculations.(Editor, n.d.).Despite being a ratio of variances, We can use F-tests in a wide variety of situations. Unsurprisingly, the F-test can assess the equality of variances. However, by changing the variances that are included in the ratio, the F-test becomes a very flexible test.And can use F-statistics and F-tests to test the overall significance for a regression model, to compare the fits of different models, to test specific regression terms, and to test the equality of means.

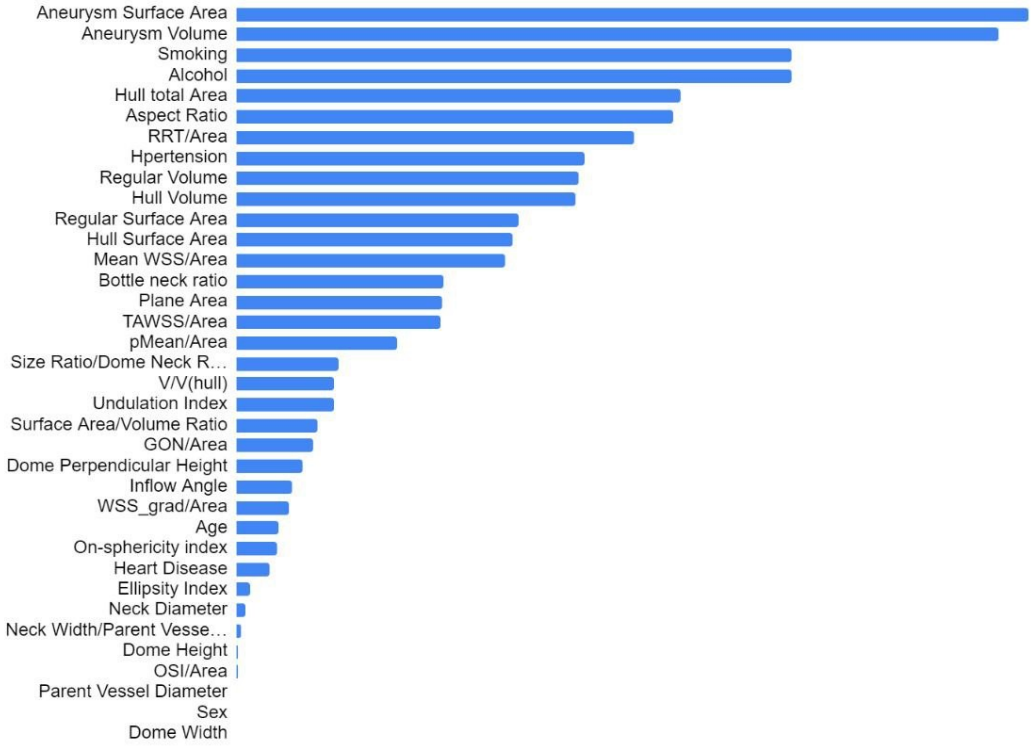

Fig 4.6 – ANOVA f- Test

From Fig 4.6 we understand that our ML dataset is highly imbalanced with multicollinearity . Imbalanced data refers to datasets where the target class has an uneven distribution of observations. For instance, one class label has a very high number of observations, and the other has a very low. In our case, we have a very high number of ruptured geometries and fewer unruptured geometries. And To make a robust ML model, it is beneficial to have a large and balanced dataset with minimal multicollinearity.

That multicollinearity detected by **variance inflation factors** (*VIF*)

The inclusion of all parameters leads to redundancy in modeling and interpretation of datasets. Hence we chose one parameter among a set of highly correlating group. This is achieved by comparison of their statistical significance, where the most significant parameter is selected for data analysis.

A variance inflation factor (VIF) is a measure of the amount of multicollinearity in regression analysis. Multicollinearity exists when there is a correlation between multiple independent variables in a multiple regression model. This can adversely affect the regression results. Thus, the variance inflation factor can estimate how much the variance of a regression coefficient is inflated due to multicollinearity(*Investopedia*, n.d.)

Removing multicollinearity by using only selected parameters and keeping Variation inflation Factor under 3 for both morphological and hemodynamic properties.

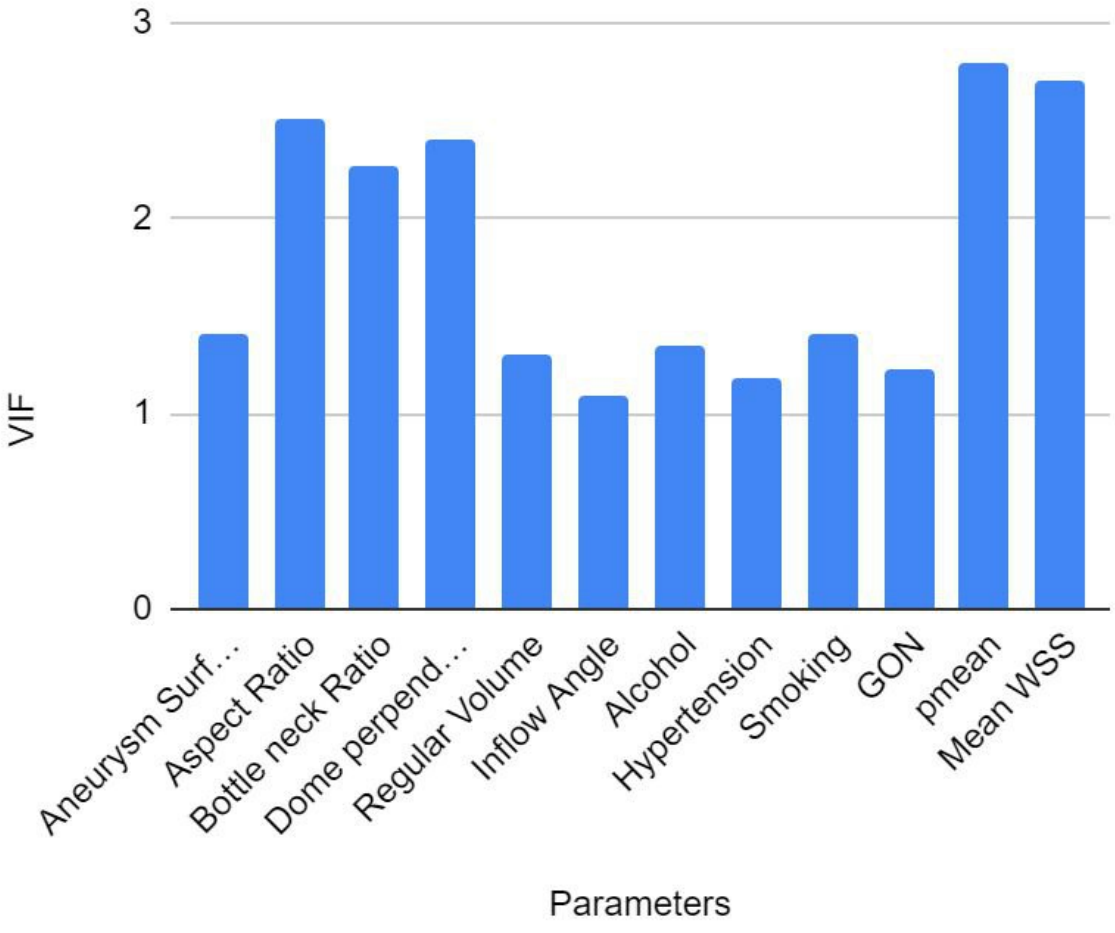

Fig- 4.7 VIF for both morphological and hemodynamic factor under 3

Principal component analysis (PCA) involves a mathematical procedure that transforms a number of (possibly) correlated variables into a (smaller) number of uncorrelated variables. It reduces the dimensionality of the data set and identifies a new meaningful underlying variable.

So we have use principal component analysis performed on Morphologic parameters and hemodynamic parameters so 16 components are enough to capture the whole variance for both.

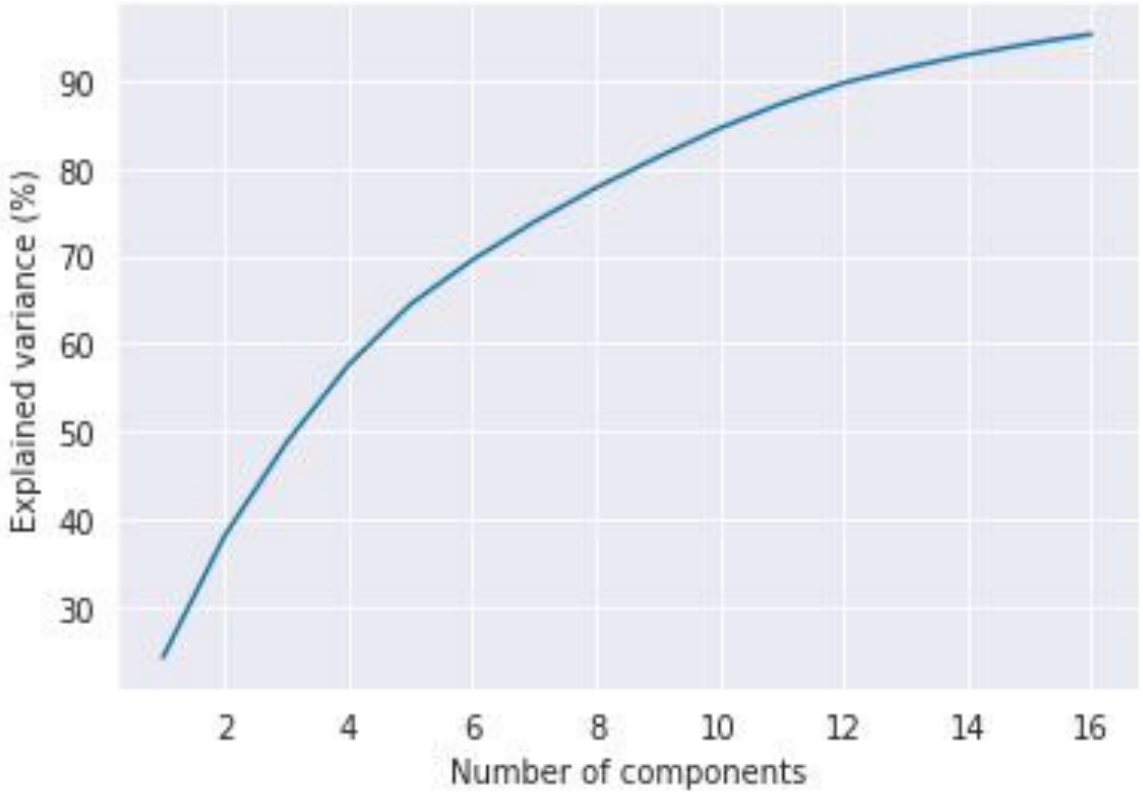

Fig 4.8 - Principal component analysis

Artificial Neural Networks (ANN)

This algorithms based on brain function and are used to model complicated patterns and forecast issues. The Artificial Neural Network (ANN) is a deep learning method that arose from the concept of the human brain Biological Neural Networks. The development of ANN was the result of an attempt to replicate the workings of the human brain. The workings of ANN are extremely similar to those of biological neural networks, although they are not identical. (Kalita, 2022)

ANN algorithm accepts only numeric and structured data.

An Artificial Neural Network (ANN) is a computational model inspired by the human brain's neural structure. It consists of interconnected nodes (neurons) organized into layers. Information flows through these nodes, and the network adjusts the connection strengths (weights) during training to learn from data, enabling it to recognize patterns, make predictions, and solve various tasks in machine learning and artificial intelligence.

There are three layers in the network architecture: the input layer, the hidden layer (more than one), and the output layer. Because of the numerous layers are sometimes referred to as the MLP (Multi-Layer Perceptron)

It is possible to think of the hidden layer as a "distillation layer," which extracts some of the most relevant patterns from the inputs and sends them on to the next layer for further analysis. It accelerates and improves the efficiency of the network by recognizing just the most important information from the inputs and discarding the redundant information.

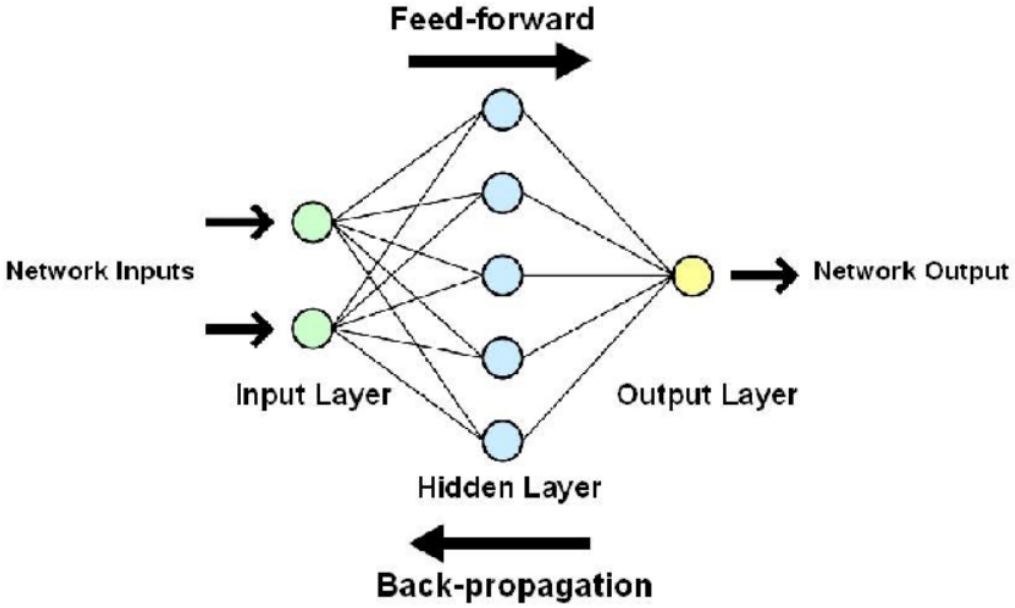

Fig 4.9- Artificial Neural Network (ANN)

We trained our ANN model with 12 parametrs by keeping Variation inflation Factor under 3 for both morphological and hemodynamic properties to get single output

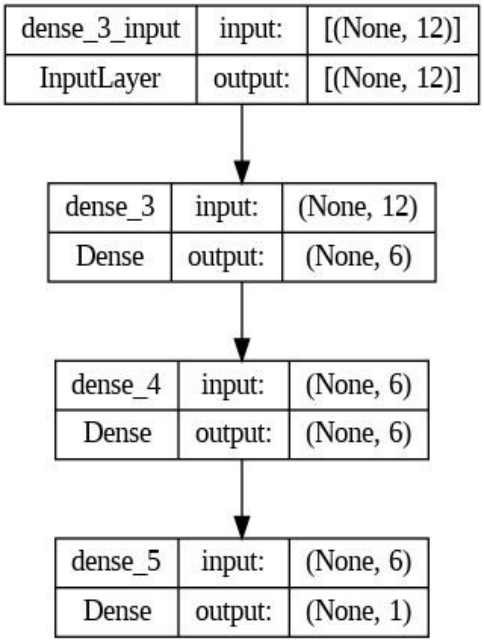

Fig 4.10- Layers of Artificial Neural Network model in sequential.

Results of supervised machine learning algorithms

Accuracy Score- The accuracy score tells the ratio of the predictions correctly predicted over the total sample size.

In a classification problem involving only two classes, the accuracy score is defined as follows:

Accuracy Score = (True Positive Samples + True Negative Samples) / Total Number of Samples Given for Prediction

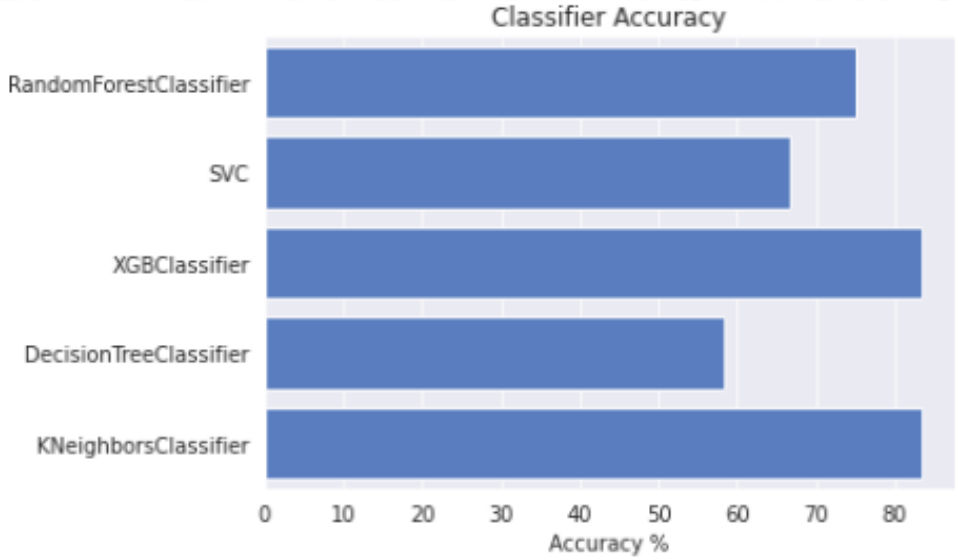

Fig 4.11- Average accuracy by machine learning algorithms after removing multicollinearity for morphological data

Morphological data gives us the maximum accuracy of around 82 % in XGB classifier and K Neighbors classifier.

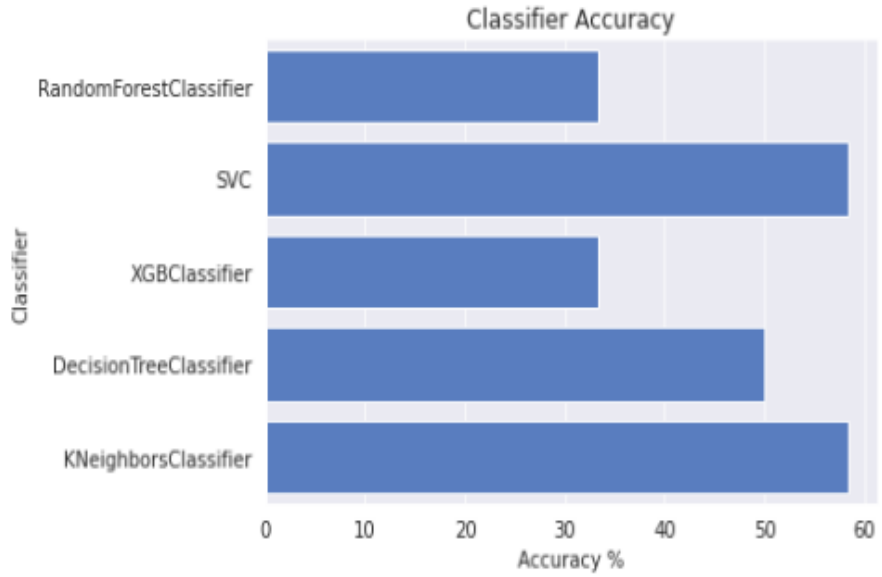

Fig 4.12- Average accuracy by machine learning algorithms after removing multicollinearity for hemodynamic data

Hemodynamics data gives us the maximum accuracy of around 60 % in Support Vector Machine and K Neighbors classifier.

When both morphological and hemodynamics parameters was used combinely the results are described with help of 3 methods

Method 1 gives the results when model is trained using all parameters and showed ANN model giving maximum accuracy of around 75 %.

Medhod 2 with Uncorrelated parameters(VIF),shows highest accuracy of around 80% for ANN model and logistic regression.

Method 3 with Principal Component Analysis shows accuracy of more than 70% for ANN model and logistic regression models

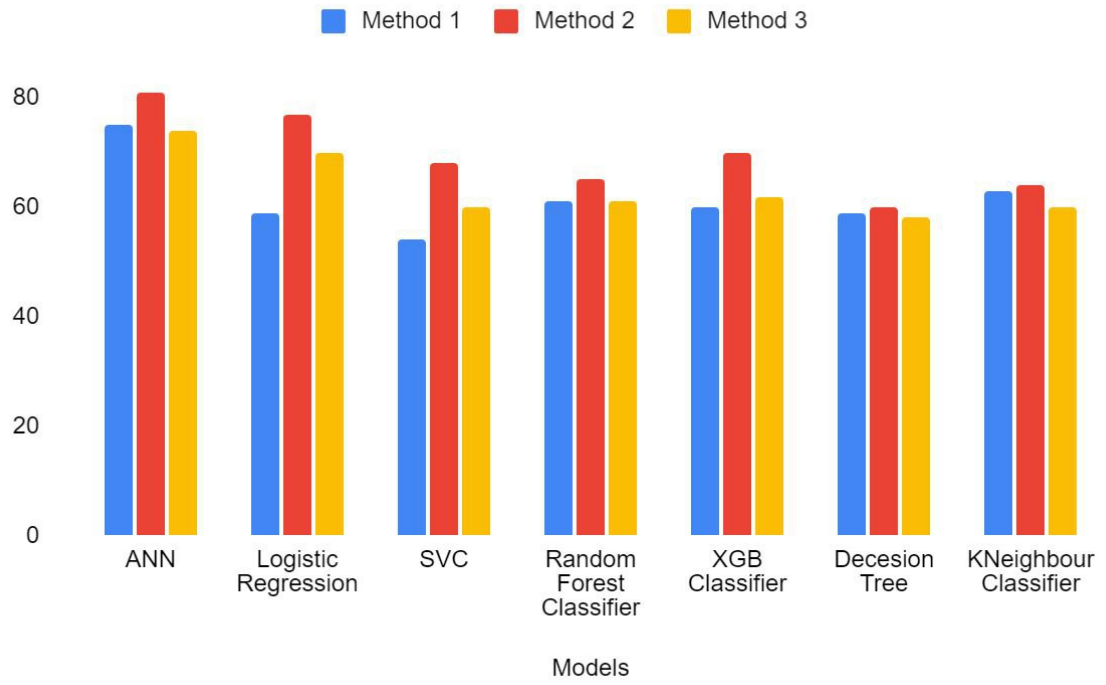

Fig4.13- Performance of the models,

Method 1- Trained using all parameters, Method 2-Uncorrelated parameters(VIF),Method 3 – Principal Component Analysis.

So we can conclude that ANN model followed by Logistic regression proved to be effective in predicting the rupture status.

Unsupervised learning algorithms

Selection of Parameters

As we discussed in Supervised learning algorithms the inclusion of all parameters leads to redundancy in modeling and interpretation of clusters. Hence we chose one parameter among a set of highly correlating group.

This is achieved by comparison of their statistical significance, where the most significant parameter is selected for clustering analysis.

Morhphological	Hemodynamic
Parent Vessel Diamter	RRT
Aneurysm Volume	GON
Inflow Angle	OSI
Neck Diameter	MeanWSS
Aspect Ratio	
Dome Height	

Table 4.6: Selected parameters for clustering based on correlation and statistical significance

Results

All the three algorithms (K-Means,DBSCAN and Spectral Clustering) were producing similar clustering results. The robustness or efficiency of each algorithm is discussed in the next section using silhouette coefficient comparison. The results from the spectral algorithm which gave the most efficient grouping are discussed in this section.

The Python programming language (version 3.9.7; Python Software Foundation, Wilmington, Del; https://www.python.org/) and its libraries, Pandas (version 1.3.4; https://pandas.pydata.org/), NumPy (version 1.20.3; https://www. numpy.org/), scikit-learn (version 1.0.2; https://scikit-learn.org/stable/), and matplotlib (version 3.4.3; https://matplotlib.org/), were used for all data processing. The programming code was executed in Jupyter Notebook (version 5.2.2; https://jupyter.org/) using a computer with general performance (AMD Ryzen 7 5800H central processing unit with 3.50 GHz, 16 cores and 16

GB of RAM). The final dataset consisted of the parameters mentioned in the above section (6 morphological and 4 hemodynamic). Normalization was done using the min-max scaling method before applying the algorithms.

Clustering Morphological Data

The elbow method is a technique used to determine the optimal number of clusters, denoted as K, in a clustering algorithm. It is commonly applied in situations where the number of clusters is not known beforehand. The elbow method involves calculating the inertia for different values of K and plotting it against the number of clusters. Inertia measures the compactness of the clusters by computing the sum of squared distances between each data point and its centroid within a cluster. A lower inertia indicates that the data points within each cluster are closer to their respective centroids.

When using the elbow method, the plot of inertia versus K typically shows a decreasing trend as K increases. This is because increasing the number of clusters allows for more precise fitting of the data. However, there is a point where the decrease in inertia becomes less significant with each additional cluster. This point is referred to as the "elbow" of the curve. We can see that the elbow formation occurs at $K = 3$ after which there is not much appreciable decrease in inertia 3.6. Hence we infer that 3 groups of aneurysms are forming based on the morphological parameters.

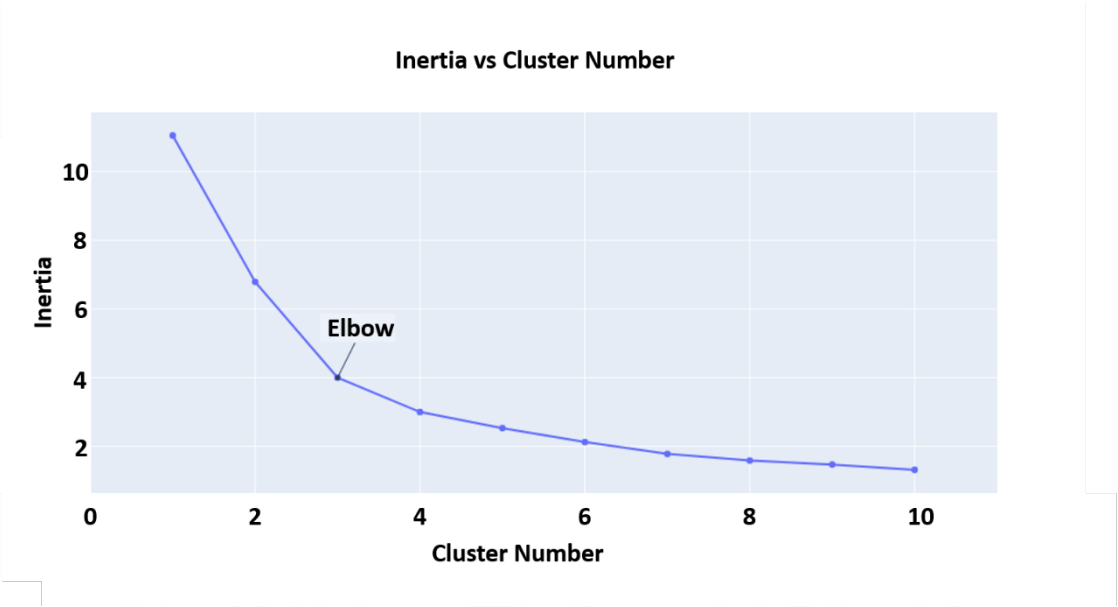

Fig4.14- Optimal number of clusters using elbow method.

Figure 4.15 represents the cluster formation by using a spider plot. The lines of colour blue, red and green are representing clusters 0,1 and 2 respectively. 47 aneurysms were grouped in cluster 0 followed by 45 in cluster 2 and 8 in cluster1

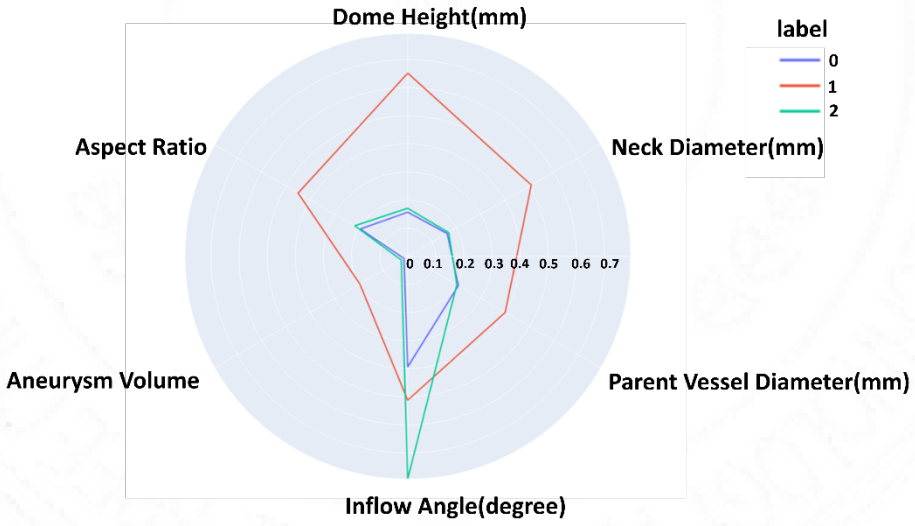

Fig 4.15: Spider plot of mean values in cluster. The values toward the circumference represents relatively larger values.

1. The split of the clusters with respect to rupture status is shown in figure 4.16

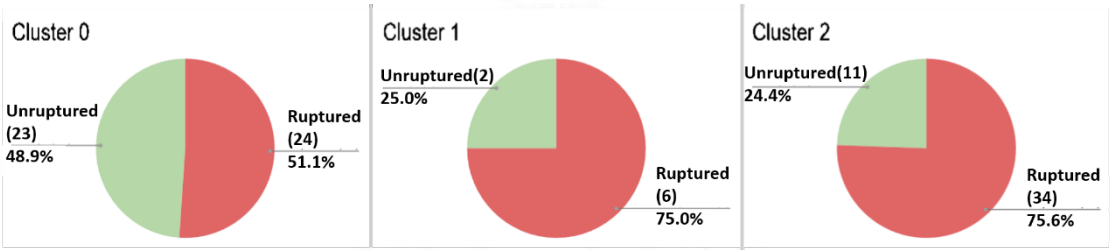

Figure 4.16 Rupture status distribution of aneurysms in each cluster

Cluster 2 contains the highest proportion of ruptured aneurysms. The samples in that cluster are morphologically small aneurysms with a high inflow anlge. Most of the abnormally large aneurysms belong to cluster 1 which also has a high proportion of rupture. Almost equal split of unruptured and ruptured cases were observed in cluster 0 which contained normal sized samples with relatively low inflow angle. The summary of results are shown in table 4.7

Cluster	Dome Height	Parent vessel diameter	Aneurysm volume	Neck diameter	Inflow angle	Aspect Ratio	Rupture Status
2	4.64561	2.78931	136.84704	5.20256	156.16093	0.73447	**High**
1	17.56010	6.51681	2131.95067	16.36049	139.89449	1.37105	**High**
0	5.75932	2.90381	896.88968	5.66268	117.39788	0.97382	**Inconclusive**

Table 4.7: Mean values of parameters in each cluster and association with rupture status

Clustering Hemodynamic Data

Hemodynamic parameters also led to formation of 3 clusters 4.17. Figure 4.18 represents the cluster formation by using a spider plot. The lines of colour blue, red and green are representing clusters 0,1 and 2 respectively. 63 aneurysms were grouped in cluster 1 followed by 21 in cluster 0 and 3 in cluster 2. The split of the clusters with respect to rupture status is shown in figure 4.19

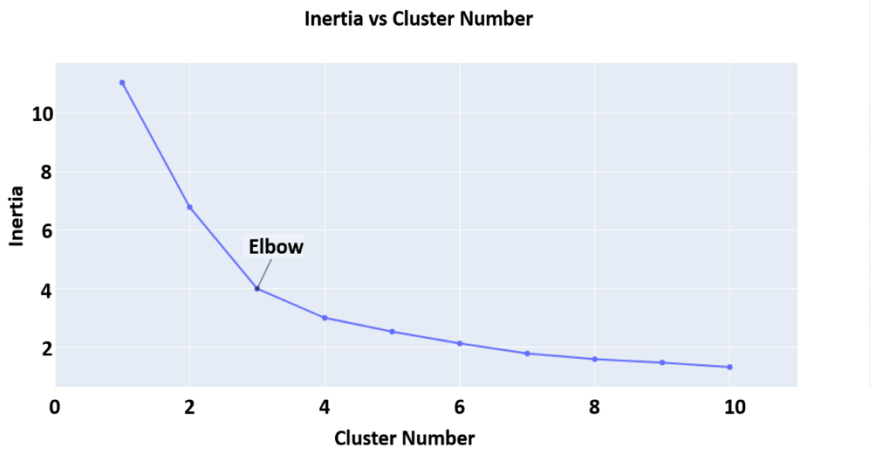

Figure 4.17: Optimal number of clusters using elbow method

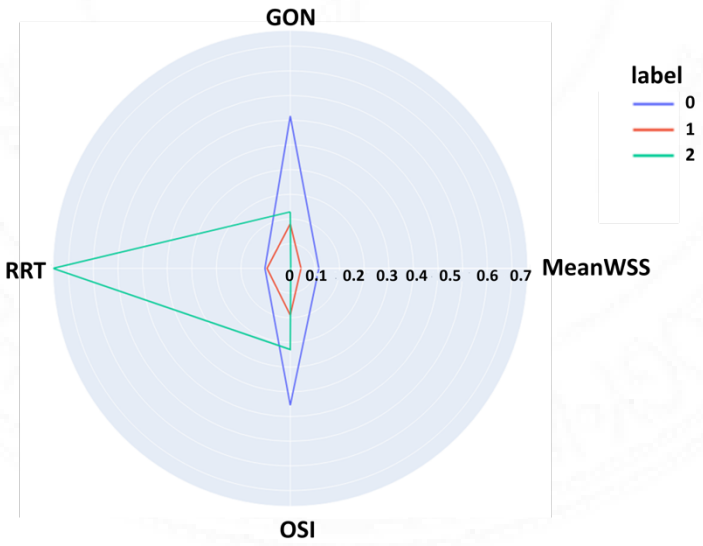

Figure 4.18: Spider plot of mean values in cluster. The values toward the circumference represents relatively larger values

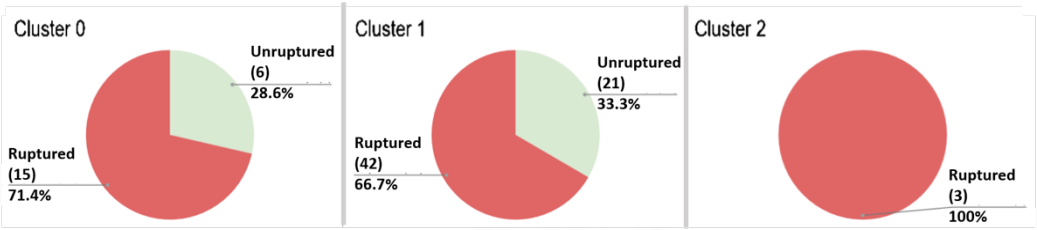

Figure 4.19: Rupture status distribution of aneurysms in each cluster

The hemodynamic data is highly class imbalanced as we only have 27 unruptured samples with 60 ruptured ones. The vast majority (78%) of unruptured aneurysms were grouped in cluster 1 which had low values of all the four hemodynamic parameters. Cluster 2 contained 3 aneurysms with abnormally high RRT and correspondingly low values of Wall Shear Stress, and all of them were ruptured. The samples in cluster 0 had high values of OSI and GON parameters and most of them were ruptured. The summary of results are shown in Table 4.8

Cluster	GON	MeanWSS	OSI	RRT	Rupture Status
2	0.08333	0.29533	0.02366	10.71633	High
0	0.20095	9.63540	0.03927	1.16262	Moderately High
1	0.06858	3.70863	0.01407	1.06695	Inconclusive

Table 4.8: Mean values of parameters in each cluster and association with rupture status

Cluster Validation and Inferences

Silhouette Score

The efficiency of clustering algorithms can be validated by a metric called Silhouette Score which checks for the separataion between different clusters and the density of points within a cluster Shahapure and Nicholas (Shahapure and Nicholas, 2020). Scikit-learn's silhouette score function computes the mean silhouette coefficient of all samples. The silhouette coefficient is calculated by taking into account the mean intracluster distance a and the mean nearest-cluster distance *b* for each data point. The silhouette coefficient (*s*) for a sample is given by

$$s = (b - a)/\max(a,b)$$

In Figure 4.20 a clustering representation in a two-dimensional space is shown Madeira and Jacob (Madeira and Jacob, 2022). The interpretation of the silhouette scores in this context is as follows:

1. A silhouette score close to +1 indicates that the data point is appropriately assigned to its cluster, suggesting a good clustering result.

2. A silhouette score close to 0 suggests that the data point could potentially belong to multiple clusters or that its assignment is ambiguous.

3. A silhouette score close to -1 indicates that the data point is likely assigned to the wrong cluster, indicating a poor clustering outcome.

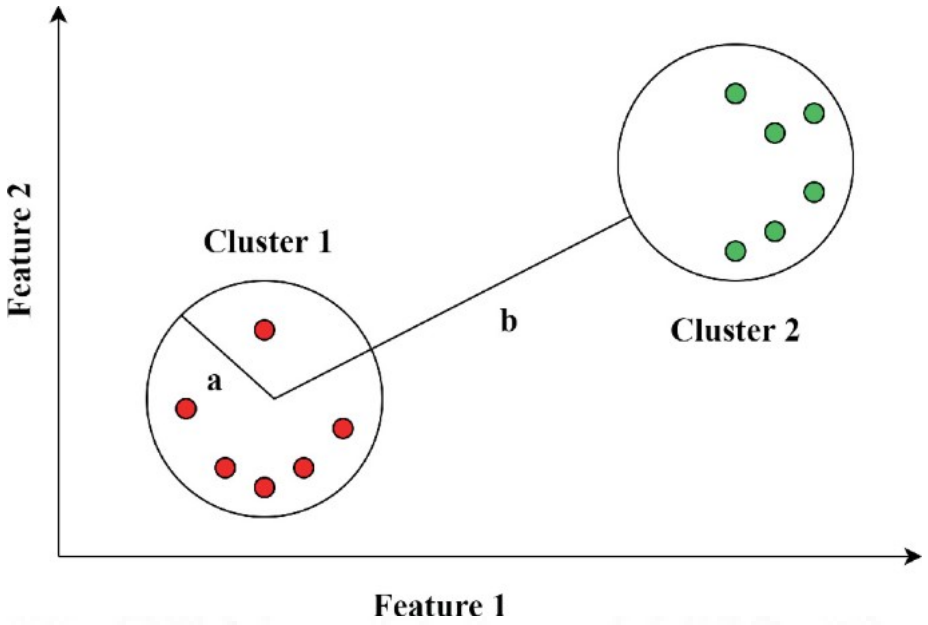

Figure 4.20: Illustration of cluster robustness measure

	Silhouette Score		
	K-Means	DBSCAN	Spectral Clustering
Morphology	0.65	0.71	0.76
Hemodynamic	0.59	0.44	0.68.

Table 4.9: Cluster validation using silhouette scores. It is clear that the spectral clustering algorithm has best performance for both morphological and hemodynamic clustering.

INFERENCES

1. Cluster 2 among morphology parameters point to higher inflow angle being a factor related to higher rupture status. This inference is aligned with previous studies Baharoglu *et al.* , Mo *et al.*(Mo et al., 2020)where it has been concluded that a significantly more obtuse inflow angle (> 125°) contributes to rupture and is associated with higher energy transmission to the dome, which they verified using Computatuional Fluid Dynamics analysis. In our scenario, these aneurysms were also relatively smaller compared to others in the population. Larger aneurysms with higher aspect ratio (> 1.2) were also associated with higher rupture status as inferred from cluster 1, which are in-line with results proposed by Dhar *et al.*(S et al., 2008).

2. Cluster 1 among hemodynamic parameters which grouped aneurysms with abnormally high RRT and correspondingly low Wall Shear Stress had 3 aneurysms, all of which were ruptured. Although in our case it is not entirely conclusive owing to the small sample size of 3, very low WSS (< 1*Pa*) has earlier been found to be a factor for rupture by previous studies Miura *et al.*(Ishida et al., 2021) .

DISCUSSION

CHAPTER 5

DISCUSSION

Clinical judgement of the rupture status of an aneurysm relies on multiple factors including a proper clinical history and review of the angiographic images. Larger and irregular aneurysms are deemed to have ruptured; but the situation is complicated if there is a mismatch with the amount of cisternal blood.(Björkman et al., 2017)

In clinical practice, we sometimes encounter cases of aneurysm in which the judgment of rupture status is difficult but important to determine the treatment strategy with multiple intracranial aneurysms. In following images (Fig 4.21), predominance of cisternal bleed was noted on the side of a smaller, smooth-walled aneurysm, while the aneurysm on the side opposite to the bleed was larger and irregular in shape. In such situations, there is a need for advanced techniques, which can predict the rupture status of aneurysm .

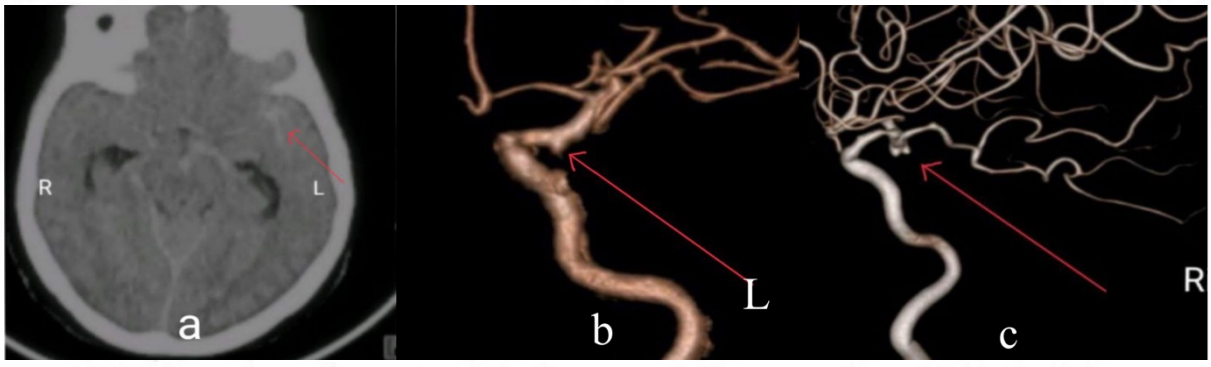

Figure 4.21.- Radiology images of a patient with multiple intracranial aneurysms. Cisternal blood is dominant on the left side (a), indicated by the red arrow. A small ICA aneurysm is noted on the left side (b) A large irregular PCom aneurysm is present on the right side (c).

Sometimes, it can be challenging to determine if a subarachnoid haemorrhage caused by a head injury or aneurysm rupture occurred in a patient who had been admitted after suffering a head injury and also had an aneurysm next to the cisternal clots. Similar to the scenario described above, if the ML models could accurately determine if an aneurysm was ruptured, we could avoid the surgery of performing on an unruptured aneurysm during the acute posttraumatic phase. However, in this case, more accurate models need to be developed because the clinical decision is whether a patient should undergo the surgery.

According to a retrospective study, irregular shape was the most important predictor of aneurysm rupture regardless of size, accounting for 18% of ruptured aneurysms that were under 4 mm and 38% that were over 7 mm.(Thompson, Brown, Amin-Hanjani, Broderick, Cockroft, Connolly, Duckwiler, Harris, Howard, SCC Johnston, et al., 2015)Several researchers have attempted to apply objective parameters in judging the rupture status of an aneurysm. Attempts have been made to quantify the irregularity of an aneurysm's structure.

Ellipticity index, non-sphericity index and undulation index are a few parameters used to quantify an aneurysm's irregular shape.In an attempt to identify the morphologic determinants of aneurysm rupture status. Xiang et al, found that non-sphericity index, undulation index, and ellipticity index heavily influenced the discrimination between ruptured and unruptured aneurysms.(Xiang et al., 2011b)

Other morphological parameters of aneurysms have also been linked to rupture risk or rupture status prediction. These include the Aspect ratio, Dome Neck Ratio, Bottleneck Ratio, and Neck Width to Parent Vessel Width Ratio. Most of these parameters have been linked to a rupture potential rather than a rupture status. While these parameters are based on 2-D

measurements, the indices representing irregularity of aneurysms are based on 3-D measurements.

Perera R et al (Perera et al., 2020) used morphologic parameters to differentiate ruptured from unruptured aneurysms. They found that aneurysm size, volume and size ratio ere the best indicators of rupture status of cerebral aneurysms.

Morphological parameters like Dome Height, Neck Diameter, Parent Vessel Diameter, Inflow Angle, Surface Area, Volume and Aspect Ratio were found to be statistically significant discriminators of rupture status in our study and Hemodynamic parameters exhibited less significant differences in ruptured and unruptured aneurysms, with the most significant parameter being RRT followerd by GON, MeanWSS and OSI.

These parameters are significantly different for ruptured versus unruptured aneurysms. Due to the multiplicity of factors considered for the statistical analysis, it is often difficult to use statistical methods to understand the collective role of these factors.

Ying zhang et al found Irregular shape, larger size, higher aspect ratio, lower WSSmin and more LSA may indicate a higher risk for their rupture(Zhang et al., 2010),which is similar to our study.

Other study by Qingyuan liu(Liu et al., 2019) AR, NWSSm, and OSI are considered three independent risk factors for intraoperative aneurysm rupture, which could serve as predictors.

Investigators have used machine-learning and deep-learning algorithms to improve the prediction of rupture status. Tanioka et al (Tanioka et al., 2020) used morphological and haemodynamic parameters to identify the rupture status of aneurysms. Using machine-learning they were able to classify ruptured aneurysms using parameters such as projection ratio, irregular shape, and size ratio. The investigators reported 77% accuracy in predicting the rupture status of aneurysm(supervised machine learning algorithms).

Detmer et al also used morphological and haemodynamic parameters and compare a previously developed aneurysm rupture logistic regression probability model (LRM) to other machine learning (ML) classifiers for discrimination of aneurysm rupture status and found performance of the LRM was overall comparable to that of the other ML classifiers, confirming its potential for aneurysm rupture assessment.The accuracy of there model ranged between 76 % to 79 %.

Another study by Dhar et al based morphological parameters that correlate with human intracranial aneurysm (IA) rupture, logistic regression analysis revealed that size ratio and undulation index had the strongest independent correlation with ruptured IA (Dhar et al., 2008)

A study by Bisbal et al used morphological and hemodynamic parameters to predicting the rupture of cerebral aneurysms and after analysing the results with supporting vector machines offer the best results with accuracy rates as high as 95%.(Bisbal et al., 2011)

Liu et al studied morphology of ACOM aneurysm and ANN model was used predict their rupture risk and found overall prediction accuracy of 94.8 %.(Liu et al., 2018b)

Detmer et al trained an aneurysm rupture probability model using logistic group lasso regression and was able to discriminate between ruptured and unruptured aneurysms with accuracy of 86%.(Detmer et al., 2018)

We used both supervised and unsupervised machine learning algorithms(K-Means, DBSCAN and Spectral clustering) to improve our reults. With supervised learning methods our results shows that ANN model followed by logistic regression proved to be effective in predicting the rupture status with accuracy of around 80 %.

The unsupervised machine learning algorithms shows that a higher inflow angle, abnormally large aneurysms and low wall shear stress can be related to higher rupture status which were consistent with other studies. Spectral algorithm grouped aneurysms with a silhouette score of 0.76 and 0.68 for both types of data.

There are no previous studies in literature with unsupervised machine learning algorithms to compare the results of our study.

In our study with supervised learning algorithms the accuracy in with only morphologic variables was higher than that with only hemodynamic parameters. The findings indicate that morphology of cerebral aneurysms is still important in judging rupture status in the current era of developing CFD analysis. However, when both morphologic and hemodynamic parameters classified rupture status as accurate as morphological parameter. However, study by Tanioka et al showed that adding consideration of hemodynamics to morphologic analysis brings more accurate classification of rupture status.

In our study important morphological parametrs like Aspect ratio, bottle neck ratio, dome height, parent vessel diameter, aneurysm surface area and surface area/volume ratio and hemodynamic parameters like RRT, mean WSS and p Mean associated with rupture status or risk.

Tanioka et al, reported projection ratio, irregular shape, size ratio, low shear area ratio, and oscillatory shear index have correlation with rupture status or risk.

In study by Detmer et al , non-sphericity index (NSI), Gaussian surface curvature, size ratio (SizeR),ellipticity index (EI), height-to-width ratio (HWR), isoperimetric ratio and aspect ratios (AR and Aspect) have correlation with rupture status or risk.

In study by Müller et al Observers (experienced neurosurgeons) assessed the aneurysm morphology obtained from stereolithography together with the patient's age, sex, and aneurysm site, and they graded the rupture state by adding their prior knowledge. The accuracy of our machine learning model with morphological parameters was higher than that of the observers' judgements, despite the fact that evaluation points of the observers were thought to coincide with features of morphological parameters.

This fact indicates the characteristics of ML well, in which a simple program with a large collection of features of ruptured and unruptured aneurysms is enough for an algorithm to classify rupture status better than human experts

In our study we used both supervised classifications which shows accuracy of around 80 % and unsupervised classifications of around 76 %.

In generally the supervised classification is more accurate than unsupervised classification because the user has control over the classification process and can ensure that training data is representative of whole dataset.

As there are no previous studies in literature with unsupervised machine learning algorithms to compare the results of our study. Further studies will be required in the future which can compare the results of both supervised classifications and unsupervised classifications.

Machine learning-based methods have the potential to influence clinical judgements in identifying the rupture status of cerebral aneurysm. Information delivered to neurosurgeons/ interventionists could equip them with objective measures to take clinically relevant and appropriate decisions to intervene. Situations such as those mentioned above, where it is difficult to decide on the side of emergency surgery could be handled using the results of such studies.

\

Conclusion and Future work

CHAPTER 6

CONCLUSION AND FUTURE WORK

Supervised and Unsupervised clustering analysis was performed on morphological and hemodynamic data of cerebral aneurysms of 100 patients. Supervised learning algorithms shows ANN model followed by Logistic regression proved to be effective in predicting the rupture status.

Unsupervised clustering like, K-Means, DBSCAN and Spectral clustering algorithms were used, out of which spectral algorithm grouped aneurysms with a silhouette score of 0.76 and 0.68 for both types of data. From the results, it can be concluded that a higher inflow angle, abnormally large aneurysms and low wall shear stress can be related to higher rupture status which were consistent with other studies.

This study has various limitations. A larger database is required to validate these results. Lack of balance database between ruptured and unruptured aneurysms (significantly more ruptured cases). The cluster inferences can be further improved and robustness can be achieved once the above limitations are tackled with sufficient database.

REFERENCES

1. Alleyne CH (2010) Editorial: Aneurysmal subarachnoid hemorrhage: Have outcomes really improved? *Neurology* 74(19): 1486-1487,. DOI: 10.1212/WNL.0B013E3181E0EF1A.
2. Ambekar S, Khandelwal P, Bhattacharya P, et al. (2016) Treatment of unruptured intracranial aneurysms: a review. *Expert Review of Neurotherapeutics* 16(10): 1205–1216. DOI: 10.1080/14737175.2016.1199958.
3. Bilker WB and Wang MC (1996) A semiparametric extension of the Mann-Whitney test for randomly truncated data. *Biometrics* 52(1): 10–20.
4. Bisbal J, Engelbrecht G, Villa-Uriol M-C, et al. (2011) Prediction of Cerebral Aneurysm Rupture Using Hemodynamic, Morphologic and Clinical Features: A Data Mining Approach. In: Hameurlain A, Liddle SW, Schewe K-D, et al. (eds) *Database and Expert Systems Applications*. Lecture Notes in Computer Science. Berlin, Heidelberg: Springer Berlin Heidelberg, pp. 59–73. DOI: 10.1007/978-3-642-23091-2_6.
5. Björkman J, Frösen J, Tähtinen O, et al. (2017) Irregular Shape Identifies Ruptured Intracranial Aneurysm in Subarachnoid Hemorrhage Patients With Multiple Aneurysms. *Stroke* 48(7): 1986–1989. DOI: 10.1161/STROKEAHA.117.017147.
6. Can A. and Du R (2016) Association of hemodynamic factors with intracranial aneurysm formation and rupture: systematic review and meta-analysis. *Neurosurgery* 78: 510–520.
7. Can Anil and Du R (2016) Association of Hemodynamic Factors With Intracranial Aneurysm Formation and Rupture: Systematic Review and Meta-analysis. *Neurosurgery* 78(4): 510–520. DOI: 10.1227/NEU.0000000000001083.

8. Cebral JR and Raschi M (2013) Suggested connections between risk factors of intracranial aneurysms: a review. *Annals of Biomedical Engineering* 41(7): 1366–1383. DOI: 10.1007/s10439-012-0723-0.

9. Cebral JR, Duan X, Chung BJ, et al. (2015) Wall Mechanical Properties and Hemodynamics of Unruptured Intracranial Aneurysms. *AJNR. American journal of neuroradiology* 36(9): 1695–1703. DOI: 10.3174/ajnr.A4358.

10. Decision Tree Algorithm in Machine Learning - Javatpoint (n.d.). Available at: https://www.javatpoint.com/machine-learning-decision-tree-classification-algorithm (accessed 13 August 2023).

11. Detmer FJ, Chung BJ, Mut F, et al. (2018) Development and internal validation of an aneurysm rupture probability model based on patient characteristics and aneurysm location, morphology, and hemodynamics. *International Journal of Computer Assisted Radiology and Surgery* 13(11): 1767–1779. DOI: 10.1007/s11548-018-1837-0.

12. Detmer FJ, Chung BJ, Jimenez C, et al. (2019) Associations of hemodynamics, morphology, and patient characteristics with aneurysm rupture stratified by aneurysm location. *Neuroradiology* 61(3): 275–284. DOI: 10.1007/s00234-018-2135-9.

13. Detmer FJ, Hadad S, Chung BJ, et al. (2019) Extending statistical learning for aneurysm rupture assessment to Finnish and Japanese populations using morphology, hemodynamics, and patient characteristics. *Neurosurgical Focus* 47(1): E16. DOI: 10.3171/2019.4.FOCUS19145.

14. Dhar S, Tremmel M, Mocco J, et al. (2008) Morphology Parameters for Intracranial Aneurysm Rupture Risk Assessment. *Neurosurgery* 63(2): 185–197. DOI: 10.1227/01.NEU.0000316847.64140.81.

15. DO W (2003) Unruptured intracranial aneurysms: natural history, clinical outcome, and risks of surgical and endovascular treatment. *Lancet* 362(9378): 103-110,. DOI: 10.1016/S0140-6736(03)13860-3.

16. Doddasomayajula R, Chung B, Hamzei-Sichani F, et al. (2017) Differences in Hemodynamics and Rupture Rate of Aneurysms at the Bifurcation of the Basilar and Internal Carotid Arteries. *AJNR. American journal of neuroradiology* 38(3): 570–576. DOI: 10.3174/ajnr.A5088.

17. Dolan JM, Kolega J and Meng H (2013) High wall shear stress and spatial gradients in vascular pathology: a review. *Annals of Biomedical Engineering* 41(7): 1411–1427. DOI: 10.1007/s10439-012-0695-0.

18. Editor MB (n.d.) Understanding Analysis of Variance (ANOVA) and the F-test. Available at: https://blog.minitab.com/en/adventures-in-statistics-2/understanding-analysis-of-variance-anova-and-the-f-test (accessed 15 August 2023).

19. Etminan N, Brown RD, Beseoglu K, et al. (2015) The unruptured intracranial aneurysm treatment score: a multidisciplinary consensus. *Neurology* 85(10): 881–889. DOI: 10.1212/WNL.0000000000001891.

20. *GeeksforGeeks* (2017) K-Nearest Neighbor(KNN) Algorithm. Available at: https://www.geeksforgeeks.org/k-nearest-neighbours/ (accessed 13 August 2023).

21. Greving JP, Wermer MJH, Brown RD, et al. (2014) Development of the PHASES score for prediction of risk of rupture of intracranial aneurysms: a pooled analysis of six prospective cohort studies. *The Lancet Neurology* 13(1): 59–66. DOI: 10.1016/S1474-4422(13)70263-1.

22. Hadjiathanasiou A, Schuss P, Brandecker S, et al. (2020) Multiple aneurysms in subarachnoid hemorrhage - Identification of the ruptured aneurysm, when the bleeding

pattern is not self-explanatory - Development of a novel prediction score. *BMC Neurology* 20(1). BMC Neurology: 1–12. DOI: 10.1186/s12883-020-01655-x.

23. Hoi Y, Meng H, Woodward SH, et al. (2004) Effects of arterial geometry on aneurysm growth: three-dimensional computational fluid dynamics study. *Journal of Neurosurgery* 101(4): 676–681. DOI: 10.3171/jns.2004.101.4.0676.
24. Huang X, Liu D, Yin X, et al. (2018) Morphometry and hemodynamics of posterior communicating artery aneurysms: Ruptured versus unruptured. *Journal of Biomechanics* 76: 35–44. DOI: 10.1016/j.jbiomech.2018.05.019.
25. Ingall Timothy, Asplund K, Mähönen M, et al. (2000) A multinational comparison of subarachnoid hemorrhage epidemiology in the WHO MONICA stroke study. *Stroke* 31(5): 1054–1061. DOI: 10.1161/01.STR.31.5.1054.
26. Ingall T., Asplund K, Mähönen M, et al. (2000) A multinational comparison of subarachnoid hemorrhage epidemiology in the WHO MONICA stroke study. *Stroke* 31(5): 1054-1061,. DOI: 10.1161/01.STR.31.5.1054.
27. *Investopedia* (n.d.) Variance Inflation Factor (VIF). Available at: https://www.investopedia.com/terms/v/variance-inflation-factor.asp (accessed 14 August 2023).
28. Ishida F, Tsuji M, Tanioka S, et al. (2021) Computational Fluid Dynamics for Cerebral Aneurysms in Clinical Settings. In: Esposito G, Regli L, Cenzato M, et al. (eds) *Trends in Cerebrovascular Surgery and Interventions*. Cham (CH): Springer. Available at: http://www.ncbi.nlm.nih.gov/books/NBK573767/ (accessed 30 June 2023).
29. Jain K (2016) Transition to Turbulence in Physiological Flows: Direct Numerical Simulation of Hemodynamics in Intracranial Aneurysms and Cerebrospinal Fluid Hydrodynamics in the Spinal Canal. Available at:

https://research.utwente.nl/en/publications/transition-to-turbulence-in-physiological-flows-direct-numerical- (accessed 27 July 2023).

30. Juvela S (2019) Treatment Scoring of Unruptured Intracranial Aneurysms. *Stroke* 50(9). American Heart Association: 2344–2350. DOI: 10.1161/STROKEAHA.119.025599.

31. Juvela S, Porras M and Poussa K (2000) Natural history of unruptured intracranial aneurysms: probability and risk factors for aneurysm rupture. *Neurosurgical Focus* 8(5): Preview 1.

32. Kalita D (2022) An Overview and Applications of Artificial Neural Networks. In: *Analytics Vidhya*. Available at: https://www.analyticsvidhya.com/blog/2022/03/an-overview-and-applications-of-artificial-neural-networks-ann/ (accessed 14 August 2023).

33. Kaneko N, Mashiko T, Namba K, et al. (2018) A patient-specific intracranial aneurysm model with endothelial lining: a novel in vitro approach to bridge the gap between biology and flow dynamics. *Journal of Neurointerventional Surgery* 10(3): 306–309. DOI: 10.1136/neurintsurg-2017-013087.

34. Kashiwazaki D and Kuroda S (2013) Size ratio can highly predict rupture risk in intracranial small (<5 mm) aneurysms. *Stroke* 44(8): 2169–2173. DOI: 10.1161/STROKEAHA.113.001138.

35. Kaspera W (2014) Morphological, hemodynamic, and clinical independent risk factors for anterior communicating artery aneurysms. *Stroke* 45(10): 2906-2911,. DOI: 10.1161/STROKEAHA.114.006055.

36. kassell1983.pdf (n.d.).

37. Kleinloog R, de Mul N, Verweij BH, et al. (2018) Risk Factors for Intracranial Aneurysm Rupture: A Systematic Review. *Neurosurgery* 82(4): 431–440. DOI: 10.1093/neuros/nyx238.

38. Lindgren AE, Koivisto T, Björkman J, et al. (2016) Irregular Shape of Intracranial Aneurysm Indicates Rupture Risk Irrespective of Size in a Population-Based Cohort. *Stroke* 47(5): 1219–1226. DOI: 10.1161/STROKEAHA.115.012404.

39. Liu J, Chen Y, Lan L, et al. (2018a) Prediction of rupture risk in anterior communicating artery aneurysms with a feed-forward artificial neural network. *European Radiology* 28(8). European Radiology: 3268–3275. DOI: 10.1007/s00330-017-5300-3.

40. Liu J, Chen Y, Lan L, et al. (2018b) Prediction of rupture risk in anterior communicating artery aneurysms with a feed-forward artificial neural network. *European Radiology* 28(8): 3268–3275. DOI: 10.1007/s00330-017-5300-3.

41. Liu Q, Jiang P, Wu J, et al. (2019) The Morphological and Hemodynamic Characteristics of the Intraoperative Ruptured Aneurysm. *Frontiers in Neuroscience* 13: 233. DOI: 10.3389/fnins.2019.00233.

42. Longo M, Granata F, Racchiusa S, et al. (2017) Role of Hemodynamic Forces in Unruptured Intracranial Aneurysms: An Overview of a Complex Scenario. *World Neurosurgery* 105: 632–642. DOI: 10.1016/j.wneu.2017.06.035.

43. Machine Learning Random Forest Algorithm - Javatpoint (n.d.). Available at: https://www.javatpoint.com/machine-learning-random-forest-algorithm (accessed 13 August 2023).

44. Madeira MA and Jacob T (2022) The Implementation of Enhanced K-Strange Points Clustering Method in Classifying Undergraduate Thesis Titles. In: *Sentimental*

Analysis and Deep Learning (eds S Shakya, VE Balas, S Kamolphiwong, et al.), Singapore, 2022, pp. 255–274. Advances in Intelligent Systems and Computing. Springer. DOI: 10.1007/978-981-16-5157-1_21.

45. Malhotra A (2017) Growth and rupture risk of small unruptured intracranial aneurysms a systematic review. *Annals of Internal Medicine* 167(1): 26-33,. DOI: 10.7326/M17-0246.

46. Malhotra A, Wu X, Forman HP, et al. (2017) Growth and rupture risk of small unruptured intracranial aneurysms a systematic review. *Annals of Internal Medicine* 167(1): 26–33. DOI: 10.7326/M17-0246.

47. Malik K, Alam F, Santamaria J, et al. (2023) Toward Grading Subarachnoid Hemorrhage Risk Prediction: A Machine Learning-Based Aneurysm Rupture Score. *World Neurosurgery* 172: e19–e38. DOI: 10.1016/j.wneu.2022.11.065.

48. Marchandise E, Crosetto P, Geuzaine C, et al. (2012) Quality open source mesh generation for cardiovascular flow simulations. *Modeling, Simulation and Applications* 5(Simbio): 395-414,. DOI: doi:

49. Meng H, Wang Z, Hoi Y, et al. (2007) Complex Hemodynamics at the Apex of an Arterial Bifurcation Induces Vascular Remodeling Resembling Cerebral Aneurysm Initiation. *Stroke* 38(6). American Heart Association: 1924–1931. DOI: 10.1161/STROKEAHA.106.481234.

50. Meng H, Tutino VM, Xiang J, et al. (2014) High WSS or Low WSS? Complex Interactions of Hemodynamics with Intracranial Aneurysm Initiation, Growth, and Rupture: Toward a Unifying Hypothesis. *AJNR: American Journal of Neuroradiology* 35(7): 1254–1262. DOI: 10.3174/ajnr.A3558.

51. Mo X, Meng Q, Yang X, et al. (2020) The Impact of Inflow Angle on Aneurysm Hemodynamics: A Simulation Study Based on Patient-Specific Intracranial Aneurysm Models. *Frontiers in Neurology* 11: 534096. DOI: 10.3389/fneur.2020.534096.

52. Mocco J, Brown RD, Torner JC, et al. (2018) Aneurysm Morphology and Prediction of Rupture: An International Study of Unruptured Intracranial Aneurysms Analysis. *Neurosurgery* 82(4): 491–496. DOI: 10.1093/neuros/nyx226.

53. Murayama Y, Takao H, Ishibashi T, et al. (2016) Risk Analysis of Unruptured Intracranial Aneurysms: Prospective 10-Year Cohort Study. *Stroke* 47(2): 365–371. DOI: 10.1161/STROKEAHA.115.010698.

54. Murayama Y, Fujimura S, Suzuki T, et al. (2019) Computational fluid dynamics as a risk assessment tool for aneurysm rupture. *Neurosurgical Focus* 47(1). DOI: 10.3171/2019.4.FOCUS19189.

55. Nanduri JR, Pino-Romainville FA and Celik I (2009) CFD mesh generation for biological flows: Geometry reconstruction using diagnostic images. *Computers and Fluids* 38(5): 1026-1032,. DOI: 10.1016/j.compfluid.2008.01.027.

56. Ng A, Jordan M and Weiss Y (2001) On Spectral Clustering: Analysis and an algorithm. In: *Advances in Neural Information Processing Systems*, 2001. MIT Press. Available at: https://proceedings.neurips.cc/paper/2001/hash/801272ee79cfde7fa5960571fee36b9b-Abstract.html (accessed 27 July 2023).

57. *NVIDIA Data Science Glossary* (n.d.) What is XGBoost? Available at: https://www.nvidia.com/en-us/glossary/data-science/xgboost/ (accessed 13 August 2023).

58. Ou C, Liu J, Qian Y, et al. (2020) Rupture Risk Assessment for Cerebral Aneurysm Using Interpretable Machine Learning on Multidimensional Data. *Frontiers in Neurology* 11: 570181. DOI: 10.3389/fneur.2020.570181.

59. Perera R, Isoda H, Ishiguro K, et al. (2020) Assessing the Risk of Intracranial Aneurysm Rupture Using Morphological and Hemodynamic Biomarkers Evaluated from Magnetic Resonance Fluid Dynamics and Computational Fluid Dynamics. *Magnetic resonance in medical sciences: MRMS: an official journal of Japan Society of Magnetic Resonance in Medicine* 19(4): 333–344. DOI: 10.2463/mrms.mp.2019-0107.

60. Qiu T, Jin G, Bao W, et al. (2017) Intercorrelations of morphology with hemodynamics in intracranial aneurysms in computational fluid dynamics. *Neurosciences (Riyadh, Saudi Arabia)* 22(3): 205–212. DOI: 10.17712/nsj.2017.3.20160452.

61. Raghavan ML, Ma B and Harbaugh RE (2005) Quantified aneurysm shape and rupture risk. *J Neurosurg* 102(2): 355-362,. DOI: 10.3171/JNS.2005.102.2.0355.

62. S D, M T, J M, et al. (2008) Morphology parameters for intracranial aneurysm rupture risk assessment. *Neurosurgery* 63(2). Neurosurgery. DOI: 10.1227/01.NEU.0000316847.64140.81.

63. Sforza DM, Putman CM and Cebral JR (2009) Hemodynamics of Cerebral Aneurysms. *Annual Review of Fluid Mechanics* 41: 91–107. DOI: 10.1146/annurev.fluid.40.111406.102126.

64. Shahapure KR and Nicholas C (2020) Cluster Quality Analysis Using Silhouette Score. In: *2020 IEEE 7th International Conference on Data Science and Advanced*

Analytics (DSAA), October 2020, pp. 747–748. DOI: 10.1109/DSAA49011.2020.00096.

65. Shojima M, Oshima M, Takagi K, et al. (2004) Magnitude and Role of Wall Shear Stress on Cerebral Aneurysm. *Stroke* 35(11). American Heart Association: 2500–2505. DOI: 10.1161/01.STR.0000144648.89172.0f.

66. Skodvin TØ, Johnsen L-H, Gjertsen Ø, et al. (2017) Cerebral Aneurysm Morphology Before and After Rupture: Nationwide Case Series of 29 Aneurysms. *Stroke* 48(4): 880–886. DOI: 10.1161/STROKEAHA.116.015288.

67. Soldozy S, Norat P, Elsarrag M, et al. (2019) The biophysical role of hemodynamics in the pathogenesis of cerebral aneurysm formation and rupture. *Neurosurgical Focus* 47(1): E11. DOI: 10.3171/2019.4.FOCUS19232.

68. Steinman DA, Milner JS, Norley CJ, et al. (2003) Image-Based Computational Simulation of Flow Dynamics in a Giant Intracranial Aneurysm. *AJNR: American Journal of Neuroradiology* 24(4): 559–566.

69. Sun Q, Groth A and Aach T (2012) Comprehensive validation of computational fluid dynamics simulations of in-vivo blood flow in patient-specific cerebral aneurysms. *Medical Physics* 39(2): 742–754. DOI: 10.1118/1.3675402.

70. Support Vector Machine (SVM) Algorithm - Javatpoint (n.d.). Available at: https://www.javatpoint.com/machine-learning-support-vector-machine-algorithm (accessed 13 August 2023).

71. Tanaka K (2018) Relationship between hemodynamic parameters and cerebral aneurysm initiation. In: *Proceedings of the Annual International Conference of the IEEE Engineering in Medicine and Biology Society, EMBS*, 2018, pp. 1347-1350,. DOI: 10.1109/EMBC.2018.8512466.

72. Tanioka S, Ishida F, Yamamoto A, et al. (2020) Machine Learning Classification of Cerebral Aneurysm Rupture Status with Morphologic Variables and Hemodynamic Parameters. *Radiology. Artificial intelligence* 2(1): e190077. DOI: 10.1148/ryai.2019190077.

73. Tateshima S, Viñuela F, Villablanca JP, et al. (2003) Three-dimensional blood flow analysis in a wide-necked internal carotid artery—ophthalmic artery aneurysm. *Journal of Neurosurgery* 99(3). Journal of Neurosurgery Publishing Group: 526–533. DOI: 10.3171/jns.2003.99.3.0526.

74. Thompson BG, Brown RD, Amin-Hanjani S, Broderick JP, Cockroft KM, Connolly ES, Duckwiler GR, Harris CC, Howard VJ, Johnston SCC lay, et al. (2015) *Guidelines for the Management of Patients With Unruptured Intracranial Aneurysms: A Guideline for Healthcare Professionals From the American Heart Association/American Stroke Association*. DOI: 10.1161/STR.0000000000000070.

75. Thompson BG, Brown RD, Amin-Hanjani S, Broderick JP, Cockroft KM, Connolly ES, Duckwiler GR, Harris CC, Howard VJ, Johnston SCC, et al. (2015) Guidelines for the Management of Patients With Unruptured Intracranial Aneurysms: A Guideline for Healthcare Professionals From the American Heart Association/American Stroke Association. *Stroke* 46(8): 2368–2400. DOI: 10.1161/STR.0000000000000070.

76. UCAS Japan Investigators, Morita A, Kirino T, et al. (2012) The natural course of unruptured cerebral aneurysms in a Japanese cohort. *The New England Journal of Medicine* 366(26): 2474–2482. DOI: 10.1056/NEJMoa1113260.

77. Ujiie H, Tamano Y, Sasaki K, et al. (2001) Is the aspect ratio a reliable index for predicting the rupture of a saccular aneurysm? *Neurosurgery* 48(3): 495–502; discussion 502-503. DOI: 10.1097/00006123-200103000-00007.

78. Valen-Sendstad K and Steinman DA (2014) Mind the gap: impact of computational fluid dynamics solution strategy on prediction of intracranial aneurysm hemodynamics and rupture status indicators. *AJNR. American journal of neuroradiology* 35(3): 536–543. DOI: 10.3174/ajnr.A3793.

79. Weir B (2003) The aspect ratio (dome/neck) of ruptured and unruptured aneurysms. *J Neurosurg* 99(3): 447-451,. DOI: 10.3171/JNS.2003.99.3.0447.

80. Wermer MJH, van der Schaaf IC, Algra A, et al. (2007) Risk of rupture of unruptured intracranial aneurysms in relation to patient and aneurysm characteristics: an updated meta-analysis. *Stroke* 38(4): 1404–1410. DOI: 10.1161/01.STR.0000260955.51401.cd.

81. Wiebers DO, Whisnant JP, Huston J, et al. (2003) Unruptured intracranial aneurysms: natural history, clinical outcome, and risks of surgical and endovascular treatment. *Lancet (London, England)* 362(9378): 103–110. DOI: 10.1016/s0140-6736(03)13860-3.

82. Xiang J, Natarajan SK, Tremmel M, et al. (2011a) Hemodynamic-morphologic discriminants for intracranial aneurysm rupture. *Stroke* 42(1): 144–152. DOI: 10.1161/STROKEAHA.110.592923.

83. Xiang J, Natarajan SK, Tremmel M, et al. (2011b) Hemodynamic-morphologic discriminants for intracranial aneurysm rupture. *Stroke* 42(1): 144–152. DOI: 10.1161/STROKEAHA.110.592923.

84. Xiang J, Yu J, Snyder KV, et al. (2016) Hemodynamic-morphological discriminant models for intracranial aneurysm rupture remain stable with increasing sample size. *Journal of Neurointerventional Surgery* 8(1): 104–110. DOI: 10.1136/neurintsurg-2014-011477.

85. Zhang LJ, Wu SY, Niu JB, et al. (2010) Dual-energy CT angiography in the evaluation of intra- cranial aneurysms: image quality, radiation dose, and com- parison with 3D rotational digital subtraction angiography. *AJR Am J Roentgenol* 194: 23–30.

86. Zhang Y, Yang X, Wang Y, et al. (2014) Influence of morphology and hemodynamic factors on rupture of multiple intracranial aneurysms: matched-pairs of ruptured-unruptured aneurysms located unilaterally on the anterior circulation. *BMC neurology* 14: 253. DOI: 10.1186/s12883-014-0253-5.

ANNEXURES:
CURRICULUM VITAE

Last Name	First Name	Middle Name
AKHADE	**BHUSHAN**	**SADASHIV**
Date of Birth (dd/mm/yy) :01/04/1990		Sex : MALE
Study Site Affiliation (e.g. Principal Investigator, Co-Investigator, Coordinator) : PRINCIPAL INVESTIGATOR, SCTIMST		
Professional Mailing Address (Include Institution name)		Study Site Address (Include Institution name)
DEPT OF NEUROSURGERY, SREE CHITRA TIRUNAL INSTITUTE FOR MEDICAL SCIENCES AND TECHNOLOGY THIRUVANANTHAPURAM KERALA 695011		DEPT OF NEUROSURGERY, SREE CHITRA TIRUNAL INSTITUTE FOR MEDICAL SCIENCES AND TECHNOLOGY THIRUVANANTHAPURAM KERALA 695011
Telephone (Office):		Mobile Number: 9730803299, 8850872273
Telephone (Residence): 8850872273		Email- bhushanakhade01@gmail.com

Academic Qualifications (Most recent qualification first)

Degree/Certificate	Year	Institution, Country
MS GENERAL SURGERY	2019	LOKMANYA TILAK MUNICIPAL MEDICAL COLLGE& LOKMANYA TILAK MUNICIPAL GENERAL HOSPITAL SION, MUMBAI-400022, INDIA.
MBBS	2015	Dr. S.C.GOVERMENT MEDICAL COLLEGE,NANDED,MAHARASHTRAINDIA,431606

Details of professional registration: (MCI/State Registration/Bar Council/DCI/etc. including Registration Number and Year of Registration
THE TRAVANCORE-COCHIN COUNCIL OF MODERN MEDICINE REGISTRATION

NUMBER: 80887
YEAR OF REGISTRATION: 2022

Current and previous positions (most recent position first)

Month and Year	Title	Institution/Company, Country
JANUARY, 2021	SENIOR RESIDENT, NEUROSURGERY	SCTIMST, INDIA
2019-2020	SPECIALITY MEDICAL OFFICER, GENERAL SURGERY	ESIS HOSPITAL KANDIVALI, MUMBAI, MAHARASHTRA, INDIA

Brief summary of relevant research experience:

1. INFLUENCE OF MORPHOLOGICAL PARAMETERS ON HAEMODYNAMICS IN INTERNAL CAROTID ARTERY BIFURCATION ANEURYSMS – ORIGINAL ARTICLE – AUTHOR.

Current project/s at hand:

1) Posterior Petrous Promontory as an Impediment to the Visualisation of Trigeminal Nerve during Microvascular Decompression

2)Do steroids alter the dynamics of colloid cyst with hydrocephalus: A Case report

2)MS THESIS (2019): COMPARATIVE EFFICACIES OF FNAC, TRUCUT BIOPSY & SONOMAMMOGRAM TO THE FINAL HISTOPATHOLOGY IN A CLINICALLY SUSPECTED BREASTSWELLINGS.

Conferences and Presentations

- Central Travancore Neurocon, NSI Kerala October 2022 Poster Presentation :
- Cadaveric workshop on transforaminal lumbar spine endoscopy -2022
- Chitra Neurosurgical Society : Symposium presentation - POSITIONING IN NEUROSURGERY
- NEUROVASCON 2022-Paper presentation
- Prof Damodar Rout Oration. Chitra Neurosurgery Update, February 2023
- Prof RM Varma Memorial Oration , Neurosurgery CME , May 2023
- 3rd International Rhoton Society conference 2023,Istanbul,Turkey- Poster presentation

Signature: 	25/08/23 TRIVANDRUM

APPENDIX A- INSTITUTIONAL ETHICS COMMITTEE APPROVAL

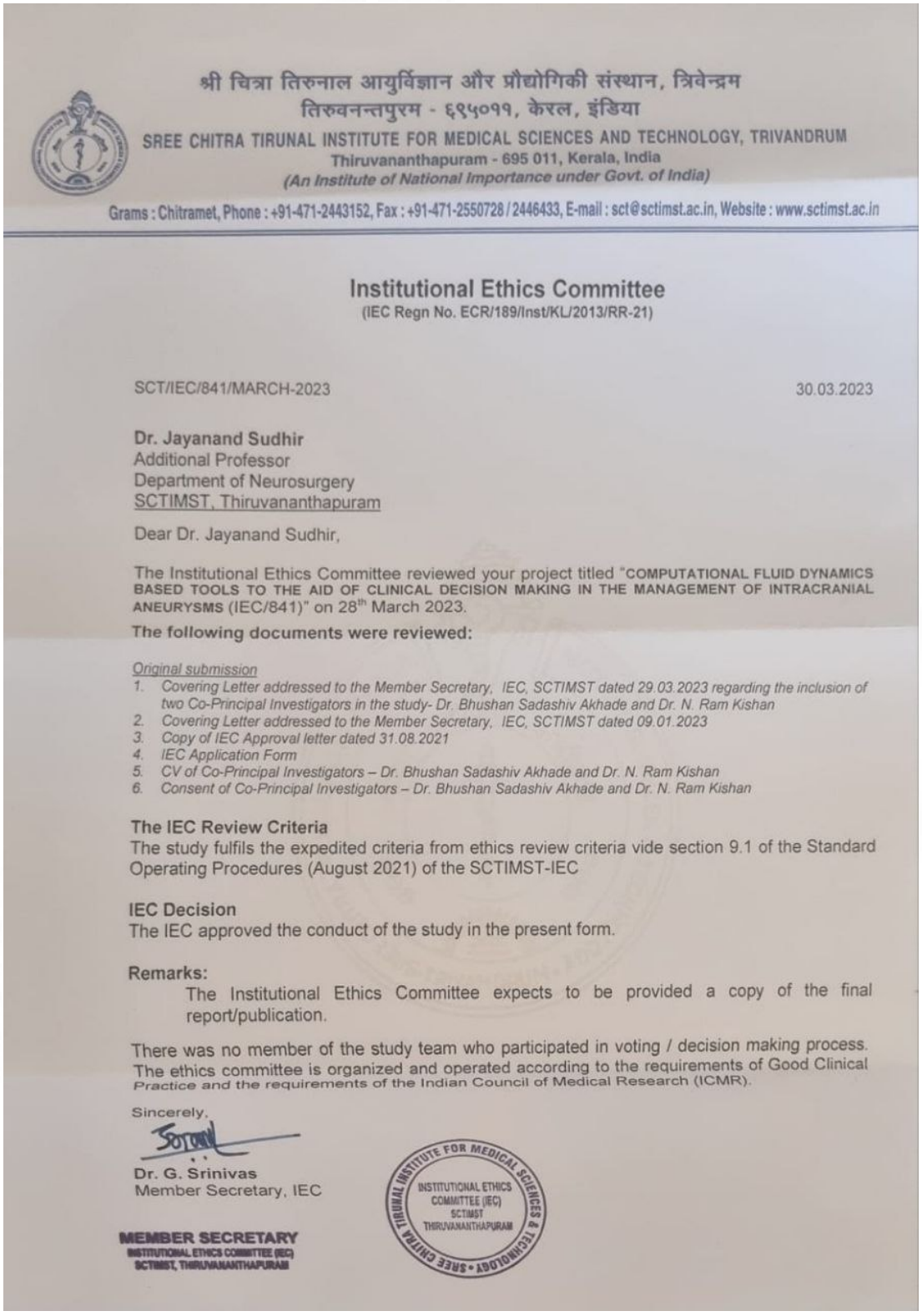

श्री चित्रा तिरुनाल आयुर्विज्ञान और प्रौद्योगिकी संस्थान, त्रिवेन्द्रम
तिरुवनन्तपुरम - ६९५०११, केरल, इंडिया

SREE CHITRA TIRUNAL INSTITUTE FOR MEDICAL SCIENCES AND TECHNOLOGY, TRIVANDRUM
Thiruvananthapuram - 695 011, Kerala, India
(An Institute of National Importance under Govt. of India)

Grams : Chitramet, Phone : +91-471-2443152, Fax : +91-471-2550728 / 2446433, E-mail : sct@sctimst.ac.in, Website : www.sctimst.ac.in

Institutional Ethics Committee

(IEC Regn No. ECR/189/Inst/KL/2013/RR-21)

SCT/IEC/841/MARCH-2023 30.03.2023

Dr. Jayanand Sudhir
Additional Professor
Department of Neurosurgery
SCTIMST, Thiruvananthapuram

Dear Dr. Jayanand Sudhir,

The Institutional Ethics Committee reviewed your project titled "**COMPUTATIONAL FLUID DYNAMICS BASED TOOLS TO THE AID OF CLINICAL DECISION MAKING IN THE MANAGEMENT OF INTRACRANIAL ANEURYSMS** (IEC/841)" on 28th March 2023.

The following documents were reviewed:

Original submission

1. *Covering Letter addressed to the Member Secretary, IEC, SCTIMST dated 29.03.2023 regarding the inclusion of two Co-Principal Investigators in the study- Dr. Bhushan Sadashiv Akhade and Dr. N. Ram Kishan*
2. *Covering Letter addressed to the Member Secretary, IEC, SCTIMST dated 09.01.2023*
3. *Copy of IEC Approval letter dated 31.08.2021*
4. *IEC Application Form*
5. *CV of Co-Principal Investigators – Dr. Bhushan Sadashiv Akhade and Dr. N. Ram Kishan*
6. *Consent of Co-Principal Investigators – Dr. Bhushan Sadashiv Akhade and Dr. N. Ram Kishan*

The IEC Review Criteria
The study fulfils the expedited criteria from ethics review criteria vide section 9.1 of the Standard Operating Procedures (August 2021) of the SCTIMST-IEC

IEC Decision
The IEC approved the conduct of the study in the present form.

Remarks:
The Institutional Ethics Committee expects to be provided a copy of the final report/publication.

There was no member of the study team who participated in voting / decision making process. The ethics committee is organized and operated according to the requirements of Good Clinical Practice and the requirements of the Indian Council of Medical Research (ICMR).

Sincerely,

Dr. G. Srinivas
Member Secretary, IEC

MEMBER SECRETARY
INSTITUTIONAL ETHICS COMMITTEE (IEC)
SCTIMST, THIRUVANANTHAPURAM

SREE CHITRA TIRUNAL INSTITUTE FOR MEDICAL SCIENCES & TECHNOLOGY
INSTITUTIONAL ETHICS COMMITTEE (IEC)
SCTIMST
THIRUVANANTHAPURAM

APPENDIX B - PAPERS AND POSTERS FROM THIS THESIS

- **NEUROVASCON 2022, RAIPUR :**

  RUPTURE STATUS PREDICTION BASED ON THE MORPHOLOGY OF CEREBRAL ANEURYSM - **Paper presentation**

- **3RD INTERNATIONAL RHOTON SOCEITY MEET 2023, ISTANBUL, TURKEY :**

  RUPTURE STATUS PREDICTION BASED ON THE MORPHOLOGY OF CEREBRAL ANEURYSM - - ePOSTER

APPENDIX C – TABLES & SCORES USED IN STUDY

PHASES aneurysm risk score	Points
(P) Population	
North American, European (other than Finnish)	0
Japanese	3
Finnish	5
(H) Hypertension	
No	0
Yes	1
(A) Age	
<70 years	0
≥70 years	1
(S) Size of aneurysm	
<7·0 mm	0
7·0–9·9 mm	3
10·0–19·9 mm	6
≥20 mm	10
(E) Earlier SAH from another aneurysm	
No	0
Yes	1
(S) Site of aneurysm	
ICA	0
MCA	2
ACA/Pcom/posterior	4

To calculate the PHASES risk score for an individual, the number of points associated with each indicator can be added up to obtain the total risk score. For example, a 55-year-old North American man with no hypertension, no previous SAH, and a medium-sized (8 mm) posterior circulation aneurysm will have a risk score of 0+0+0+3+0+4=7 points. According to figure 3, this score corresponds to a 5-year risk of rupture of 2·4%. SAH=subarachnoid haemorrhage. ICA=internal carotid artery. MCA=middle cerebral artery. ACA=anterior cerebral arteries (including the anterior cerebral artery, anterior communicating artery, and pericallosal artery). Pcom=posterior communicating artery. posterior=posterior circulation (including the vertebral artery, basilar artery, cerebellar arteries, and posterior cerebral artery).

Table 4: **Predictors composing the PHASES aneurysm rupture risk score**

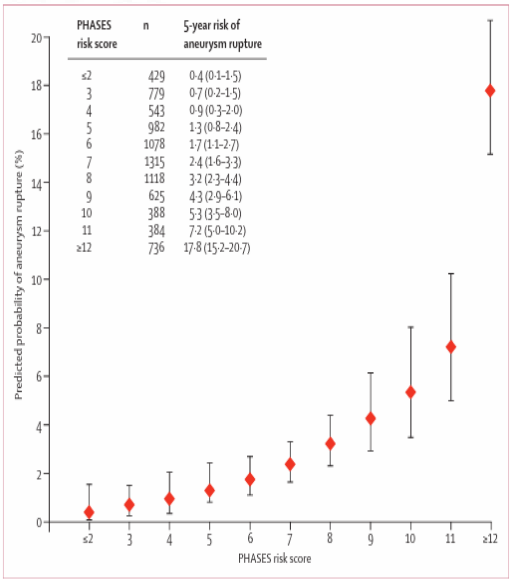

Figure 3: Predicted 5-year risk of aneurysm rupture according to PHASES score

(Greving et al., 2014)

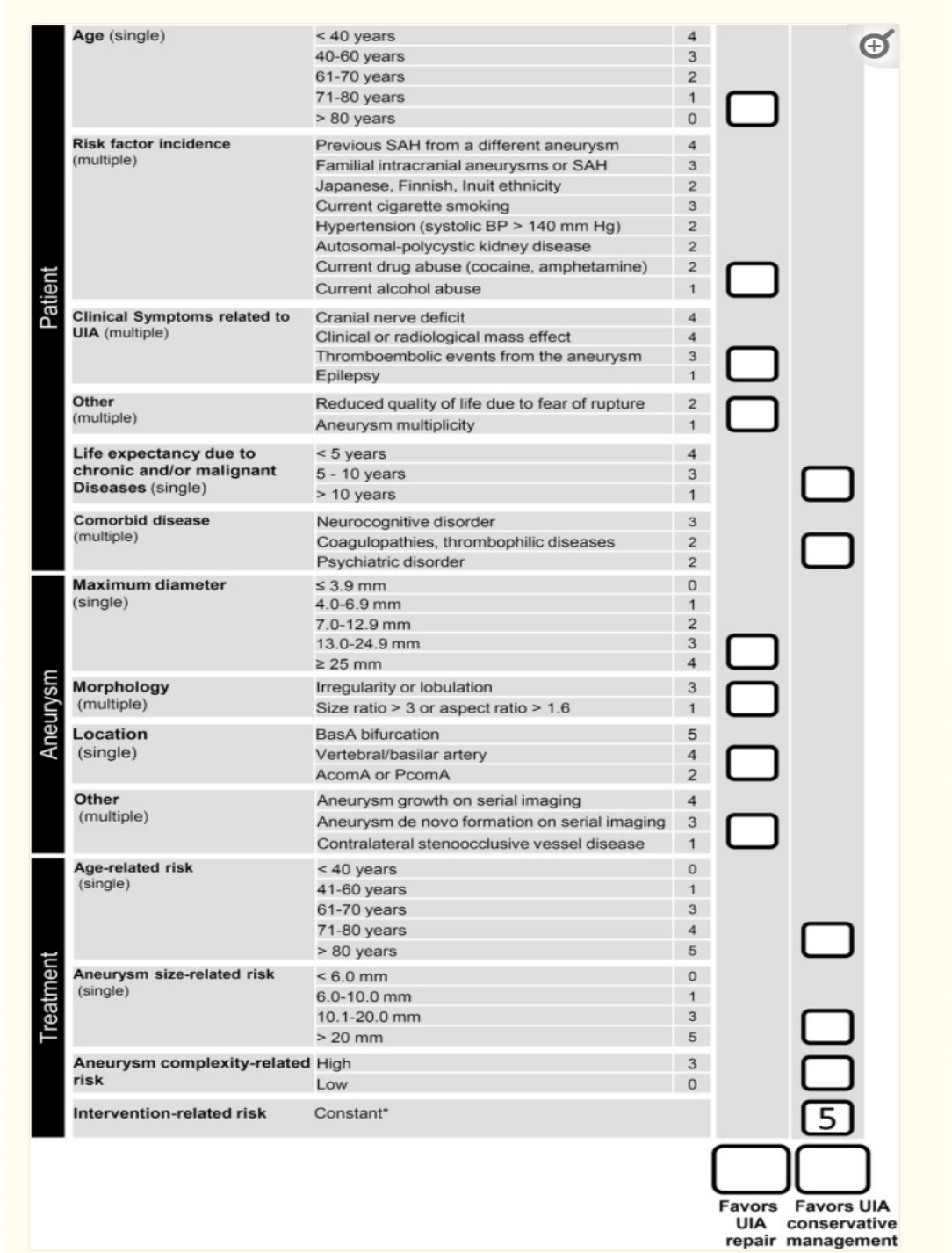

Patient	**Age** (single)	< 40 years	4		
		40-60 years	3		
		61-70 years	2		
		71-80 years	1	☐	
		> 80 years	0		
	Risk factor incidence (multiple)	Previous SAH from a different aneurysm	4		
		Familial intracranial aneurysms or SAH	3		
		Japanese, Finnish, Inuit ethnicity	2		
		Current cigarette smoking	3		
		Hypertension (systolic BP > 140 mm Hg)	2		
		Autosomal-polycystic kidney disease	2		
		Current drug abuse (cocaine, amphetamine)	2	☐	
		Current alcohol abuse	1		
	Clinical Symptoms related to UIA (multiple)	Cranial nerve deficit	4		
		Clinical or radiological mass effect	4		
		Thromboembolic events from the aneurysm	3	☐	
		Epilepsy	1		
	Other (multiple)	Reduced quality of life due to fear of rupture	2	☐	
		Aneurysm multiplicity	1		
	Life expectancy due to chronic and/or malignant Diseases (single)	< 5 years	4		
		5 - 10 years	3		☐
		> 10 years	1		
	Comorbid disease (multiple)	Neurocognitive disorder	3		
		Coagulopathies, thrombophilic diseases	2		☐
		Psychiatric disorder	2		
Aneurysm	**Maximum diameter** (single)	≤ 3.9 mm	0		
		4.0-6.9 mm	1		
		7.0-12.9 mm	2		
		13.0-24.9 mm	3	☐	
		≥ 25 mm	4		
	Morphology (multiple)	Irregularity or lobulation	3	☐	
		Size ratio > 3 or aspect ratio > 1.6	1		
	Location (single)	BasA bifurcation	5		
		Vertebral/basilar artery	4	☐	
		AcomA or PcomA	2		
	Other (multiple)	Aneurysm growth on serial imaging	4		
		Aneurysm de novo formation on serial imaging	3	☐	
		Contralateral stenoocclusive vessel disease	1		
Treatment	**Age-related risk** (single)	< 40 years	0		
		41-60 years	1		
		61-70 years	3		
		71-80 years	4		☐
		> 80 years	5		
	Aneurysm size-related risk (single)	< 6.0 mm	0		
		6.0-10.0 mm	1		
		10.1-20.0 mm	3		☐
		> 20 mm	5		
	Aneurysm complexity-related risk	High	3		☐
		Low	0		
	Intervention-related risk	Constant*			5

Favors UIA repair | Favors UIA conservative management

(Etminan et al., 2015)

APPENDIX D - PLAGIARISM CHECK REPORT

PLAGIARISM SCAN REPORT

Date	August 30, 2023
Exclude URL:	NO

Unique Content	96%
Plagiarized Content	4%
Paraphrased Plagiarism	0

Word Count	14,431
Records Found	10

CONTENT CHECKED FOR PLAGIARISM:

INTRODUCTION

Intracranial aneurysms are relatively common. The true risk arises when an aneurysm ruptures, resulting in a subarachnoid haemorrhage. However, symptoms from unruptured aneurysms may be primarily due to a mass effect or thrombosis. Spontaneous subarachnoid haemorrhage (SAH), a serious condition that can be fatal and result in permanent impairment, is primarily caused by the rupture of aneurysms. Therefore, it is highly desirable to assess the aneurysm rupture risk.

The overall 28-day case mortality rate following aneurysm rupture is 42.7 %, and survivors-dependency rates are about 50 % (Timothy Ingall et al., 2000).About 3.2 percent of adults (mean age, 50 years) globally have cerebral aneurysms, yet only 0.25 percent rupture.(Thompson, Brown, Amin-Hanjani, Broderick, Cockroft, Connolly, Duckwiler, Harris, Howard, SCC lay Johnston, et al., 2015) Treatment recommendations for unruptured aneurysms requires knowledge about the stability of the aneurysm. According to several investigators, size is the most crucial factor in determining aneurysm stability. (kassell1983.pdf, n.d.)

Due to the widespread use of computed tomography angiogram (CTA) and magnetic resonance angiogram (MRA) during the past few decades, an increase in the number of unruptured aneurysms has been discovered. Notably, a significant portion of accidentally discovered aneurysms (<87>6%) have small diameters (<3>, 2016) It is still debatable how to handle patients with small aneurysms that have not ruptured. Based on the data of the low annual growth and rupture rates of small aneurysms, some researchers advise patients with aneurysms of 3 mm to not undertake preventative treatment or imaging follow-up.(Malhotra et al. , 2017) However, in

APPENDIX D: Patient Information Sheet And Consent Form

(English and Malyalam)

Participant Information Sheet

Title of the study:

Computational Fluid Dynamics based tools to the aid of clinical decision-making in the management of intracranial aneurysms

Principal Investigator: Dr. Jayanand Sudhir, Dept of Neuro-surgery, SCTIMST

Co-PI: Dr.Bhushan Sadashiv Akhade, Dept of Neuro-surgery, SCTIMST

IEC/841/August 2021

Introduction:

You are being requested to participate in a research study on intracranial aneurysms. Intracranial aneurysms are out-pouchings of blood vessels in the brain. They pose a risk for rupture. They may also come to attention due to their pressure effects and stroke. They may also be incidentally diagnosed during scan for some other reason.

You have undergone evaluation and management of an intracranial aneurysm. We intend to conduct a study on the images of the angiography done in the institute to understand the blood flow pattern within the aneurysm. We hope to include 200 patients in this study.

You are being requested to give consent for your angiogram images to be used for this research study.

If you take part, what you have to do?

If you consent to participate in the study, a copy of your angiographic images will be processed to help understand the pattern of blood flow within the aneurysm. Enrolment into the study does not pose any risk to you. Data regarding the blood flow (blood flow velocity) and aneurysm characteristics (whether the aneurysm had ruptured or not), normally obtained during your management will be used for the study. No blood or other tissue/ biological samples will be collected for the study. No personal details will be collected. The identifier details in the scans will be masked to conceal identity.

What will be done with the angiography images?

A copy of the angiography images will be used for the study. The images will be processed using a computer in the institute hospital and transferred to Indian Institute of Technology, Madras, where further processing of the images will be done to yield the results.

Will the study influence the outcome of my medical condition?

No. The angiographic images are being requested for submission for research only after you have been subjected to the standard protocol of management in the institute hospital. The study will not affect the outcome of your management.

Are there any side-effects or complications of the study?

There are no side-effects or complications in this study. The study involves processing of the scan images only. No biological samples will be obtained from you for the study.

Will I benefit from the study?

No. There will be no personal benefit for you from the study. The results of the study may benefit the society by helping the medical fraternity in understanding intracranial aneurysms better and influence the management protocol for intracranial aneurysms in future.

Will you have to pay for the study?

No extra payment will have to be paid by you over the routine cost of management.

Will your personal details be kept confidential?

Upon enrolment, you will be identified in the study by a code. No personal details will be used for the study. Any detail relating to your identification in the angiography images will be masked. The results of this study will be published in a medical journal but you will not be identified by name in any publication or presentation of results. However, your medical notes may be reviewed by people associated with the study, without your additional permission.

If you have any further questions, please you can contact Dr. B Jayanand Sudhir (0471-2524347) or email: bjs@sctimst.ac.in.

In case you have any questions about the ethics approvals for this study, you can contact the Member Secretary of the SCTIMST-IEC. Phone: 0471 2524689 or email: iec.mem.sec@sctimst.ac.in

Informed Consent form

I_____aged _____, son/daughter of _____

• declare that I have read the above information provide to me regarding the study: *Haemodynamic imaging of 200 cases of intracranial aneurysms using computational fluid dynamics* and have clarified any doubts that I had. [ ]

• I also understand that my participation in this study is entirely voluntary and that I am free to withdraw permission to continue to participate at any time without affecting my usual treatment or my legal rights [ ]

• I understand that my angiography images will be used for the study and that my participation in the study will not influence the usual course of my treatment in the hospital [ ]

• I also understand that my blood or other biological samples are not being used in the study. [ ]

• I permit the study staff and institutional ethics committee members to look at my health records and use the data including images for the study, maintaining confidentiality and not revealing the patient identity. I agree to this access

• I understand that the study staff and institutional ethics committee members will not need my permission to look at my health records even if I withdraw from the trial. I agree to this access [ ]

• I understand that my identity will not be revealed in any information released to third parties or published [ ]

• I voluntarily agree to take part in this study [ ]

• I received a copy of this signed consent form [ ]

Name: Signature:

Date:

Name of witness:

Relation to participant:

Date:

(Person Obtaining Consent) I attest that the requirements for informed consent for the medical research project described in this form have been satisfied. I have discussed the research project with the participant and explained to him or her in nontechnical terms all of the information contained in this informed consent form, including any risks and adverse reactions that may reasonably be expected to occur. I further certify that I encouraged the participant to ask questions and that all questions asked were answered.

Name and Signature of Person Obtaining Consent:

സമ്മതപത്രം

പഠനത്തിന്റെ പേര്

ഫ്ലൂയിഡ് ഡൈനാമിക്സ് ഉപയോഗിച്ച് ഇൻട്രാക്രേനിയൽ അനൂറിസമുള്ള 200 കേസുകളുടെ ഹീമോഡൈനാമിക് ചിത്രീകരണം

ആമുഖം

ഇൻട്രാക്രേനിയൽ അന്യൂറിസത്തെപ്പറ്റിയുള്ള ഗവേഷണ പഠനത്തിൽ പങ്കെടുക്കുവാനായി താങ്കളോട് അപേക്ഷിക്കുന്നു. തലച്ചോറിലെ രക്തക്കുഴലുകളുടെ പുറത്തേക്ക് തള്ളുന്ന വീക്കമാണ് ഇൻട്രാക്രേനിയൽ അനൂറിസങ്ങൾ. അവ പൊട്ടാനിടയുണ്ട്. അവയുടെ സമ്മർദ്ദത്തിന്റെ പ്രഭവവും സ്ട്രോക്കും മൂലവും അവ ശ്രദ്ധയാകർഷിക്കുന്നു. മറ്റുകാരണങ്ങളാൽ സ്കാൻചെയ്യുമ്പോൾ സന്ദർഭവശാലും രോഗം കണ്ടെത്താറുണ്ട്.

താങ്കൾ ഇൻട്രാക്രേനിയൽ അന്യൂറിസത്തിന് ഈ ഇൻസ്റ്റിറ്റ്യൂട്ടിൽ വിലയിരുത്തപ്പെടുകയും ചികിത്സക്ക് വിധേയമാവുകയും ചെയ്തിട്ടുണ്ട്. അന്യൂറിസത്തിനുള്ളിലെ രക്തപ്രവാഹത്തെപ്പറ്റി ഇൻസ്റ്റിറ്റ്യൂട്ടിൽ നടത്തിയിട്ടുള്ള ആൻജിയോഗ്രാം ചിത്രങ്ങളുപയോഗിച്ച് ഒരു പഠനം നടത്താൻ ഞങ്ങളുദ്ദേശിക്കുന്നു.

ഈ പഠനത്തിൻ 20 രോഗികളെ ഉൾപ്പെടുത്തുവാൻ ഞങ്ങൾ ഉദ്ദേശിക്കുന്നു.

താങ്കളുടെ ആൻജിയോഗ്രാം ചിത്രങ്ങൾകൂടി ഈ പഠനത്തിൽ ഉൾപ്പെടുത്തുവാൻ സമ്മതം തരണമെന്ന് അപേക്ഷിക്കുന്നു.

ഇതിൽ പങ്കെടുക്കുവാൻ താങ്കൾ ചെയ്യേണ്ടത് എന്തെല്ലാം

താങ്കൾ ഈ പഠനത്തിൽ പങ്കെടുക്കുവാൻ സമ്മതിക്കുകയാണെങ്കിൽ താങ്കളുടെ ആൻജിയോഗ്രാം ചിത്രങ്ങളുടെ ഒരു പകർപ്പ് എടുത്ത് രക്തചംക്രമണരീതി മനസ്സിലാക്കുന്നതിനായി ഉപയോഗിക്കുന്നതാണ്. ഈ പഠനത്തിൽ പങ്കെടുക്കുകയാണെങ്കിൽ താങ്കൾക്ക് അപകടസാദ്ധ്യത ഒന്നും തന്നെയില്ല. താങ്കളുടെ രക്തചംക്രമണത്തിന്റെ (രക്തത്തിന്റെ ഒഴുക്കിന്റെ വേഗതയുടെ) സാധാരണ ചികിത്സയുടെ ഭാഗമായി ലഭ്യമാക്കപ്പെടുന്ന വിവരങ്ങളും അന്യൂറിസത്തിന്റെ സ്വഭാവവും (അന്യൂറിസം പൊട്ടിയോ ഇല്ലയോ) ഈ പഠനത്തിൽ ഉൾപ്പെടുത്തുന്നതാണ്. രക്തത്തിന്റെയോ മറ്റ് ശരീര കോശങ്ങളുടെയോ സാമ്പിളുകൾ ഈ പഠനത്തിനായി എടുക്കുന്നതല്ല. വ്യക്തിപരമായ ഒരു വിവരങ്ങളും ഈ പഠനത്തിനായി എടുക്കുന്നതല്ല. തിരിച്ചറിയാതിരിക്കാനായി താങ്കളുടെ സ്കാൻ റിപ്പോർട്ടിലുള്ള താങ്കളുടെ തിരിച്ചറിയൽ വിവരങ്ങൾ മറയ്ക്കുന്നതാണ്.

ആൻജിയോഗ്രാഫി ചിത്രങ്ങൾ കൊണ്ട് എന്തെല്ലാം ചെയ്യും

ആൻജിയോഗ്രാഫി ചിത്രങ്ങളുടെ ഒരു പകർപ്പ് ഈ പഠനത്തിനായി ഉപയോഗിക്കും. വേണ്ട വിവരങ്ങൾ കിട്ടുന്നതിനായി ഈ ചിത്രങ്ങൾ ഇൻസ്റ്റിറ്റ്യൂട്ട് ആശുപത്രിയിലെ കംപ്യൂട്ടർ ഉപയോഗിച്ച് പ്രോസസ്സ് ചെയ്യുന്നതും 'മറ്റൊരു കേന്ദ്രത്തിലേക്ക് (ഇൻഡ്യൻ ഇൻസ്റ്റിറ്റ്യൂട്ട് ഓഫ് ടെക്നോളജി,

മദ്രാസ്) നൽകുന്നതും അവിടെ ഫലം ലഭിക്കാനായി കൂടുതൽ പ്രക്രിയകൾക്ക് വിധേയമാക്കുന്നതുമാണ്

താങ്കളുടെ ആരോഗ്യപരമായ അവസ്ഥയെ ഈ പഠനം ബാധിക്കുമോ

ഇല്ല. ചികിത്സയ്ക്കായി ഇൻസ്റ്റിറ്റ്യൂട്ട് ആശുപത്രിയിൽ ക്രമീകരിച്ചിട്ടുള്ള സ്റ്റാൻഡേർഡ് ചികിത്സാക്രമങ്ങൾക്ക് താങ്കളെ വിധേയമാക്കിയശേഷമാണ് ഗവേഷണത്തിന് സമർപ്പിക്കുവാനായി ആൻജിയോഗ്രാം ചിത്രങ്ങൾ ചോദിക്കുന്നത്. ഈ പഠനം താങ്കളുടെ ചികിത്സാക്രമത്തെ ഒരുതരത്തിലും ബാധിക്കുന്നതല്ല.

ഈ പഠനത്തിന് എന്തെങ്കിലും പാർശ്വഫലങ്ങളോ ദൂഷ്യഫലങ്ങളോ ഉണ്ടോ

മദ്രാസ്)

ചിത്രങ്ങൾ പ്രോസസ് ചെയ്യുക മാത്രമേ ചെയ്യുന്നുള്ളു. പഠനത്തിനായി താങ്കളിൽ നിന്ന ഒരു വിധ ശാരീരിക സാമ്പിളുകളും എടുക്കുന്നതല്ല.

ഈ പഠനം കൊണ്ട് താങ്കൾക്ക് എന്തെങ്കിലും ലാഭമുണ്ടോ.
ഒന്നും ഇല്ല. താങ്കൾക്ക് വ്യക്തിപരമായി ഒരു ലാഭവുമുണ്ടാകില്ല. ഇൻട്രാക്രേനിയൽ അന്യൂറിസത്തെപ്പറ്റി കൂടുതൽ അറിയുവാനും അതിന്റെ ചികിത്സാക്രമീകരണങ്ങൾ മെച്ചപ്പെടുത്തുവാനും ആരോഗ്യ ചികിത്സാരംഗത്തുള്ളവരെ ഈ പഠനഫലങ്ങൾ സഹായിച്ചേക്കാം.

ഈ പഠനത്തിനായി താങ്കൾ പണം മുടക്കേണ്ടതണ്ടോ
ഇല്ല. താങ്കളുടെ സാധാരണ ചികിത്സാ ചെലവുകളല്ലാതെ ഈ പഠനത്തിൽ ഉൾപ്പെടുന്നതിനാൽ താങ്കൾക്ക് ഒരു വിധ ചെലവുകളുമില്ല.

താങ്കളുടെ വ്യക്തിപരമായ വിവരങ്ങൾ രഹസ്യമായി സൂക്ഷിക്കുമോ
ഈ പഠനത്തിൽ ചേരുന്നതോടെ താങ്കൾക്ക് ഒരു പ്രത്യേക കോഡ് തന്ന് ആ കോഡ് മാത്രമായിരിക്കും ഈ പഠനത്തിൽ ഉപയോഗിക്കുക. വ്യക്തിപരമായ ഒരു വിവരങ്ങളും ഈ പഠനത്തിൽ ഉപയോഗിക്കുകയില്ല. ആൻജിയോഗ്രഫി ചിത്രങ്ങളിൽ താങ്കളെ തിരിച്ചറിയുന്നതിനുള്ള എല്ലാ വിവരങ്ങളും മറച്ചിരിക്കും. ഈ പഠനത്തിലെ ഫലങ്ങൾ മെഡിക്കൽ ജേർണലിൽ പ്രസിദ്ധീകരിക്കുമെങ്കിലും താങ്കളുടെ പേര് ഒരു പ്രസിദ്ധീകരണത്തിലും ഫലപ്രകാശനങ്ങളിലും ഉണ്ടായിരിക്കുന്നതല്ല. എന്നാൽ താങ്കളെ സംബന്ധിക്കുന്ന മെഡിക്കൽ നോട്ടുകൾ ഈ പഠനവുമായി ബന്ധപ്പെട്ടിരിക്കുന്നവർ താങ്കളുടെ പ്രത്യേക അനുവാദമില്ലാതെ പുനപരിശോധിച്ചേക്കും,

താങ്കൾക്ക് അധികമായി എന്തെങ്കിലും അറിയണമെന്നുണ്ടെങ്കിൽ ദയവായി ഡോ. ബി. ജയാനന്ദ് സുധീർ (0471-2524347) അല്ലെങ്കിൽ ഇമെയിൽ bjs@sctimst.ac.in

യഥാസ്ഥാനങ്ങളിൽ ( ) അടയാളപ്പെടുത്തുക

..... ന്റെ മകൻ/മകൾ/മാതാവ്/പിതാവായ .....വയസ്സുള്ള..... എന്ന ഞാൻ ഫ്ലൂയിഡ് ഡൈനാമിക്സ് ഉപയോഗിച്ച് ഇൻട്രാക്രേനിയൽ അനൂറിസമുള്ള 200 കേസുകളുടെ ഹീമോഡൈനാമിക് ചിത്രീകരണം എന്ന പഠനത്തെ സംബന്ധിച്ച് മേൽ വിവരിച്ചിരിക്കുന്ന കാര്യങ്ങൾ മുഴുവൻ വായിക്കുകയും സംശയനിവൃത്തി വരുത്തി കാര്യങ്ങൾ മുഴുവനായി മനസ്സിലാക്കിയതായും ഇതിനാൽ സാക്ഷ്യപ്പെടുത്തിക്കൊള്ളുന്നു. [ ]

താഴെപ്പറയുന്ന കാര്യങ്ങൾകൂടി ഞാൻ മനസ്സിലാക്കുന്നു.

- ഈ പഠനത്തിൽ സ്വമനസ്സാലെയും സ്വമേധയായും ആണ് ഞാൻ പങ്കെടുക്കുന്നത്. എന്റെ സാധാരണ ചികിത്സയ്ക്കോ നിയമപരമായ പരിരക്ഷക്കോ ഭംഗം കൂടാതെതന്നെ എതുസമയത്തും ഇതിൽതുടരുവാനുള്ള അനുവാദം എനിക്ക് പിൻവലിക്കാവുന്നതാണ്. [ ]
- ഈ പഠനത്തൽ എന്റെ ആൻജിയോഗ്രഫി ചിത്രങ്ങൾ ഉപയോഗിക്കാം. [ ]
- ഞാൻ ഈ പഠനത്തിൽ പങ്കെടുക്കുന്നത് ആശുപത്രിയിലെ എന്റെ സാധാരണ ചികിത്സാക്രമത്തെ ബാധിക്കുകയില്ല. [ ]
- എന്റെ രക്തത്തിന്റെയോ മറ്റ് ശരീരസാമ്പിളുകളോ ഈ പഠനത്തിൽ ഉപയോഗിക്കുകയില്ല []
- ഞാൻ ഈ പഠനത്തിൽനിന്ന് പിൻമാറിയാലും എന്റെ ആരോഗ്യരേഖകൾ നോക്കുന്നതിലേക്ക് പഠനം നടത്തുന്നവർക്കോ സ്ഥാപനത്തിലെ എത്തിക്സ് കമ്മറ്റി അംഗങ്ങൾക്കോ എന്റെ അനുവാദം ആവശ്യമില്ലാത്തതാകുന്നു. [ ]
- ഏതെങ്കിലും തേർഡ് പാർട്ടിക്ക് കൊടുക്കുന്നതോ പ്രസിദ്ധീകരിക്കുന്നതോ ആയ വിവരങ്ങളിലൊന്നും എന്നെ തിരിച്ചറിയാനുതകുന്ന വിവരങ്ങൾ ഉണ്ടായിരിക്കുന്നതല്ല എന്നു ഞാൻ മനസ്സിലാക്കുന്നു. [ ]
- ഈ പഠനത്തിൽ സ്വമനസ്സാലെയാണ് പങ്കെടുക്കുന്നതെന്നും ഞാൻ സമ്മതിക്കുന്നു [ ]
- സമ്മതപത്രത്തിന്റെ ഒപ്പിട്ട ഒരു കോപ്പി എനിക്കു കിട്ടി [ ]

പേര് ഒപ്പ്

തിയതി

സാക്ഷിയുടെ പേര് ഒപ്പ്
മേൽപ്പറയുന്നയാളുമായുള്ള ബന്ധം

തീയതി

(സമ്മതം വാങ്ങുന്നയാൾ)

മെഡിക്കൽ റിസർച്ച് പ്രോജക്ടിനാവശ്യമായ സമ്മതപത്രത്തിനു വേണ്ടുന്ന എല്ലാ ഘടകങ്ങളും തൃപ്തികരമായി നിർവഹിച്ചിരിക്കുന്നുവെന്ന് ഞാൻ ബോധ്യപ്പെടുത്തുന്നു. പഠനപങ്കാളിയുമായി ഗവേഷണപദ്ധതിയെപ്പറ്റി സാങ്കേതികേതര പദങ്ങളുപയോഗിച്ച് എല്ലാ വിവരങ്ങളെപ്പറ്റിയും ചർച്ച നടത്തുകയും പ്രതീക്ഷിക്കാവുന്ന അപകടസാധ്യതകളും പാർശ്വഫലങ്ങളും വിശദീകരിക്കുകയും

ചെയ്തു. പങ്കാളിയെ ചോദ്യങ്ങൾ ചോദിക്കാൻ പ്രേരിപ്പിക്കുകയും എല്ലാ ചോദ്യങ്ങൾക്കും ഉത്തരം നൽകുകയും ചെയ്തു എന്നും ഞാൻ സാക്ഷ്യപ്പെടുത്തുന്നു.

സമ്മതപത്രം വാങ്ങുന്ന ആളുടെ പേരും ഒപ്പും തീയതിയും